2
7002

This is to certify that the

dissertation entitled

INDUCTION OF LEUKOCYTE APOPTOSIS
BY TRICHOTHECENE MYCOTOXINS

presented by

Rebecca Lynne Uzarski

has been accepted towards fulfillment
of the requirements for

Ph.D. degree in Food Science/
Environmental Toxicology

James J Pestka
Major professor

Date 5/10-02

O-12771

INDUCTION OF LEUKOCYTE APOPTOSIS BY TRICHOTHECENE MYCOTOXINS

By

Rebecca Lynne Uzarski

A DISSERTATION

Submitted to
Michigan State University
in partial fulfillment of the requirements
for the degree of

DOCTOR OF PHILOSOPHY

Department of Food Science and Human Nutrition

2002

ABSTRACT

INDUCTION OF LEUKOCYTE APOPTOSIS BY TRICHOTHECENE MYCOTOXINS

By

Rebecca Lynne Uzarski

Trichothecenes are secondary fungal metabolites produced by food-borne and environmental molds including *Fusarium*, *Stachybotrys*, and *Myrothecium*. Human and animal exposure may occur via consumption of mold-contaminated grains, inhalation of fungal spores present on water-damaged building materials, or airborne exposure during suspected chemical warfare. Trichothecenes are potent translational inhibitors which bind to the ribosomes of actively dividing leukocytes of the immune system. Exposure to trichothecenes results in decreased leukocyte numbers and impaired resistance to pathogens. The overall hypothesis of this dissertation is that trichothecene-induced immune suppression is mediated in part by the induction of leukocyte death by apoptosis. The specific objectives of these studies were to compare apoptosis induction by trichothecenes and other naturally occurring translational inhibitors, determine the physico-chemical components of the trichothecenes critical for the induction of apoptosis, investigate the augmentation of trichothecene-induced cell death by inflammatory agents, and determine the signal transduction mechanisms critical for trichothecene-induced apoptosis. Comparisons of translational inhibitors suggested that trichothecenes were among the most potent inducers of leukocyte apoptosis when compared to other natural toxins. Multiple physico-chemical factors critical to transport and ribosomal binding contribute to the apoptotic actions of the trichothecenes including

lipophilicity, electrostatic interactions, and molecular shape. Trichothecene-induced leukocyte apoptosis may be augmented by signal components of stress and inflammation such as TNF-α and Fas ligand. Activation of mitogen activated protein kinases (MAPKs) appears to be an early, critical step in the development of leukocyte apoptosis induced by trichothecenes or potentiated by inflammatory agents. Taken together, these studies contribute to our knowledge of the mechanism of leukocyte apoptosis by the trichothecene mycotoxins and may facilitate risk assessment studies for this group of natural toxins.

ACKNOWLEDGMENTS

I would like to thank Drs. James Pestka, John Linz, Jay Schroeder, and Norb Kaminski for their guidance, support, and patience. I would like to acknowledge my many friends and colleagues in the Pestka and Linz lab groups and members of the Department of Food Science and Human Nutrition who have provided support and assistance in many different forms. The Department of Food Science and Human Nutrition, College of Agriculture and Natural Resources, Institute for Environmental Toxicology, and the Society of Toxicology all provided funding for this research. A final thank you goes to "The Dons" for both statistical and moral support.

TABLE OF CONTENTS

LIST OF TABLES

LIST OF FIGURES

CHAPTER 1

Literature Review

General aspects of trichothecene mycotoxins

Fusarium, *Stachybotrys*, and *Myrothecium* produce biologically active secondary fungal metabolites called trichothecenes (Bondy and Pestka, 2000). This group of mycotoxins is comprised of 182 compounds (Grove 1993; 1996) characterized by a tetracyclic scirpenol ring system (Figure 1.1) and further categorized into four subtypes (A – D) based on the presence or absence of specific functional groups (Ueno, 1983). Three of these subtypes, Type A, B, and D, are common in the air and soil and therefore, pose the greatest health risk to humans and animals. Type A trichothecenes are characterized by a hydroxy or acyl moiety at the R_1, R_2, R_3, or R_5 position(s) and include T-2 toxin and diacetoxyscirpenol (Table 1.1). Type B trichothecenes, such as deoxynivalenol (DON) and nivalenol (NIV) possess a carbonyl at R_5 in addition to the Type A moieties previously described. The satratoxins are examples of Type D (macrocyclic) trichothecenes which possess a diester or triester ring system at the R_2 and R_3 positions (Figure 1.2).

Environmental exposure to trichothecenes and adverse health effects

Exposure to trichothecenes occurs via consumption of mold-contaminated grains, inhalation of fungal spores present in heating ducts and building materials, and airborne exposure during suspected chemical warfare (Peraica et al., 1999). Alimentary toxic aleukia, the first recorded human mycotoxicosis attributed to the trichothecenes, occurred in the Soviet Union between 1932 and 1947. *F. sporotrichoides* was isolated from 40%

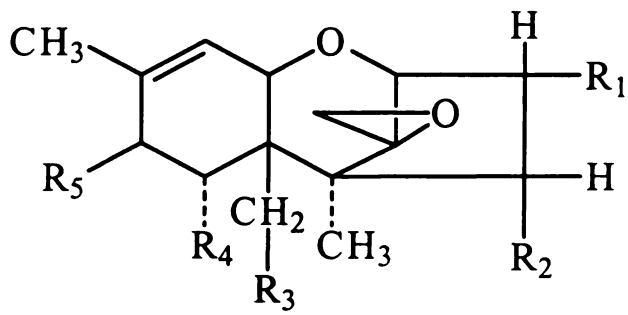

Figure 1.1. Common tetracyclic scirpenol ring system of the trichothecene mycotoxins. Functional group location is depicted by R_1, R_2, R_3, R_4, and R_5. Functional groups for individual trichothecenes are listed in Table 1.1.

Table 1.1. Type A and Type B trichothecene mycotoxin functional groups.

Trichothecene	Abbreviation	R_1	R_2	R_3	R_4	R_5
Type A						
T-2 Toxin	A1	OH	OAc[a]	OAc	H	ISV[b]
HT-2 Toxin	A2	OH	OH	OAc	H	ISV
Diacetoxyscirpenol	A3	OH	OAc	OAc	H	H
Acetyl T-2 Toxin	A4	OAc	OAc	OAc	H	ISV
T-2 Tetraol	A5	OH	OH	OH	H	OH
T-2 Triol	A6	OH	OH	OH	H	ISV
3'OH T-2 Toxin	A7	OH	OAc	OAc	H	$OCOCH_2C(OH)(CH_3)_2$
3'OH HT-2 Toxin	A8	OH	OH	OAc	H	$OCOCH_2C(OH)(CH_3)_2$
Neosolaniol	A9	OH	OAc	OAc	H	OH
Isotrichodermin	A10	H	OAc	H	H	H
Isotrichodermol	A11	H	OH	H	H	H
3,15 Didecalonectrin	A12	OH	H	OH	H	H
Verrucarol	A13	H	OH	OH	H	H
Type B						
Deoxynivalenol	B1	OH	H	OH	OH	=O
Fusarenon-X	B2	OH	OAc	OH	OH	=O
Nivalenol	B3	OH	OH	OH	OH	=O
15-Acetyldeoxynivalenol	B4	OH	H	OAc	OH	=O
3-Acetyldeoxynivalenol	B5	OAc	H	OH	OH	=O
4, 15 Diacetylnivalenol	B6	OH	OAc	OAc	OH	=O

[a]OAc: $-OC{=}OCH_3$

[b]ISV: $-OC{=}OCH_2CH(CH_3)_2$

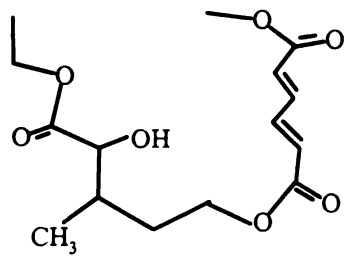

Verrucarin A (D1)

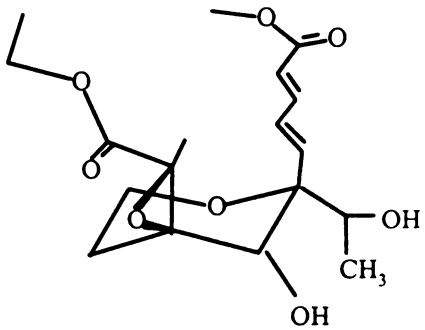

Satratoxin G (D2)

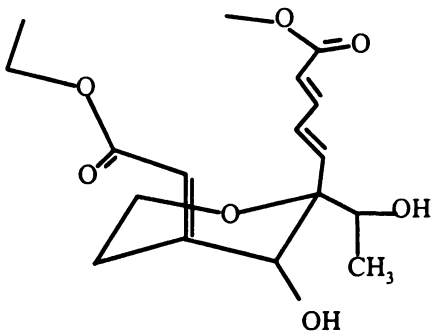

Satratoxin H (D3)

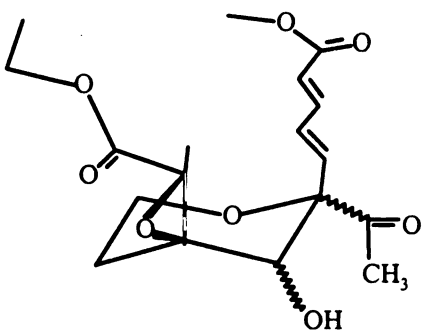

Satratoxin F (D4)

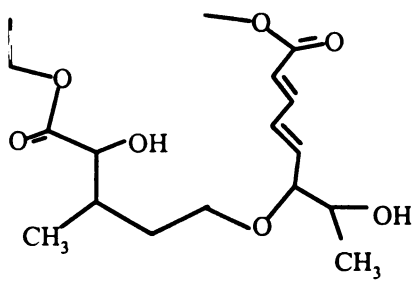

Roridin A (D5)

Figure 1.2. Type D (macrocyclic) trichothecene functional groups. Type D abbreviations are noted in parenthesis.

of grain samples. With a mortality rate of 60%, continuous consumption of the toxic grain was a determinant in severity of the disease. Between 1960 and 1991, 53 outbreaks of human food poisoning associated with moldy cereal occurred throughout China affecting approximately 130,000 people (Li, 1999). Stachybotryotoxicosis in horses, sheep, and cattle has been associated with consumption of *Stachybotrys*-infested hay and straw (Bamburg et al., 1968). Moldy corn toxicosis has been recorded in pigs and cattle in the Midwestern United States and linked to *Fusarium* growth.

Recent attention has focused on the contribution of molds to indoor air illness and specifically, the role of trichothecene-producing molds in indoor environments. Trichothecenes are estimated to be between 10- and 40-times (FAO/WHO, 2002; Peraica et al., 1999) more toxic when inhaled. Both *Fusarium* and *Stachybotrys* isolates have been collected from ventilation systems of homes of allergen sensitized children (Wickman et al., 1992). *Stachybotrys* has been found in water damaged homes, schools, and public buildings where the occupants have reported building-related respiratory disease (Mahmoudi and Gershwin, 2000). Thirty-seven cases of infant pulmonary hemorrhage were reported and linked to water damaged homes containing *Stachybotrys* in Cleveland, OH (Dearborn et al., 1999). *Stachybotrys* spores were isolated from lung tissue of one child.

Trichothecenes have the potential to be used as chemical warfare agents. The toxins are believed to exist in the arsenals of some countries (McGovern et al., 1999; Heyndrickx et al., 1984; Zilinskas, 1997) and were reportedly used as chemical warfare agents in South-East Asia between 1975 and 1981(Peraica et al., 1999).

Mycotoxin levels have not always been determined in food-borne and inhalation exposures due to unsuitable diagnostic methods or lack of samples (Bamburg, 1972).

However, trichothecene levels were recently determined in samples from a food poisoning outbreak in Anhui, China in 1991 (Li et al., 1999). Cereal samples contained up to 51.4, 6.9, 2.5, and 2.5 mg/kg deoxynivalenol (DON, vomitoxin), nivalenol (NIV), 3-acetyl-DON, and 15-acetyl-DON, respectively. T-2 toxin was detected at concentrations up to 420 μg/kg in moldy rice implicated in a food-borne outbreak in Zhejiang, China (Wang et al., 1993a). In addition, T-2 toxin, DON, and NIV are routinely detected in raw agricultural products (Scott, 1997; WHO, 1990) and commercial grain-based foods (Abouzied et al., 1991) intended for human consumption.

Of the trichothecenes, DON is among the most commonly encountered relative to frequency and concentration in wheat, corn, and barley worldwide (Rotter et al., 1996). DON levels can vary widely on a year-to-year and region-to-region basis due to weather and storage conditions. DON at low levels (< 1 ppm) is frequently encountered but may occasionally reach 5 to 20 ppm in processed foods (Abouzied et al., 1991).

The U. S. Food and Drug Administration has established a tolerance limit of 1 ppm DON for bran, flour, and germ targeted for human consumption. Health Canada designated guidelines of 2 ppm DON in uncleaned soft wheat used for nonstaple goods and 1 ppm for infant foods. Maximum tolerated levels of 0.5 ppm, 1 ppm, and 1 ppm have been set by Austria, Hungary, and the Soviet Union, respectively (Pestka, submitted). The Food and Agriculture Organization of the United Nations and World Health Organization have recently recommended the development of DON equivalency factors to assess human health risks from trichothecene exposure (FAO/WHO, 2002).

Trichothecenes are immunotoxins

The common mechanism of action of all trichothecenes is inhibition of protein

synthesis following binding to the 60S ribosomal subunit. Ribosomal binding occurs rapidly and drastically impacts cells that are actively dividing. Cells of the intestinal mucosa and immune system are particularly sensitive to trichothecenes (Bondy and Pestka, 2000). Ingestion of trichothecenes leads to gastrointestinal disorders including nausea, vomiting, and diarrhea. Airborne exposure to this group of toxins results in respiratory tract irritation, fatigue, and dermatitis. In addition, alterations of immune cell function, dysregulation of the humoral immune response, and impairment of host resistance to pathogens have been described for both exposure scenarios (Bondy and Pestka, 2000; Nikulin et al., 1997; Nikulin et al., 1996). Symptoms described in food-borne outbreaks and reported for suspected inhalation mimic symptoms of experimental animals exposed to trichothecenes and provide a useful model for toxicity studies.

DON, the most extensively studied trichothecene, may stimulate or suppress the immune system dependent on dose and duration of exposure. Mice exposed to low concentrations of DON exhibit increased cytokine production, increased serum IgA, and IgA immune complex deposition in the kidney (Bondy and Pestka, 2000). The development of IgA nephropathy in the mouse mimics human IgA nephropathy. Mice exposed to high concentrations of DON have impaired host-resistance to challenge with *Listeria* and *Salmonella* and decreased lymphocyte numbers.

Trichothecenes induce lymphocyte apoptosis

Cell death by apoptosis (Yang et al., 2000; Okumura et al., 2000; Shifrin and Anderson, 1999) has been widely reported for the trichothecenes and is likely to contribute to the observed immunotoxic effects. Apoptosis is a regulated form of cell

death that removes damaged or unnecessary cells. Scheduled cell death regulates embryogenesis, maintains tissue homeostasis, and prevents autoimmunity (Dong et al., 2002; Cohen et al., 1992; Koury et al., 1992). However, apoptosis may also result from cellular stress (i.e. UV light, cytokines, and heat shock), chemical insult (Saini and Walker, 1998), or ribotoxic stress resulting from ribosomal cleavage (Iordanov et al., 1997) or ribosomal binding (Shifrin and Anderson, 1999) by translational inhibitors. Down regulation of apoptosis in lymphocytes of the immune system may lead to autoimmunity and inflammation whereas up-regulation of apoptosis may lead to immune suppression and increased susceptibility to pathogens.

Trichothecene toxicity is potentiated by bacterial lipopolysaccharide

Signaling components of both stress (Albers et al., 1996; Pruett et al., 1993) and inflammation (Luster et al., 2000; Emmendoerffer et al., 2000) may play a critical role in chemically-induced toxic responses. Recent studies indicate that exposure to low levels of lipopolysaccharide (LPS), the biologically active component of gram negative bacteria, can influence the magnitude of a toxic response to xenobiotic agents (Roth et al., 1997). Increased hepatotoxic responses have been observed for carbon tetrachloride, ethanol, and ally alcohol. Previous in vivo studies demonstrate increased trichothecene toxicity in the presence of LPS. LD_{50} doses decreased and mortality increased in mice exposed to Salmonella and T-2 toxin simultaneously (Tai and Pestka, 1988). Increased lymphocyte apoptosis and mortality was observed in LPS and DON-treated mice (Zhou et al., 2000; Zhou et al., 1999). The mechanisms involved in this synergistic toxicity have not been elucidated. However, LPS induces its biological effects by stimulating host cells to produce a variety of mediators including bioactive lipids (i.e prostaglandins),

glucocorticoids (i.e. corticosterone), and proinflammatory cytokines (i.e. TNF-α). These mediators may interact with trichothecenes to alter immune cell responses.

Rationale

Despite the high potential for human exposure, little information exists on the role of apoptosis in VT-induced immunosuppression and the signaling mechanisms involved in apoptosis induction. The objectives of this research were as follows:

1. To compare the induction of apoptosis and cytotoxicity by several trichothecenes and other translational inhibitors in three murine lymphocyte cell lines.
2. To determine the structural aspects of the trichothecenes that impart biological activity in the induction of cell death in murine lymphocytes.
3. To investigate the potentiation of trichothecene-induced cell death by inflammatory agents in primary murine lymphocytes.
4. To characterize the dose dependent induction of apoptosis and alterations in apoptotic signal transduction mechanisms in human lymphocytes exposed to trichothecenes.
5. To assess the potentiation of trichothecene-induced apoptosis and apoptotic signal transduction mechanisms by TNF-α in a human lymphocyte model.

The aforementioned issues were addressed in the following five chapters. Chapter 2 compares the induction of apoptosis and cytotoxicity by trichothecenes and several

naturally occurring translational inhibitors in murine B lymphocytes. The B lymphocyte lines studied represent phenotypically immature B cells (CH31, WEHI-231), and mature B cells (CH12.LX). These cells are differentially sensitive to apoptotic agents. For

example, CH31 and WEHI-231 unlike CH12.LX, express surface IgM and are sensitive to apoptosis induced by antigenic mimics such as anti-IgM (Warner et al., 1992). Both immature and mature B cells express prostaglandin receptors, however, only immature CH31 and WEHI-231 cells undergo apoptosis in response to PGE_2 (Brown and Phipps, 1995). Finally, CH31, WEHI-231, and CH12.LX express FasR, however, mature B cells are most susceptible to apoptosis induced by Fas ligand (Onel et al., 1995). Therefore, differential sensitivity to translational inhibitors could be addressed using this lymphocyte model system. Chapter 3 describes physical and chemical characteristics of the trichothecenes that influence murine B lymphocyte apoptosis and cytotoxicity induction and may be used to predict the toxicity of uncharacterized trichothecenes. Chapter 4 investigates the potentiation of trichothecene-induced toxicity by inflammatory agents in several primary murine lymphocytes. Chapter 5 compares dose response induction of apoptosis and alterations in cell signal transduction mechanisms of trichothecenes in human lymphocytes. In addition, the induction of apoptosis and alterations in cell signaling in the potentiation of trichothecene-induced apoptosis by TNF-α are addressed. Chapter 6 summarizes these inter-related studies.

CHAPTER 2

Differential Induction of B Cell Cytotoxicity and Apoptosis By Trichothecene Mycotoxins and Other Translational Inhibitors

INTRODUCTION

A number of natural toxins including trichothecene mycotoxins, shiga like toxins (SLT), and ricin are potent translational inhibitors. Ribosomal binding by the trichothecenes, secondary fungal metabolites produced by *Fusarium* species, inhibits the initiation/elongation step of protein synthesis. Both SLT, bacterial toxins produced by *Escherichia coli* and *Shigella dysenteriae*, and ricin, a lectin produced by *Ricinus communis*, cleave the ribosome to cause inhibition of protein synthesis. While these three translational inhibitors are diverse in their mechanism of action, all induce cell death by apoptosis (Chen et al., 1998; Griffiths et al., 1987; Kiyokawa et al., 2001; Yang et al., 2000).

Apoptosis is a regulated form of cell death that removes damaged or unnecessary cells. Scheduled cell death regulates embryogenesis, maintains tissue homeostasis and prevents autoimmunity in the immune system (Dong et al., 2002; Cohen et al., 1992; Koury et al., 1992). However, apoptosis may also result from cellular stress (i.e. UV light, cytokines, and heat shock), chemical insult (Saini and Walker, 1998), or ribotoxic stress resulting from ribosomal cleavage (Iordanov et al., 1997) or ribosomal binding (Shifrin and Anderson, 1999) by translational inhibitors. Down-regulation of apoptosis in lymphocytes of the immune system may lead to autoimmunity and inflammation

whereas upregulation of apoptosis may lead to increased susceptibility to pathogens.

Trichothecenes, SLT, and ricin pose a health risk to humans and animals exposed to these toxins in food or the environment. Trichothecene mycotoxicosis has been linked to consumption of *Fusarium*-contaminated grain-based food and feeds (Bondy and Pestka, 2000). Recent attention has focused on the contribution of molds to indoor air illness through inhalation of trichothecene-producing spores (Smoragiewicz et al., 1993; Johanning et al., 1996; Tuomi et al., 1998). The most common symptoms described for trichothecene mycotoxicosis include vomiting, diarrhea, respiratory tract irritation, leukopenia, and impaired immune function (Bondy and Pestka, 2000). Exposure to SLT occurs through consumption of meat, apple juice, and vegetables contaminated with toxin-producing *E. coli* (Sandvig and vanDeurs, 2000). This group of toxins plays a critical role in the pathogenesis of the epidemic form of hemolytic uremic syndrome (HUS) which may ultimately lead to kidney failure. Following consumption of castor beans or castor seed oil containing ricin, symptoms of gastroenteritis, hepatoxicity, and teratogenicity were documented (Palatnick and Tenenbein, 2000; El Mauhoub et al., 1983).

Clinical signs described following exposure to translational inhibitors may be partially due to apoptosis induction. Germinal centers containing actively dividing B cell lineages are particularly sensitive to protein synthesis inhibition. Of these lineages, the immature B cell is the most susceptible to apoptosis (Carsetti et al., 1995; Garvy et al., 1993). The objective of this study was to compare the sensitivity of three murine B cell lines to apoptosis and cytotoxicity induction by several trichothecene mycotoxins, SLT-1, and ricin to cycloheximide (CHX), a prototypical protein sythesis inhibitor commonly used to study cell signal transduction mechanisms. The differential sensitivity observed

among immature (CH31, WEHI-231) and mature (CH12.LX) B cell lineages to these toxins may contribute to our understanding of mechanisms of toxicity of the aforementioned translational inhibitors.

MATERIALS AND METHODS

Chemicals and reagents

Chemicals and reagents were purchased from Sigma Chemical Company (St. Louis, MO) unless otherwise noted. Satratoxin G, satratoxin F, and satratoxin H were obtained from Dr. Bruce Jarvis (University of Maryland, College Park, MD). 3'OH metabolites were produced by the procedure of Yoshizawa et al. (1981; 1984). Trichothecenes, cycloheximide (CHX), and ricin were dissolved in 100% ethanol and diluted in RPMI-1640 supplemented with 100 U/ml penicillin, 100 μg/ml streptomycin, 50 μM 2-mercaptoethanol, 2 mM glutamine, 1 mM sodium pyruvate (Gibco Life Technologies, Rockville, MD), and 1 mM non-essential amino acids (Gibco). Final ethanol concentration in the culture medium was less than 0.01% (v/v) which did not induce apoptosis or cytotoxicity. SLT1 (10^7 units/mg, Toxin Technology Inc., Sarasota, FL) was dissolved in 0.01M PBS and diluted in supplemented RPMI-1640 medium.

Cell lines and culture

WEHI-231 and CH31 cells, phenotypically immature B cells, were obtained from Dr. David Scott (American Red Cross Holland Laboratory, Rockville, MD). CH12.LX cells, phenotypically mature B cells, were obtained from Dr. Geoffrey Haughton (University of North Carolina, Chapel Hill, NC). Cell number and viability were

assessed microscopically by trypan blue dye exclusion using a hemocytometer (Stiles, 1986). Cells were cultured in supplemented RPMI-1640 medium with 5% (v/v) heat-inactivated fetal bovine serum at a concentration of 5 x 10^5/ml in 200 µl/well in 96 well flat bottom plates at 37°C in a 5% CO_2 humidified incubator. Triplicate cultures were treated with three concentrations of each translational inhibitor diluted in supplemented RPMI-1640 for 18 h. All experiments were repeated (n=6).

MTT conversion assay for cytotoxicity

Following treatment, 20 µl of a 5 mg/ml solution of 3- (4,5 dimethylthiazol-2-ul)-2,5-diphenyl tetrazolium bromide (MTT) in 0.01 M PBS was added to each well for the final 2 h of the 18 h incubation period (Marin et al., 1996). Microtiter plates were centrifuged at 450 x g for 20 min and media were aspirated to minimize formazan crystal loss. The resultant crystals were dissolved in 150 µl dimethylsulfoxide (DMSO) for 15 min. Optical density was measured using a Vmax Microplate Reader (Molecular Devices, Menlo Park, CA) at dual wavelengths, 570 nm and 690 nm. Percent MTT inhibition was calculated as follows: ((1 - absorbance of treatment)/ absorbance of control) x 100. Mean values were used to graphically determine ED_{50} values.

Apoptosis assay

Apoptotsis, as determined by cell morphology, was quantitated by fluorescence microscopy as described (Duke and Cohen, 1995). Briefly, following trichothecene treatment, microtiter plates were centrifuged at 450 x g for 10 min and 150 µl of supernatant was removed. Five µl of DNA staining reagent (acridine orange (100 µg/ml) and ethidium bromide (100 µg/ml) in 0.01 M phosphate buffered saline (PBS)) was

added to each well. Cells were classified as apoptotic or normal based on chromatin organization. A normal nucleus appeared large with an organized structure while an apoptotic nucleus appeared small and highly condensed or fragmented. Percent apoptosis was calculated as follows: number of cells with apoptotic nuclei/total cell number x 100. Mean values were used to graphically determine the effective dose causing 50% apoptosis (ED_{50}).

Statistical analysis

The data were analyzed using Systat version 5.0 (Evanston, IL). A Student's t test was used to compare two groups while multiple groups were compared using a one way analysis of variance (ANOVA) and a Tukey test for mean separation. A p value <0.05 was considered statistically significant.

RESULTS AND DISCUSSION

Induction of cytotoxicity and apoptosis by cycloheximide (CHX)

Cycloheximide (CHX), an antibiotic produced by *Streptomyces griseus*, interferes with the translocase enzyme to block the translocation step of protein synthesis. CHX is widely used as a pharmacological tool to study cell signal trasduction mechanisms and has been used to study superinduction of proteins (Zinck et al., 1995), to block apoptosis (Takahashi et al., 2002; Liao et al., 2001), and to potentiate apoptosis (Li et al., 2001). Induction of B cell cytotoxicity by CHX was evaluated at 18 h by the MTT conversion assay. CHX significantly increased immature and mature B cell cytotoxicity (Figure 2.1). ED_{50} values for cytotoxicity were 0.25, 0.33, and 0.15 μg/ml for CH31, CH12.LX,

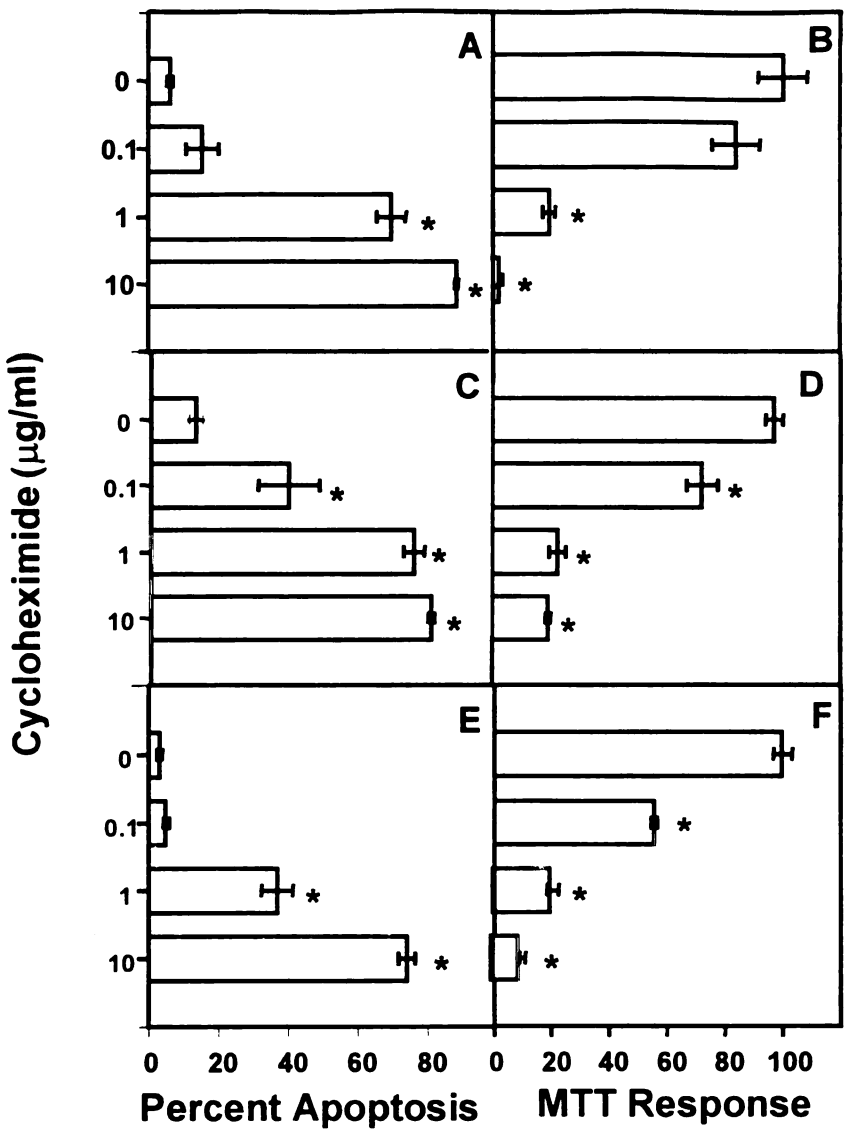

Figure 2.1. Cycloheximide-(CHX)-induced apoptosis and cytotoxicity in immature and mature murine B cells. Murine CH31 (A, B), CH12.LX (C, D), and WEHI-231 (E, F) B cells (5 X 10^5/ml) were exposed to CHX for 18 h prior to determination of apoptosis (A, C, and E) and cytotoxicity (B, D, and F) as described. Asterisk indicates values significantly different from vehicle control ($p < 0.05$).

and WEHI-231 cells, respectively. Induction of apoptosis at 18 h was evaluated by fluorescence microscopy. CHX significantly increased apoptotic morphology in all cell lines (Figure 2.1). ED_{50} values for apoptosis were 0.4, 0.15, and 2.0 μg/ml for CH31, CH12.LX and WEHI-231 cells, respectively. These results suggest both immature and mature B cells are similarly sensitive to cell death induced by CHX. The similarity in apoptosis and cytotoxicity ED_{50} values suggests cell death was primarily due to apoptosis. In previous studies, CHX-induced cell death was observed at higher doses (10 - 50 μg/ml) and later time points (24 - 72 h) in MDA-231, MCF-7, or Burkitt lymphoma cells than reported here (Geier et al., 1996; Ishii et al., 1995; Geier et al., 1992) suggesting murine B cells may be a more sensitive to CHX-induced cell death than these aforementioned cell lines. However, ED_{50} values were not determined in these studies.

Induction of cytotoxicity and apoptosis by trichothecene mycotoxins

Trichothecene mycotoxins consist of 182 family members (Grove 1993; 1996) divided into three subtypes based on the presence or absence of specific functional groups (Figure 1.1, 1.2 and Table 1.1; Snyder, 1986). Ribosomal binding by the trichothecenes inhibits protein synthesis in actively dividing cells (Bondy and Pestka, 2000). Induction of cytotoxicity and apoptosis by trichothecenes was evaluated at 18 h. Deoxynivalenol (DON), a representative trichothecene, induced cytotoxicity and apoptosis after exposure to 100 - 1000 ng/ml and 1000 ng/ml respectively (Figure 2.2). ED_{50} values for WEHI-231 cells were derived for 24 trichothecenes and are summarized in Table 2.1. Similar values were calculated for CH12.LX and CH31 cells suggesting immature and mature B cells are equally sensitive to trichothecene induced cell death (summarized in Table 3.4).

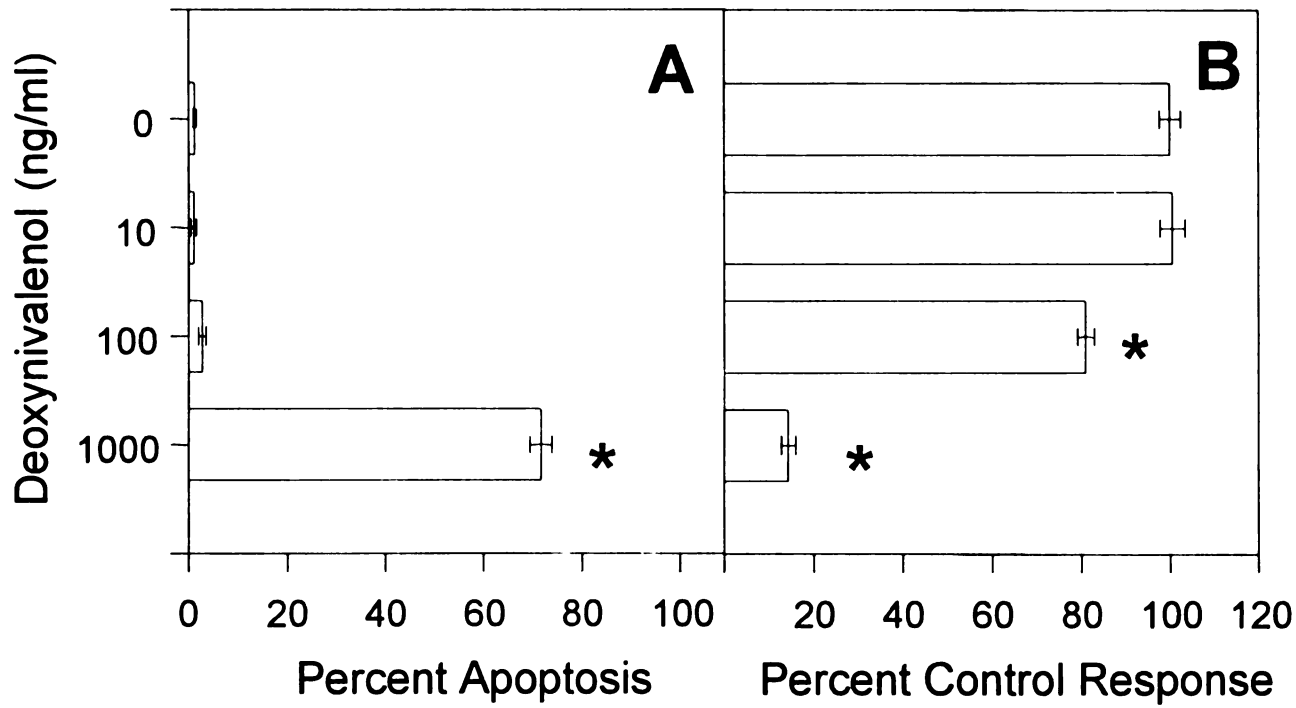

Figure 2.2 Deoxynivalenol (DON, Vomitoxin,)-induced apoptosis and cytotoxicity in immature and mature murine B cells. Murine WEHI-231 B cells (5 X 10^5/ml) were exposed to DON for 18 h prior to determination of apoptosis (A) and cytotoxicity (B) as described. Asterisks indicate values significantly different from the vehicle control ($p < 0.05$). CH31 and CH12.LX apoptosis and cytotoxicity were similarly affected.

Table 2.1. The effective dose (ED_{50}, ng/ml) resulting in 50% apoptosis and cytotoxicity in WEHI-231 immature B cells exposed to several Type A, Type B, and Type D trichothecenes.

Trichothecene	Apoptosis (ED_{50})	Cytotoxicity (ED_{50})
Type A		
T-2 Toxin	2.0	0.8
HT-2 Toxin	6.5	2.75
Diacetoxyscirpenol	4.0	4.0
Acetyl T-2 Toxin	70	55
T-2 Tetraol	>1000	40
T-2 Triol	>1000	45
3'OH T-2 Toxin	250	10
3'OH HT-2 Toxin	1000	50
Neosolaniol	100	70
Isotrichodermol	800	650
Isotrichodermin	4000	700
3'15 Didecalonectrin	4500	1500
Verrucarol	>10000	>10000
Type B		
Deoxynivalenol	500	300
Fusarenon X	400	200
Nivalenol	475	400
15 AcDeoxynivalenol	500	300
3 AcDeoxynivalenol	>10000	5000
4, 15 DiAcNivalenol	550	100
Type D		
Verrucarin A	0.4	0.35
Satratoxin G	2.0	0.5
Satratoxin H	9.0	3.75
Isosatratoxin F	3.0	2
Roridin A	0.4	0.35

Trichothecenes demonstrated a characteristic rank toxicity in which Type D > Type A > Type B (Table 2.1). Exceptions occurred when parent compounds, such as T-2 toxin, were compared to a less toxic form, such as T-2 tetraol and T-2 triol. Cytotoxicity values reported are similar to values previously reported for this group of translational inhibitors (Ueno, 1983). ED_{50} values derived for cytotoxicity were generally lower than values calculated for apoptosis. This suggests inhibition of MTT conversion may be indicative of an earlier stage of apoptosis or cell growth inhibition without development of a distinct apoptotic morphology by 18 h. No significant increase in necrotic cells was noted by fluorescence microscopy. Differences in apoptotic and cytotoxic values were not observed in CH31 or CH12.LX cell lines (Table 3.4) suggesting this may be a cell line specific effect.

Differential Induction of cytotoxicity and apoptosis by shiga like toxin 1 (SLT1)

SLT1 is a bacterial toxin composed of two subunits. The B subunit binds to surface glycolipids and the A subunit cleaves ribosomes and inhibits protein synthesis. The induction of apoptosis by SLT1 has been reported in several cell types and may contribute to the development of HUS (Pijpers et al., 2001; Nakao and Takeda, 2000; Kodama et al., 1999). Induction of cytotoxicity and apoptosis by SLT1 was evaluated in murine B cells at 18 h (Figure 2.3). The ED_{50} value for CH12.LX cytotoxicity, determined by MTT conversion assay, was 7 ng/ml. The dose resulting in 50% apoptosis, measured using fluorescence microscopy, was 3 ng/ml. CH31 and WEHI-231 immature B cell viability were not significantly altered when treated with SLT1 concentrations up to 100 ng/ml.

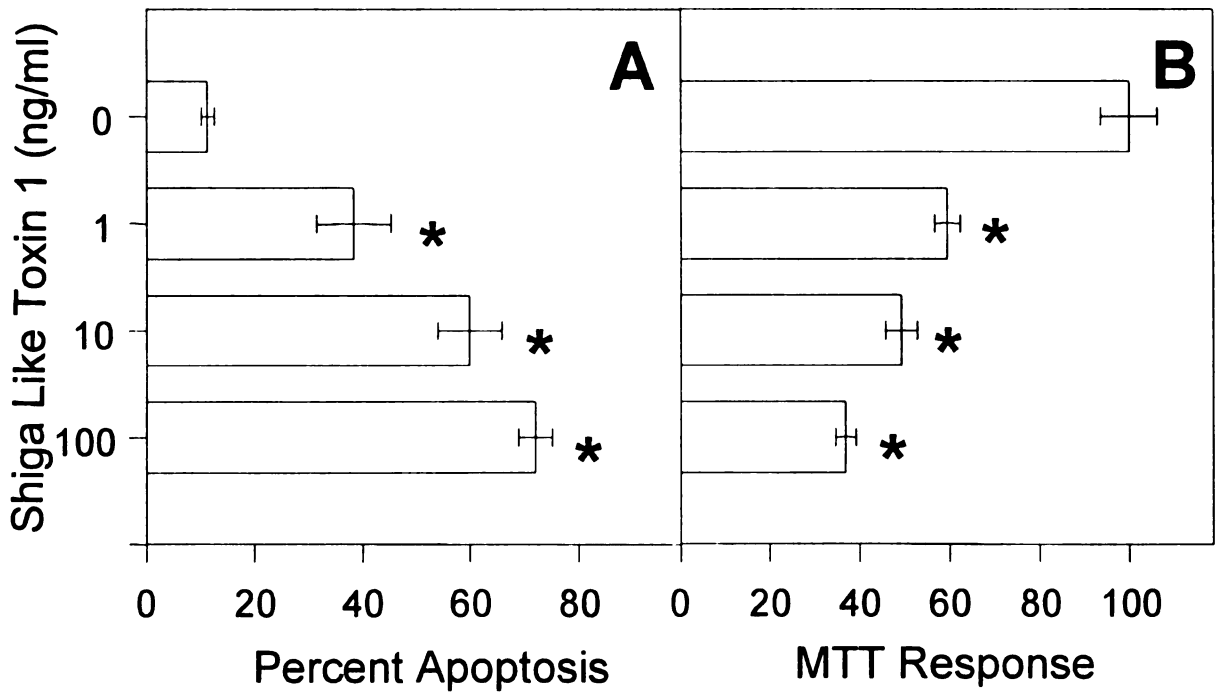

Figure 2.3. Shiga Like Toxin 1 (SLT1)-induced apoptosis and cytotoxicity in mature murine B cells. Murine CH12.LX B cells (5 X 10^5/ml) were exposed to SLT1 for 18 h prior to determination of apoptosis (A) and cytotoxicity (B) as described. Asterisk indicates values significantly different from vehicle control. Apoptosis and cytotoxicity were not affected in CH31 and WEHI-231 cell lines.

Differential sensitivity in B cell subpopulations to SLT1-induced cell death has been observed in human B cells. Cohen et al. (1990) observed most IgG- and IgA-committed subsets were sensitive to SLT1-induced cell death while IgM- and IgD-committed subsets were resistant. In contrast, we demonstrated sensitivity of IgM expressing CH12.LX cells to SLT1-induced apoptosis. This differential sensitivity may relate to glycolipid expression differences on cell surfaces rather than Ig expression. Relatedly, Daudi cells are resistant to SLT1 toxic effects due to deficient levels of SLT glycolipid receptor Gb3/CD77 (Cohen et al., 1990) while renal tissue expresses the highest levels of Gb3/CD77 thereby accounting for the high sensitivity of these cells to SLT (Lingwood, 1996). It is possible that CH12.LX cells may express higher levels of Gb3/CD77 than other IgM+ B cell subsets and explain the sensitivity of this cell line. However, to our knowledge, cell surface expression of Gb3/CD77 on CH12.LX cells has not been reported. SLT1 uptake by a cell appears to be an early critical step in apoptosis induction.

Interestingly, surface binding of SLT1 may initiate apoptosis independent of ribosomal cleavage. The sequence of CD19 is similar to shiga B chain and binds to the Gb3/CD77 receptor. The CD19-Gb3/CD77 complex is endocytosed and leads to the induction of apoptosis in the absence of ribosomal cleavage (Sandvig and vanDeurs, 2000). Mori et al. (2000) demonstrated that surface receptor binding in this pathway leads to Gb3/CD77-IgM clustering, cross-linking, and activation of the antigen receptor ligation mediated apoptosis pathway.

Differential Induction of cytotoxicity and apoptosis by ricin

Similar to SLT1, ricin, a plant toxin, is composed of two subunits. The B subunit

binds to glycolipids or glycoproteins present in the cell membrane while the A subunit cleaves ribosomal RNA to inhibit protein synthesis. One molecule of ricin has been estimated to inactivate approximately 2000 ribosomes per minute (Sandvig and vanDeurs, 2000). Induction of cytotoxicity and apoptosis by ricin was evaluated at 18 h (Figure 2.4). ED_{50} values derived using the MTT conversion assay were 3.0, 0.05, and 4.0 μg/ml for CH31, CH12.LX, and WEHI-231 cells, respectively. Apoptotic morphology was assessed by fluorescence microscopy. ED_{50} values for apoptosis induction in CH31, CH12.LX, and WEHI-231 cells were 2.25, 0.03, and 4.0 μg/ml, respectively. These results suggest mature B cells were more sensitive to ricin-induced cell death than immature B cells. As with SLT1, the differential sensitivity to ricin may result from differences in glycolipid or glycoprotein expression that influence cellular uptake of ricin. Similar ED_{50} values for apoptosis and cytotoxicity were calculated for each individual cell line suggesting cell death was primarily due to apoptosis. A previous study evaluating ricin-induced cell death reported approximately 60% death in MDA-231 cells following exposure to 250 pg/ml (Geier et al., 1996). This difference in dose may reflect differences in cellular uptake of ricin which would be critical to the induction of cell death.

SUMMARY

Trichothecenes, SLT, and ricin, natural toxins encountered in food and the environment, pose a health risk to humans and animals. Upon exposure, these toxins induce a ribotoxic stress response which may ultimately lead to apoptosis induction. This study compared induction of cytotoxicity and apoptosis by the aforementioned natural toxins to CHX, a translational inhibitor commonly used to study cell signaling events.

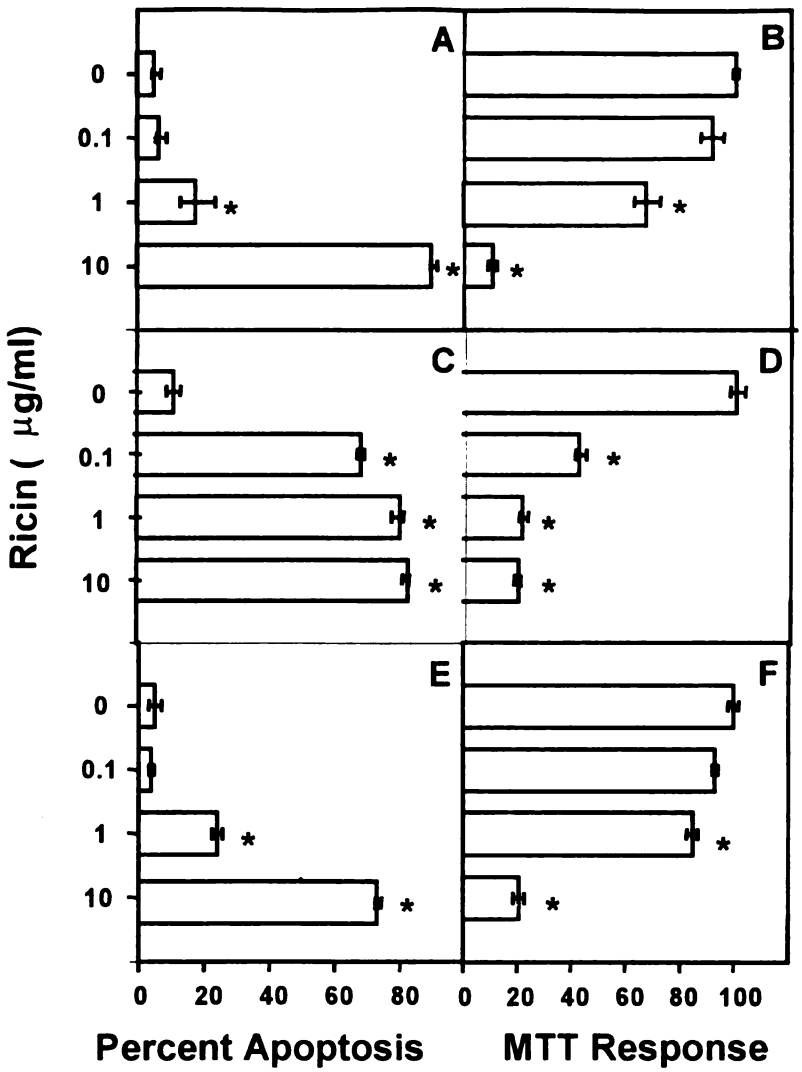

Figure 2.4. Ricin-induced apoptosis and cytotoxicity in immature and mature murine B cells. Murine CH31 (A, B), CH12.LX (C, D) and WEHI-231 (E, F) B cells (5 X 10^5/ml) were exposed to ricin for 18 h prior to determination of apoptosis (A, C, and E) and cytotoxicity (B, D, and F) as described. Asterisk indicates values significantly different from vehicle controls ($p < 0.05$).

These results suggest lymphocytes of the immune system were particularly sensitive to the toxic effects of translational inhibitors. Comparisons among the translational inhibitors tested suggest Type D and Type A trichothecenes, ricin, and SLT1 were more potent inducers of apoptosis than CHX (Table 2.2). Type B, and Type A trichothecene metabolites were less potent inducers of apoptosis when compared to CHX in this immunotoxicity model. CHX and the trichothecenes tested demonstrated non-preferential induction of cytotoxicity and apoptosis in immature or mature B cells suggesting toxic effects of these natural toxins may be non-specific upon exposure. However, mature B cells were more sensitive to ricin and SLT1-induced cytotoxicity and apoptosis than immature B cells. This differential sensitivity may be due to glycolipid and glycoprotein cell membrane expression which would result in variable cellular uptake. Taken together, these data may be critical to identification and treatment following accidental or deliberate exposure to the trichothecenes, SLT1 or ricin. Up-regulation of apoptosis in B lymphocytes may contribute to the impairment of the immune response and other symptoms described following exposure to these naturally occurring translational inhibitors.

Table 2.2. Translational inhibitor dose (molarity) required to induce 50% apoptosis in murine B cell lines.

Translational Inhibitor	Apoptosis (ED_{50})
Type D Trichothecenes	1 – 16 nM
Type A Trichothecenes	5 – 10 nM
Shiga Like Toxin 1	10 nM
Ricin	1 – 100 nM
Cycloheximide	0.5 μM
Type A Trichothecene Metabolites	0.5 – 50 μM
Type B Trichothecenes	1 – 2 μM

CHAPTER 3

Induction of B Cell Cytotoxicity and Apoptosis by Environmental and Food-borne Trichothecenes: Quantitative Structure Activity Relationships

INTRODUCTION

Trichothecene mycotoxins are naturally occurring environmental contaminants produced by molds common in the air and soil. These fungal metabolites are characterized by a tetracyclic scirpenol ring system (Figure 1.1) and categorized into four subtypes based on the presence or absence of specific functional groups (Ueno, 1983). Three of these subtypes, Type A, B, and D, pose the greatest health risk to humans and animals and therefore, are the focus of this study. Type A trichothecenes are characterized by a hydroxy or acyl moiety at R_1, R_2, R_3, or R_5 position(s) (Table 1.2). Type B trichothecenes possess a carbonyl at R_5 in addition to the Type A moieties. Type D (macrocyclic) trichothecenes contain a diester or triester ring system at the R_2 and R_3 positions (Figure 1.2) (Snyder, 1986).

Historically, outbreaks of human and animal disease have been linked to trichothecene- producing molds such as *Fusarium*, associated with production of Type A and B toxins, and *Stachybotrys*, associated with production of Type D toxins (reviewed by Bamburg, 1968). Alimentary toxic aleukia in the Soviet Union and red mold disease in Japan were linked to human consumption of *Fusarium* contaminated grains. Outbreaks of stachybotryotoxicosis in horses, sheep, and cattle have been associated with consumption of *Stachybotrys*-infested hay and straw. Moldy corn toxicosis has been

recorded in pigs and cattle in the Midwestern United States and linked to *Fusarium* growth.

Between 1960 - 1991, 53 outbreaks of human food poisoning associated with moldy cereal occurred throughout China (Li et al., 1999). Trichothecene levels were recently determined in samples from a food poisoning outbreak in Anhui, China in 1991 (Li et al., 1999). Moldy cereal samples contained up to 51.4, 6.9, 2.5, and 2.5 mg/kg deoxynivalenol (DON), nivalenol (NIV), 3-acetyl-DON, and 15-acetyl-DON, respectively. Approximately 130,000 people were affected by gastrointestinal disorders including nausea and vomiting. In addition, T-2 toxin was detected at concentrations up to 420 μg/kg in moldy rice implicated in a food-borne outbreak in Zhejiang, China (Wang et al., 1993a). Trichothecene levels have not always been determined in the above mentioned outbreaks due to unsuitable diagnostic methods or lack of samples (Bamburg, 1972). However, Type A (T-2 toxin) and Type B toxins (DON and NIV) are routinely detected in raw agricultural products as well as commercial grain based foods intended for human consumption (Scott, 1997; WHO, 1990; Abouzied et al., 1991).

Recent attention has focused on the contribution of molds to indoor air illness and specifically, the role of trichothecene-producing molds in indoor environments. Both *Fusarium* and *Stachybotrys* isolates have been collected from ventilation systems of homes of allergen sensitized children (Wickman et al., 1992). *Stachybotrys* has been found in water damaged homes, schools, and public buildings where the occupants have reported building-related respiratory disease (reviewed by Mahmoudi and Gershwin, 2000). Thirty-four cases of infant pulmonary hemorrhage were reported and linked to water damaged homes containing *Stachybotrys* in Cleveland, OH (Dearborn et al., 1999). Type A (T-2 toxin, HT-2 toxin, and diacetoxyscirpenol) and Type D (satratoxins and

verrucarins) trichothecenes have been identified in indoor air samples in which respiratory disease has been reported (Smoragiewicz et al., 1993; Johanning et al., 1996; Tuomi et al., 1998; Malmoudi and Gershwin, 2000). *Stachybotrys* was isolated from the bronchoalveolar lavage fluid of one infant with pulmonary hemosideriosis but the involvement of Type D trichothecenes was not determined (Elidemir et al., 1999).

Trichothecenes also have the potential to be used as chemical warfare agents and are believed to exist in the arsenals of some countries (McGovern et al., 1999; Heyndrickx et al., 1984; Zilinskas, 1997). The ability to predict toxicity of trichothecenes would be of paramount importance to military medical personnel and public health officials encountering these agents during military or terrorist attack.

Symptoms described in food-borne outbreaks (nausea, vomiting, diarrhea, and leukopenia) and reported for suspected inhalation (respiratory tract irritation, fatigue, dermatitis, impaired immune function, and nasal hemorrhage) mimic symptoms of experimental animals exposed to trichothecene mycotoxins (Bondy and Pestka, 2000; Nikulin et al., 1997; Nikulin et al., 1996). The primary target, both in vivo and in vitro, of all trichothecenes is the 60S ribosomal subunit.

Ribosomal binding by trichothecenes occurs rapidly and blocks protein synthesis in actively dividing immune cells in the bone marrow, spleen, thymus, and lymph nodes (Ueno, 1983). Exposure to trichothecenes leads to alteration of immune cell function, dysregulation of the humoral immune response, and impairment of host resistance to pathogens (reviewed by Bondy and Pestka, 2000). Direct cytotoxicity (Hanelt et al., 1994; Anderson et al., 1989; Yike et al., 1999) and induction of apoptosis (Yang et al., 2000; Okumura et al., 2000; Shifrin and Anderson, 1999) are widely reported for this group of compounds and likely to contribute to these immunotoxic effects. A general

rank order of toxicity is observed in which Type D > Type A > Type B (Ueno, 1983) suggesting that the functional groups on the scirpenol ring system contribute greatly to the biological action of this group of mycotoxins. Although the trichothecene family contains 182 structurally related metabolites (Grove, 1993; 1996), the toxicity has been well-characterized for only a few compounds. Recently, a joint committee on food additives organized by the Food and Agriculture Organization of the United Nations and World Health Organization recommended the development of DON equivalency factors to assess human risk from trichothecene exposure (FAO/WHO, 2001).

Quantitative structure activity relationship (QSAR) analysis may contribute to our ability to understand trichothecene mechanism of action. QSAR links biological properties of a chemical to its molecular structure (Barratt, 1998a). Consequently, a hypothesis can be proposed to identify the physical or chemical parameters which are crucial to the structure activity relationship of a group of chemicals. QSAR analysis is commonly used to predict the toxic action of chemicals (Benigni and Andreoli, 1993; Purdy, 1996; Kulkarni et al., 2002), to predict receptor binding (Tong et al., 1997) or to address mechanisms involved in a toxic endpoint (Lopez de Compadre, 1990). Trichothecenes possess the structural similarity and the common mechanism of action (in vivo and in vitro) necessary to develop a robust model (Barratt, 1998b). Such a model can ultimately be used to predict the toxicity of untested trichothecenes. The goal of this project was to apply QSAR using principal component analysis to identify the physico-chemical characteristics which clearly separate the trichothecene mycotoxins into subtypes (Type A, B, and D) and gain insight into trichothecene mechanisms of action.

MODEL DESIGN AND RATIONALE

Three dimensional trichothecene structures were drawn and analyzed using Chem 3D version 4.0 (CambridgeSoft, Cambridge, MA) and Cache (Oxford Molecular Group Inc., Beaverton, OR). Briefly, the dihedral driver was used to identify and access conformational space. Allinger's molecular mechanics (MM2) force field parameters were used to describe the energy of each molecule. The resultant stable conformation with the lowest energy was selected following each pass. The geometry was re-optimized and semi-empirical Austin Model 1 (AM1) calculations were implemented using the closed shell wave function for the final optimization of each trichothecene structure. Structures were systematically aligned and 34 physical and chemical properties were calculated using Molecular Modeling Pro version 2.4 (WindowChem Software Inc., Fairfield, CA; Table 3.1).

Variables were selected for further analysis based on (1) statistical correlation between variables and (2) the relation of each variable to uptake, transport, and reactivity properties relevant to biological activity. Several variables were highly correlated (Pearson correlation, $p < 0.05$ (data not shown)) likely due to the similarities in variable calculation. Eight variables were selected for further analysis (Table 3.2). Hansen solubility parameter (SOL) and hydrophilic-lipophilic balance (HLB) are indicators of membrane penetration or uptake of the molecule. Hansch Log P (Log P), Crippen Log P (CRIP), and CNDO Log P (CNDO) are measurements of lipophilicity which influences transportation of a molecule to the site of action. Kier connectivity index (KIER) is an indicator of molecular size and shape and can reflect binding at the site of action. Highest Occupied Molecular Orbital (HOMO) and Lowest Unoccupied Molecular

Table 3.1 Physical and chemical properties generated for the trichothecene mycotoxins.

CNDO Log P[a]	**Crippen's Log P**
Density	Dipole Moment
Hansch Log P	Hansen Dispersion
Hansen Hydrogen Bonding	Hansen Polarity
Hansen Solubility Parameter	**Highest Occupied Molecular Orbital**
Hydrogen Bond Acceptor	Hydrogen Bond Donor
Hydrophilic Lipophilic Balance	Hydrophilic Surface
Kier Connectivity 0	Kier Connectivity 1
Kier Connectivity 2	Kier Connectivity 3
Kier Connectivity Index 4	Kier Shape Index Kappa 1
Lowest Unoccupied Molecular Orbital	Molecular Depth
Molecular Length	Molecular Volume
Molecular Weight	Molecular Width
Surface Area	Valence 0
Valence 1	Valence 2
Valence 3	Valence Index 4
Water of Hydration	Water Solubility

[a]Properties in bold type were selected for further analysis.

Table 3.2. Physical and chemical descriptor values selected for principal component analysis.

Trichothecene[a]	SOL[b]	HLB[c]	LogP[d]	CRIP[e]	CNDO[f]	Kier[g]	HOMO[h]	LUMO[i]
A1	18.065	13.641	3.103	0.846	6.724	11.601	-0.396	0.145
A2	19.381	13.815	0.457	0.716	5.965	10.879	-0.404	0.124
A3	17.035	15.076	0.943	0.275	5.037	9.773	-0.402	0.136
A4	24.222	14.599	2.118	0.975	7.699	12.203	-0.416	0.137
A5	26.172	12.680	-1.709	-0.897	3.012	8.980	-0.405	0.137
A6	20.264	13.187	-0.449	0.587	4.779	10.567	-0.396	0.143
A7	22.012	14.433	1.152	1.248	5.918	12.020	-0.436	0.131
A8	18.753	14.039	0.993	1.118	4.931	11.237	-0.437	0.129
A9	17.474	13.655	2.827	0.275	5.107	9.773	-0.392	0.136
A10	21.427	8.955	1.385	1.444	3.871	7.752	-0.421	0.135
A11	18.306	11.226	2.511	1.573	4.740	8.389	-0.435	0.144
A12	25.345	13.727	-0.427	-0.363	2.615	8.167	-0.412	0.119
A13	22.054	12.400	-0.602	0.441	3.561	8.329	-0.407	0.132
B1	24.600	16.077	-3.488	-0.050	3.181	9.323	-0.422	0.070
B2	23.169	16.663	-3.845	-0.545	3.839	10.428	-0.414	0.081
B3	26.716	16.407	-4.448	-0.674	2.974	9.700	-0.425	0.069
B4	21.789	16.386	-2.582	0.079	4.077	9.557	-0.418	0.079
B5	22.992	16.386	-2.335	0.079	3.988	9.923	-0.411	0.075
B6	21.953	16.864	-3.469	-0.416	4.727	10.669	-0.421	0.078
D1	20.779	13.699	3.161	1.966	7.453	12.259	-0.408	0.027
D2	22.249	14.223	1.757	0.382	7.260	15.890	-0.415	0.047
D3	21.688	13.593	1.349	1.050	7.440	14.272	-0.416	0.056
D4	19.634	14.464	1.431	0.750	7.706	15.890	-0.420	0.048
D5	20.406	13.001	2.067	2.144	7.772	12.753	-0.404	0.061

[a]Abbreviations as described in Table 1.1 and Fig 1.2.
[b]Hansen Solubility Parameter
[c]Hydrophilic Lipophilic Balance
[d]Hansch Log P
[e]Crippen Log P
[f]CNDO Log P
[g]Kier Connectivity Index
[h]Highest Occupied Molecular Orbital
[i]Lowest Unoccupied Molecular Orbital

Orbital (LUMO) are indicators of electrophilic interactions and the ability of a molecule to donate or accept electrons, respectively. HOMO and LUMO may be indicators of specific binding at the site of action (Mekenyan and Veith, 1993). These variables were again tested for collinearity using Gittins condition number (data not shown) (Gittins, 1985).

BIOLOGICAL TESTING

Relative toxicity of 24 trichothecene mycotoxins was determined using induction of cell death by apoptosis or cytotoxicity in several cloned murine B cell lines as follows:

Cell lines and culture

70Z/3 cells, phenotypically pre-B lymphoblasts, were obtained from Dr. Richard Schwartz (Michigan State University, E. Lansing, MI). CH31 cells, phenotypically immature B cells, were obtained from Dr. David Scott (American Red Cross Holland Laboratory, Rockville, MD). CH12.LX cells, phenotypically mature B cells, were obtained from Dr. Geoffrey Haughton (University of North Carolina, Chapel Hill, NC). Cell number and viability were assessed microscopically by trypan blue dye exclusion using a hemocytometer (Stiles, 1986). Cell culture media and chemicals were purchased from Sigma Chemical Company (St. Louis, MO) unless otherwise noted. Cells were cultured at a concentration of 5 x 10^5/ml in 200 µl/well in 96 well flat bottom plates at 37°C in a 5% CO_2 humidified incubator. Cells were grown in RPMI-1640 medium supplemented with 100 U/ml penicillin, 100 µg/ml streptomycin, 50µM 2-mercaptoethanol, 2 mM glutamine, 1 mM sodium pyruvate (Gibco Life Technologies,

Rockville, MD), and 1 mM non-essential amino acids (Gibco). CH31 and CH12.LX media was supplemented with 5% (v/v) heat-inactivated fetal bovine serum (FBS, Gibco). 70Z/3 media was supplemented with 10% (v/v) FBS.

Trichothecenes

Satratoxin G, satratoxin F, and satratoxin H were obtained from Dr. Bruce Jarvis (University of Maryland, College Park, MD). 3'OH metabolites were produced by the procedure of Yoshizawa et al. (1981;1984). All other trichothecenes were purchased from Sigma. Toxins were dissolved in 100% ethanol and diluted in RPMI-1640. Final ethanol concentration in the culture medium was less than 0.01% (v/v) which did not induce apoptosis or cytotoxicity. Triplicate cultures were treated with toxin in 10-fold dilutions or RPMI-1640 (control) for 18 h.

MTT conversion assay for cytotoxicity

Following trichothecene treatment, 20 µl of a 5 mg/ml solution of 3- (4,5 dimethylthiazol-2-ul)-2,5-diphenyl tetrazolium bromide (MTT, Sigma) in 0.01 M PBS was added to each well for the final 2 h of the 18 h incubation period (Marin, et al., 1996). Microtiter plates were centrifuged at 450 x g for 20 min and media were aspirated to minimize formazan crystal loss. The resultant crystals were dissolved in 150 µl dimethylsulfoxide for 15 min. Optical density was measured using a Vmax Microplate Reader (Molecular Devices, Menlo Park, CA) at dual wavelengths, 570 nm and 690 nm. Percent MTT inhibition was calculated as follows: ((1 - absorbance of treatment)/ absorbance of control) x 100. Mean values were used to graphically determine ED_{50} values.

Apoptosis assay

Apoptotic cells were quantitated by fluorescence microscopy as described by Duke and Cohen (1995). Briefly, following trichothecene treatment, microtiter plates were centrifuged at 450 x g for 10 min and 150 µl of supernatant was removed. Five µl of DNA staining reagent (acridine orange (100 µg/ml) and ethidium bromide (100 µg/ml) in 0.01 M phosphate buffered saline (PBS)) was added to each well. Cells were classified as apoptotic or normal based on chromatin organization. Briefly, a normal nucleus appears large with an organized structure while an apoptotic nucleus appears small and highly condensed or fragmented. Percent apoptosis was calculated as follows: number of cells with apoptotic nuclei/total cell number x 100. Mean values were used to graphically determine the effective dose causing 50% apoptosis (ED_{50}).

Statistical analysis

Modeled physico-chemical parameters were compared between trichothecene subgroups using a one-way analysis of variance (ANOVA) and a Tukey test for mean separation. Pearson correlation was used to identify correlations between each physico-chemical parameter and apoptosis or cytotoxicity using Systat, version 5.0 (Evanston, IL). The ability of these parameters and toxicity to differentiate between trichothecene subgroups was assessed using principal components analysis (PCA). All data sets were tested for multivariate normality and log transformations were used as needed. Characteristics of the trichothecenes which acted as surrogates for toxicity were then identified. PCA was performed using Statistical Analysis Software (SAS) version 6.12.

RESULTS

Trichothecene physical and chemical descriptors

Physical and chemical variables calculated using Molecular Modeling Pro version 2.4 were compared between trichothecene subgroups (Table 3.3). Type B trichothecene HLB measurements (16.46 ± 0.11) were significantly higher ($p<0.01$) than both Type A (13.19 ± 0.45) and Type D (13.80 ± 0.26) subgroups while Log P calculations (-3.36 ± 0.32) were significantly lower ($p<0.01$). Mean Log P values for Type A and Type D were 0.946 ± 0.41 and 1.953 ± 0.33, respectively. CRIP measurements of Type B toxins (-0.255 ± 0.14) were also significantly lower ($p<0.01$) than both Type A (0.634 ± 0.20) and Type D (1.258 ± 0.34). CNDO and KIER measurements of Type D trichothecenes (7.526 ± 0.09 and 14.213 ± 0.76, respectively) were significantly higher ($p<0.01$) than both Type A (4.920 ± 0.40 and 9.975 ± 0.43, respectively) and Type B (3.80 ± 0.26 and 9.933 ± 0.21) values. LUMO values for Type A (0.134 ± 0.002), Type B (0.076 ± 0.002), and Type D (0.048 ± 0.006) trichothecenes were all significantly different from each other ($p<0.01$). No significant differences were noted between subgroups for SOL and HOMO calculations. These data suggest: (1) one subgroup can be separated from the remaining groups on the basis of lipophilicity (Log P, CRIP, CNDO) (2) molecular branching is greater in Type D than Type A and B toxins (KIER) and (3) trichothecene subgroups exhibit a broad range of ability to accept electrons (LUMO).

Trichothecene-induced B cell apoptosis and cytotoxicity

Previous studies suggest that germinal centers of the spleen and Peyer's patch are sensitive to DON-induced apoptosis, thus B cells are highly susceptible (Zhou et al.,

Table 3.3. Effective dose (ED_{50}, ng/ml) resulting in 50% apoptosis or cytotoxicity in three murine B cell lines following 18 h trichothecene mycotoxin exposure.

	70Z/3		CH31		CH12.LX	
	Apoptosis	Cytotoxicity	Apoptosis	Cytotoxicity	Apoptosis	Cytotoxicity
Trichothecene[a]						
A1	4.5	0.6	2.0	1.5	3.0	2.5
A2	8.0	3.0	3.5	3.0	3.5	3.5
A3	40	40	20	25	30	20
A4	400	250	400	500	350	250
A5	400	150	250	200	350	150
A6	25	30	20	25	10	10
A7	150	45	15	30	70	20
A8	3.5	2.5	3.25	3.0	3.5	3.5
A9	45	25	30	50	35	25
A10	500	200	400	350	350	350
A11	400	100	250	250	50	30
A12	600	300	500	550	350	300
A13	>10000	>10000	>10000	>10000	>10000	>10000
B1	400	90	400	225	400	250
B2	450	200	450	250	400	325
B3	375	275	450	350	400	325
B4	550	125	450	225	400	375
B5	>10000	2000	3000	5000	4000	3500
B6	60	30	40	40	40	40
D1	1.5	0.85	0.4	0.35	2.0	3.25
D2	3.0	4.25	2.75	3.25	2.0	4.0
D3	0.5	0.7	0.35	0.3	1.0	1.25
D4	3.0	5.75	2.5	2.75	3.0	2.75
D5	4.0	3.0	0.4	0.35	3.25	3.0

[a]Trichothecene abbreviations as described in Table 1.1 and Fig. 1.2. Results are representative of duplicate experiments (n=6).

2000). Induction of apoptosis or general cytotoxicity was assessed for 24 trichothecenes in three B lymphocyte cell lines representing three distinct lineages. The cell lines tested represent pre-B (70Z/3), immature (CH31), and mature (CH12.LX). Of these lineages, the immature B cell is the most susceptible to apoptosis (Carsetti, 1995; Garvy, 1993). The effective doses resulting in 50% apoptosis or cytotoxicity (ED_{50}) were graphically determined for these cell lines and these data are summarized in Table 3.4.

Apoptosis and cytotoxicity exhibited a general rank toxicity in which Type D > Type A > Type B. Exceptions to this rank toxicity occurred when considering the metabolized forms of the parent compounds. For example, subsequent reductions in ED_{50} values from 10 to 100-fold were observed when T-2 toxin was compared to several of its metabolites (Table 3.3). However, cytotoxicity values reported here are similar to values previously reported for this group of toxins (Ueno, 1983). ED_{50} values for apoptosis and cytotoxicity were similar suggesting that cell death was primarily due to apoptosis. ED_{50} values for apoptosis and cytotoxicity were similar in all three cell lines suggesting that the level of differentiation did not influence B cell susceptibility to trichothecene-induced cell death.

Pearson Correlation indicated that no significant ($p<0.05$) relationship existed between trichothecene-induced cell death and any single physical or chemical descriptor (data not shown). Interestingly, when toxicity values were log transformed to reduce the effect of outliers and to ensure the data approximated a normal distribution, significant correlations were observed with Log P, SOL, KIER, CNDO, and CRIP (Table 3.4). CNDO and KIER showed the strongest correlations with log transformed toxicity. The correlation with log transformed apoptosis was slightly higher than with log transformed

Table 3.4. Significant correlations observed between log transformed toxicity values and physico-chemical descriptors of the trichothecene mycotoxins.

	70Z/3		CH31		CH12.LX	
	Apoptosis	Cytotoxicity	Apoptosis	Cytotoxicity	Apoptosis	Cytotoxicity
Log P[a]						
r	-0.502	-0.496	-0.548	-0.510	-0.560	-0.571
p	0.012	0.014	0.006	0.016	0.014	0.011
SOL						
r	0.488	0.555	0.527	0.507	0.527	0.555
p	0.016	0.005	0.008	0.011	0.008	0.005
KIER						
r	-0.750	-0.690	-0.762	-0.751	-0.716	-0.681
p	0.001	0.001	0.001	0.001	0.001	0.001
CNDO						
r	-0.834	-0.786	-0.859	-0.844	-0.824	-0.805
p	0.001	0.001	0.001	0.001	0.001	0.001
CRIP						
r	0.440	0.416	0.503	0.488	0.493	0.509
p	0.032	0.043	0.012	0.016	0.014	0.011

[a]Physico-chemical abbreviations as described in Model Design and Rationale.

cytotoxicity for these descriptors. Multivariate techniques were used to simultaneously examine physico-chemical descriptor values and cell death by apoptosis or cytotoxicity.

Principal component analysis (PCA) of trichothecene-induced cell death

The effects of physicochemical parameters and the induction of apoptosis and cytotoxicity on separating trichothecene subtypes were assessed using PCA. Vector loadings of the first PC of each analysis indicated that Log P, CRIP, and CNDO weighted heavily in structuring both the 70Z/3 pre-B cell apoptosis (0.500, 0.462, and 0.463, respectively) and cytotoxicity (0.504, 0.469, and 0.439, respectively) data (Figures 3.1 A and 3.1 B). LUMO and KIER weighted heavily (-0.524 and 0.514, respectively) for the apoptosis and (-0.515 and 0.504, respectively) cytotoxicity data sets in the second PC in each analysis. Similarly, vector loadings of the first PC indicated that Log P, CRIP, and CNDO also weighted heavily in CH31 immature B cell apoptosis (0.500, 0.466, and 0.442, respectively) and cytotoxicity (0.499, 0.465, and 0.441, respectively) (Figures 3.2A and 3.2B). LUMO and KIER weighted heavily (-0.514 and 0.499, respectively) for the apoptosis and (-0.517 and 0.502, respectively) cytotoxicity data sets in the second PC in each analysis for CH31 cells. Finally, Log P, CRIP, and CNDO weighted heavily in the first PC of each analyses using CH12.LX mature B cell apoptosis (0.500, 0.465, and 0.440, respectively) and cytotoxicity (0.501, 0.466, and 0.440, respectively) (data not shown). Again, LUMO and KIER weighted heavily in the second PC, (-0.518 and 0.508, respectively) for the apoptosis and (-0.517 and 0.505, respectively) cytotoxicity data sets in each analysis. The combination of PC1 and PC2 explained more than 65% of the total variation of these data. When apoptosis and cytotoxicity were log transformed, results were similar. In each analysis of log

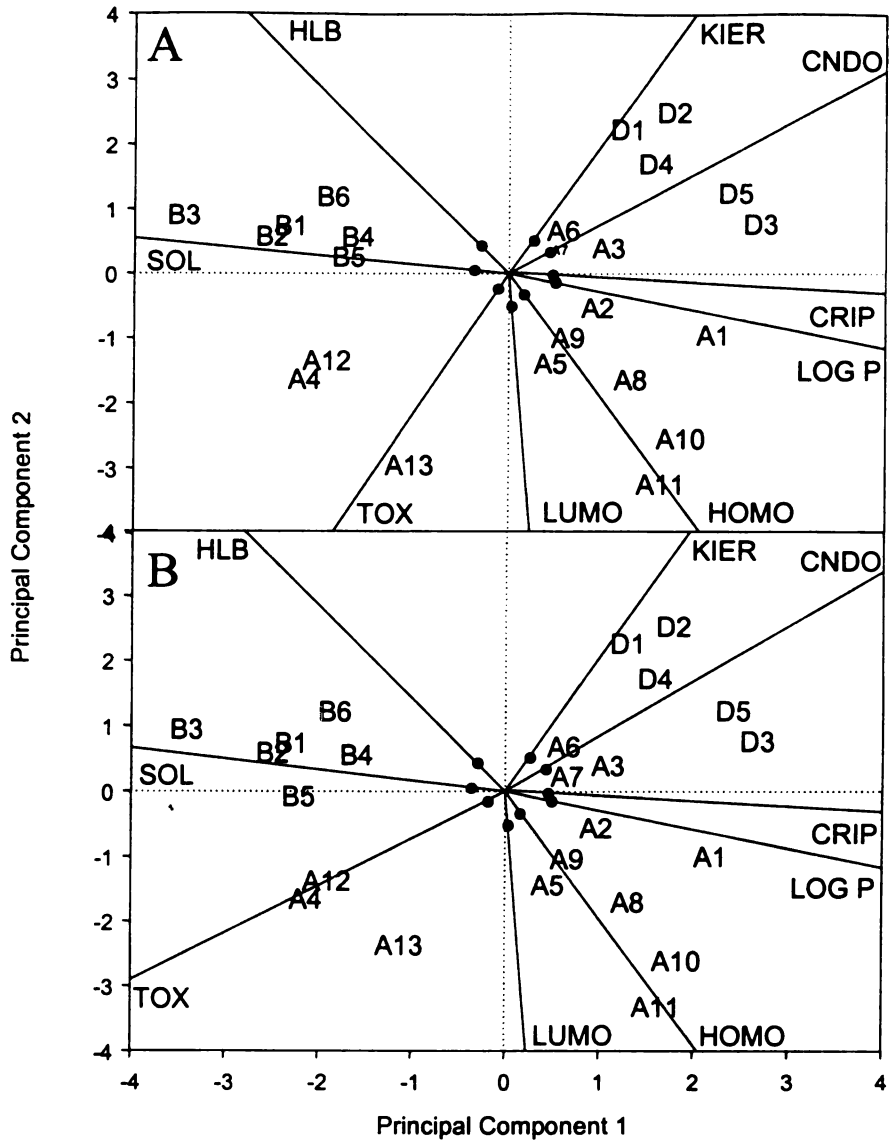

Figure 3.1. Principal component analysis (PCA) of 70Z/3 cytotoxicity (A) and apoptosis (B). PCA was performed on 8 physicochemical characteristics of the trichothecenes generated using molecular modeling and toxicity data. PC1 explained 37.7% and 38.3% while PC2 explained 27.6% and 27.0% of the variation in the cytotoxicity and apoptosis data sets respectively. Lipophilic values were weighted heavily in PC1, while LUMO weighted heavily in PC2 in each analysis. KIER and CNDO acted in conjunction with toxicity and could possibly serve as a measure of toxicity.

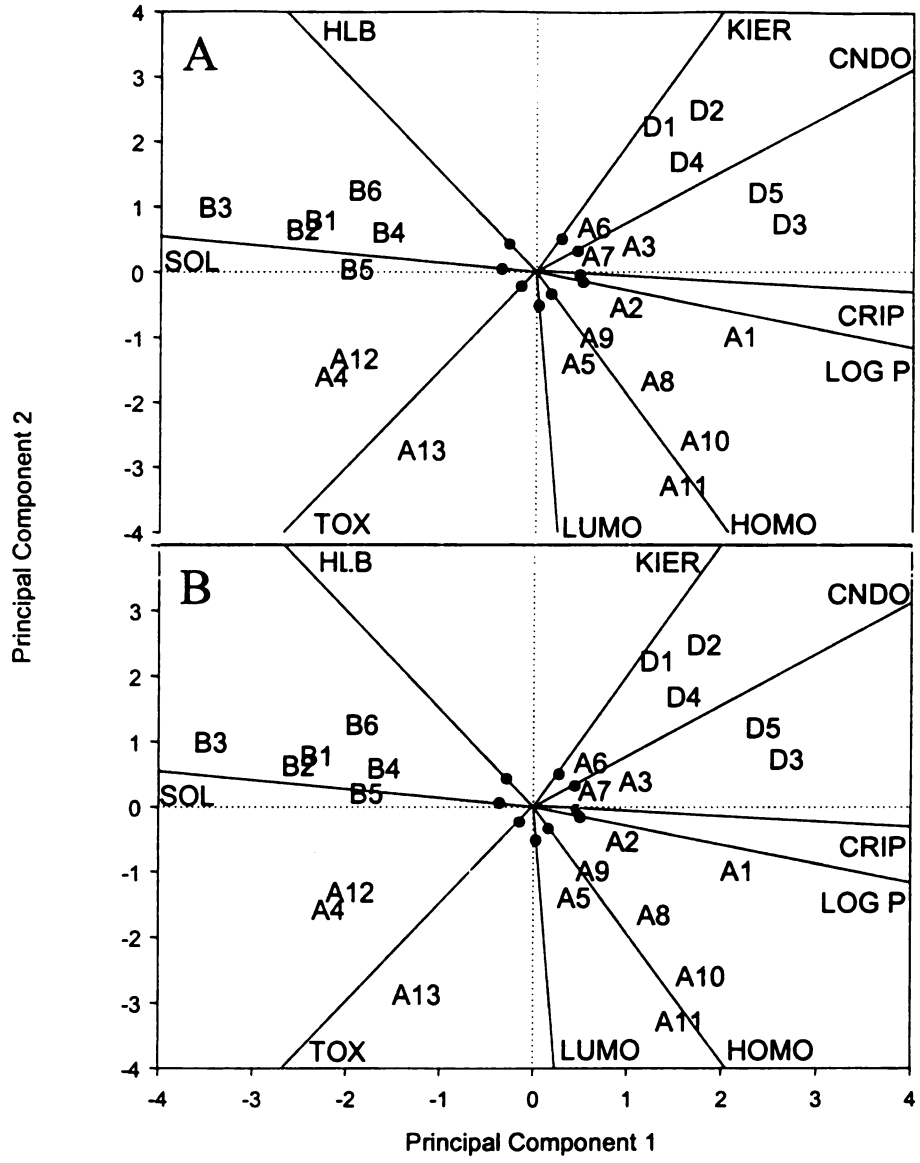

Figure 3.2. Principal component analysis (PCA) of CH31 cytotoxicity (A) and apoptosis (B). PCA was performed on 8 physicochemical characteristics of the trichothecenes generated using molecular modeling and toxicity data. PC1 explained 38.1% and 38.0% while PC2 explained 27.4% and 27.6% of the variation in the cytotoxicity and apoptosis data sets respectively. Lipophilic values were weighted heavily in PC1, while LUMO weighted heavily in PC2 in each analysis. KIER and CNDO acted in conjunction with toxicity and could possibly serve as a measure of toxicity.

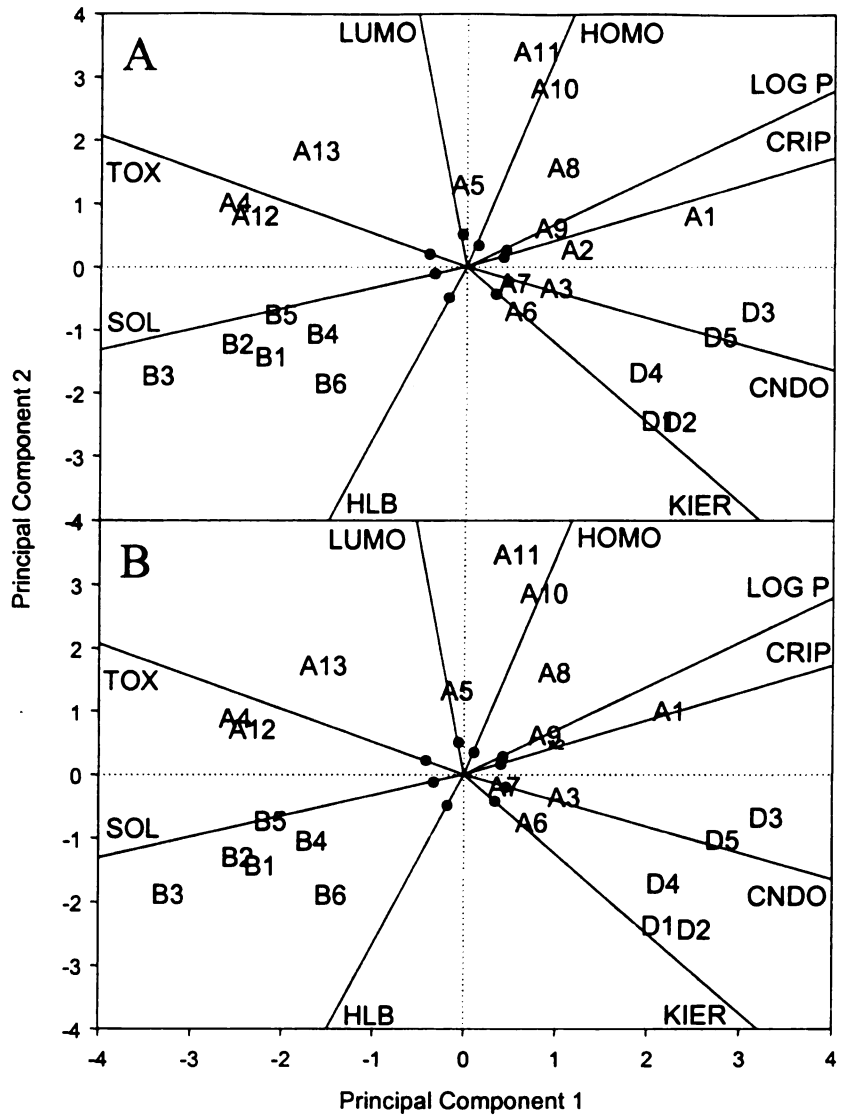

Figure 3.3. Principal component analysis (PCA) of 70Z/3 log transformed cytotoxicity (A) and apoptosis (B). PCA was performed on 8 physicochemical characteristics of the trichothecenes generated using molecular modeling and toxicity data. PC1 explained 43.3% and 43.6% while PC2 explained 28.2% and 28.6% of the variation in the cytotoxicity and apoptosis data sets respectively. Lipophilic values were weighted heavily in PC1, while LUMO weighted heavily in PC2 in each analysis. KIER and CNDO acted in conjunction with toxicity and could possibly serve as a measure of toxicity.

transformed apoptosis and cytotoxicity, CNDO and/or Log P weighted heavily in PC1 and LUMO weighted heavily in PC2 (Figures 3.3 A, 3.3 B, and data not shown). PC1 and PC2 combined always explained more than 72% of the variation in data sets using log transformed toxicity. Collectively, these results suggest that the trichothecenes exhibit a broad range of lipophilicity and LUMO binding values that, when combined, account for the major portion of the variation in the data set. Log P and LUMO can divide trichothecenes into clear subgroups without overlap, suggesting these two descriptors combined are good toxicity predictors for unknown trichothecenes.

Graphical display of PCA permitted a two-dimensional visualization of physicochemical descriptors in relation to toxicity. Thus, descriptors with the greatest influence on toxicity were identified based on the relationship of eigenvectors. Log P and LUMO played a major role in structuring these data sets and separating trichothecene subgroups, but had less influence on the toxic action of these compounds to 70Z/3 cells. However, KIER and CNDO acted in conjunction with apoptosis (Figures 3.1A, 3.3A) and cytotoxicity (Figures 3.1B, 3.3B) therefore potentially acting as surrogates in separating the data. Therefore, KIER and CNDO could possibly serve as predictors of toxicity. Similar relationships were noted for CH31 (Figures 3.2A and 3.2B) and CH12.LX cells (data not shown).

DISCUSSION

The worldwide occurrence and potential health hazard presented by the trichothecene mycotoxins requires an improved understanding of the mechanisms of toxic action of these compounds to facilitate risk assessment. The ability of

trichothecenes to inhibit protein synthesis and induce cell death of lymphocytes is central to the observed immunotoxicity (Ueno, 1983). A previous study indicated B lymphocytes in germinal centers of the spleen and Peyer's patch are particularly sensitive to trichothecene-induced apoptosis (Zhou, et. al 2000). Therefore, our model was designed using apoptosis and cytotoxicity of several B lymphocyte lineages as a measure of toxicity. To our knowledge, this is the first report of trichothecene-induced cell death in B lymphocytes and physico-chemical characteristics of individual trichothecene mycotoxins.

This study suggests that several factors may contribute to the apoptotic and cytotoxic actions of the trichothecenes. These compounds exhibit a broad range of lipophilicity, which correlated with log transformed toxicity. Therefore, when the data approached a normal distribution, toxicity increased with increasing lipophilicity. However, lipophilicity did not correlate with non-transformed data, indicating lipophilicity alone was not a good indicator of toxicity when outliers, or less toxic trichothecenes such as verrucarol and 3-Ac-DON, were included in the analysis. Lipophilicity was always weighted heavily in PC1 of each analysis, reinforcing that the trichothecenes exhibit a broad range of lipophilic values.

In a previous study addressing trichothecene structure-activity relationships Ramu et al. (1989) concluded that no clear correlation existed between toxicity and lipophilicity in the cytotoxic actions of several trichothecenes. In contrast, Grove and Mortimer (1969) demonstrated diminished cytotoxicity with decreased lipophilicity in a HEp2 cell model system. Both studies focused on Type A compounds and included less toxic outliers. Thompson and Wannemacher (1986) compared toxicity of 19 trichothecenes both in vitro and in vivo. In this study, the most potent trichothecenes possessed acetate

groups or hydrocarbon chains, which strongly influence lipid solubility. They suggest the variable potency of the trichothecenes is due to the rate of transport into the cell with other properties contributing to toxic action such as factors influencing ribosomal binding and protein synthesis inhibition.

LUMO was significantly different for all trichothecene subgroups but did not significantly correlate with toxicity data. In using PCA, LUMO always weighted heavily in PC2. The importance of LUMO in shaping the data set suggests that electrostatic interactions, specifically, the ability to accept electrons, may be important for the toxic action of these compounds. These data support previous studies which demonstrated that the C9-10 double bond and C12-13 epoxide, common to all trichothecenes, are necessary for biological activity (Wei and McLaughlin, 1974; Ehlrich and Daigle, 1987). The C9-10 double bond and C12-13 epoxide may be important for determining trichothecene conformation or may participate directly in binding to the ribosomes.

As LUMO values decrease, the binding affinity of a compound increases. Interestingly, trichothecene LUMO values suggest that Type D compounds have greater binding affinities than Type B compounds, which in turn, have greater binding affinities than Type A. Mekenyan and Veith (1993) observed an interdependence between LUMO and Log P in which compounds became more dependent on Log P with increasing LUMO values (decreased binding affinity). A similar relationship may apply to the trichothecenes. Type D compounds are very reactive and very lipophilic suggesting that they are efficiently transported to the ribosome and bind with a high affinity. Type A compounds are less reactive, but still relatively lipophilic indicating they are reaching the target site in sufficient quantities to bind to the ribosomes. As the Type A parent compounds are further metabolized, they become more soluble and may not reach the site

of action. Type B compounds are reactive, but very soluble suggesting less of the toxin reaches the target site but binds effectively when it does.

KIER values for the Type D trichothecenes were significantly higher than Type A and B values and demonstrated a significant ($p<0.05$) correlation with log transformed toxicity. KIER did not correlate with the non-transformed toxicity data suggesting KIER alone is not a good predictor of toxicity when outliers, or less toxic trichothecenes such as verrucarol and 3- Ac-DON, were included in the analysis. Trichothecenes can be divided into two groups based on the step of protein synthesis blocked. Wei and McLaughlin (1974) suggested functional group size may contribute to the ability of the toxin to block the initiation or elongation-termination step of protein synthesis. Bamburg (1968) noted that the elongation/termination inhibitors were unsubstituted or possessed only small substituents. Interestingly, KIER values for the initiation inhibitors previously characterized (Ueno, 1983) and modeled here ranged from 9.7 - 12.0, while elongation/termination inhibitors ranged from (7.8 - 8.4). These data suggest branching of the molecule is important for binding and may predict the step of protein synthesis a trichothecene blocks.

In summary, no single physico-chemical characteristic of the trichothecene mycotoxins correlated with apoptosis or cytotoxicity. Lipophilicity (Log P, CRIP, CNDO) and molecular branching (KIER) correlated with log-transformed toxicity values. Therefore, log transformation of the toxicity data would be necessary when using lipophilicity and molecular branching to predict toxicity of less toxic outliers in the data set, such as 3-Ac-DON and verrucarol. Using PCA analysis, the relationship of the physico-chemical vectors to toxicity was demonstrated. These results indicated CNDO and KIER had the greatest influence in separating the data set on the basis of toxicity.

Taken together, this study suggests CNDO and KIER, or possibly a combination of these variables, may provide the most accurate prediction of trichothecene apoptosis and cytotoxicity. Thus, the transportation of trichothecenes to the ribosome and molecular branching, which impacts binding, are critical for trichothecene-induced toxicity.

CHAPTER 4

Potentiation of Trichothecene-Induced Cytotoxicity and Apoptosis in Murine Leukocytes by TNF-α and Fas Ligand

INTRODUCTION

Vomitoxin (VT, deoxynivalenol), a trichothecene mycotoxin, is a naturally occurring environmental contaminant produced by molds commonly infesting cereal grains. Trichothecenes are not significantly reduced or removed from grains during milling and processing procedures (Wolf-Hall et al., 1999) and may enter finished food products at ppm levels (Abouzied et al., 1991). Exposure to this group of toxins leads to alteration of immune cell function, dysregulation of the humoral immune response, and impairment of host resistance to pathogens (Bondy and Pestka, 2000). The toxicity of trichothecenes, including vomitoxin, is attributed to ribosomal binding and subsequent inhibition of protein synthesis in actively dividing immune cells of the bone marrow, spleen, thymus, and lymph nodes (Ueno, 1983). Induction of apoptosis in these tissues by the trichothecenes (Islam et al., 1998; Shinozuka et al., 1997) is likely to contribute to the observed immunosuppressive effects.

Historically, outbreaks of human disease have been linked to trichothecene-producing molds such as *Fusarium* (Bamburg, 1968). Alimentary toxic aleukia in the Soviet Union and red mold disease in Japan were linked to human consumption of *Fusarium* contaminated grains. Between 1960 - 1991, 53 outbreaks of human food poisoning associated with moldy cereal occurred throughout China (Li et al.,

1999). Trichothecene levels were recently determined in samples from a food poisoning outbreak in Anhui, China in 1991 (Li et al., 1999). Moldy cereal samples contained up to 1.5 mg/kg VT. Approximately 130,000 people were affected by gastrointestinal disorders including nausea, vomiting, diarrhea, and leukopenia. Symptoms described in food-borne outbreaks mimic symptoms of experimental animals exposed to trichothecene mycotoxins (Bondy and Pestka, 2000).

Components of both stress (Albers et al., 1996; Pruett et al., 1993) and inflammatory (Luster et al., 2000; Emmendoerffer et al., 2000) signaling pathways play a critical role in chemically-induced toxic responses. Recent studies indicate that exposure to low levels of lipopolysaccharide (LPS), the biologically active component of gram negative bacteria, can influence the magnitude of a toxic response to xenobiotic agents. Increased hepatotoxic responses have been observed for carbon tetrachloride, ethanol, and ally alcohol (Roth et al., 1997). Previous in vivo studies demonstrate increased trichothecene toxicity in the presence of LPS which lowered LD_{50} doses and increased mortality in T-2 toxin treated mice (Tai and Pestka, 1988) and increased lymphocyte apoptosis and mortality in VT-treated mice (Zhou et al., 2000; Zhou et al., 1999). The mechanisms involved in this synergistic toxicity have not been elucidated.

LPS induces its biological effects by stimulating host cells to produce a variety of mediators including bioactive lipids (i.e. prostaglandins), glucocorticoids (i.e. corticosterone), and proinflammatory cytokines (i.e. TNF-α). These mediators may interact with VT to alter immune cell responses. For example, two chemicals may interact in an additive manner in which the combined effect is equal to the sum of the two, while synergism is defined by an effect that is greater than the sum. Potentiation occurs when one chemical does not elicit an effect, but when combined makes the second

chemical more toxic. Finally, an antagonistic interaction occurs when one chemical reduces or inhibits the effect of another (Casarett et al., 1996).

The objective of this study was to determine if cells exposed to low levels of the trichothecene VT could interact with LPS or other mediators of stress and inflammation including prostaglandin E_2 (PGE_2), anti-immunoglobulin, glucocorticoids, Fas ligand, or TNF-α in the induction of apoptosis and cytotoxicity in primary leukocyte cultures.

MATERIALS AND METHODS

Chemicals and reagents

Chemicals and reagents were purchased from Sigma Chemical Company (St. Louis, MO) unless otherwise noted. VT was dissolved in 100% ethanol and diluted in RPMI-1640 medium supplemented with 100 U/ml penicillin, 100 μg/ml streptomycin, 50μM 2-mercaptoethanol, 2 mM glutamine, 1 mM sodium pyruvate (Gibco Life Technologies, Rockville, MD), 1 mM non-essential amino acids (Gibco), and 10 % (v/v) fetal bovine serum (FBS, Gibco). Final ethanol concentration in the culture medium was less than 0.01% (v/v) which did not induce apoptosis or cytotoxicity. LPS (*Salmonella typhimurium*), PGE_2, dexamethasone (DEX, water-soluble) ethylenediaminetetraacetic acid (EDTA), and N-acetyl-L-cysteine (NAC) were dissolved in supplemented RPMI-1640. Anti-IgM (Pharmingen, San Diego, CA), anti-Fas (Pharmingen), and TNF-α (R&D Systems, Minneapolis, MN) were dissolved in 0.01 M phosphate buffered saline (PBS, pH 7.2) and diluted in supplemented RPMI-1640. Final concentration of TNF-α (20 ng/ml) in culture was equivalent to 1000 U/ml. BAPTA-AM, PD98059, SB203580, and Caspase 3 Inhibitor I were purchased from Calbiochem (San Diego, CA) and dissolved in cell culture grade dimethylsulfoxide (DMSO). Final DMSO

concentration in cell culture media was less than 0.1% (v/v) which did not induce apoptosis or cytotoxicity.

Animals

All animal handling was conducted humanely in accordance with the recommendations established by the National Institutes of Health and approved by Michigan State University Laboratory Animal Research Committee. Female B6C3F1 mice (8 - 10 weeks) were obtained from Charles River (Portage, MI). Animals were housed three per cage and acclimated 1 week at the MSU Laboratory Animal Resources Facility in a humidity and temperature controlled room with a 12 h light and dark cycle. Mice were provided standard rodent chow and water ad lib.

Primary cell culture

Mice were euthanized by cervical dislocation and thymus (TH), spleen (SP), femurs containing bone marrow (BM), and Peyer's patch (PP) were immediately removed. Single cells were released from TH, SP, and PP by forcing the tissue through a 40 μm nylon mesh Collector Tissue Sieve (Bellco Glass Inc., Vineland, NJ) and then submerged into cold RPMI-1640 medium. BM was flushed from the femur using RPMI-1640. SP and BM cell suspensions were treated with erythrocyte lysing buffer containing 0.83% (w/v) ammonium chloride, 0.1% (w/v) potassium bicarbonate, and 0.0037% (w/v) EDTA for 2 min at room temperature and centrifuged twice at 450 x g for 10 min. Cell number and viability were determined using a hemacytometer (Stiles, 1986). All cells (1 x 10^6/ml) were cultured in supplemented RPMI-1640 medium at 37°C in a 5% CO_2 humidified incubator in 96 well plates in a final volume of 300

μl/well. Cells were incubated with VT, each mediator, or VT plus each mediator for 18 h prior to apoptotic and cytotoxic measurements. Inhibitors or chelators (1 μM) were pre-incubated with cells for 2 h and removed prior to the addition of VT, TNF-α, or VT plus TNF-α in fresh medium. All experiments were repeated and results represent mean values from a minimum of four mice.

MTT conversion assay for cytotoxicity

Following treatment, 20 μl of a 5 mg/ml solution of 3- (4,5 dimethylthiazol-2-ul)-2,5- diphenyl tetrazolium bromide (MTT) in 0.01 M PBS was added to each well for the final 4 h of the 18 h incubation period (Marin et al., 1996). Microtiter plates were centrifuged at 450 x g for 20 min and media was aspirated to minimize formazan crystal loss. The resultant crystals were dissolved in 150 μl DMSO for 15 min. Optical density was measured using a Vmax Microplate Reader (Molecular Devices, Menlo Park, CA) at dual wavelengths, 570 nm and 690 nm. Percent control response was calculated as follows: ((1-absorbance of treatment/absorbance of control) x 100). Mean values were used to graphically determine ED_{50} values when possible.

Apoptosis assay

Apoptotic cells were quantitated using fluorescent DNA binding dyes as described by Duke and Cohen (1995). Briefly, following treatment, microtiter plates were centrifuged at 450 x g for 10 min and 250 μl of supernatant was removed. Five μl of DNA staining reagent (acridine orange (100 μg/ml) and ethidium bromide (100 μg/ml) in 0.01 M PBS) was added to each well and gently mixed. Cells were incubated on ice until sample analysis. A fluorescence microscope was used to count approximately 200

cells under 400 x magnification, 400/490 nm excitation and 520 nm emission. Cells were classified as apoptotic or normal based on chromatin organization. A normal nucleus appeared large with an organized structure whereas apoptotic nuclei appeared small and highly condensed or fragmented. Percent apoptosis was calculated as follows: ((number of cells with apoptotic nuclei/total cell number) x 100). Mean values were used to graphically determine the effective dose causing 50% apoptosis (ED_{50}) when possible.

Statistical analysis

The data were analyzed using Systat version 5.0 (Evanston, IL). A Student's t test was used to compare two groups while multiple groups were compared using a one way analysis of variance (ANOVA) and a Tukey test for mean separation. Samples receiving two treatments were analyzed for additivity, synergy/potentiation, or antagonsim by randomly combining single treatment replicates to calculate an expected mean additive response with variance. This calculated value was compared to actual co-treated samples using a Mann Whitney Rank Sum test. A p value < 0.05 was considered statistically significant.

RESULTS AND DISCUSSION

Differential sensitivity of primary murine leukocytes to VT- , LPS-, and VT plus LPS-induced apoptosis

Induction of apoptosis (Yang et al., 2000; Okumura et al., 2000; Shifrin and Anderson, 1999) and cytotoxicity (Hanelt et al., 1994; Anderson et al., 1989; Yike et al., 1999) are widely reported for the trichothecene mycotoxins and likely contribute to their toxic effects. Sensitivity of unstimulated primary leukocyte cultures prepared from TH,

SP, BM, and PP to VT was assessed. Induction of apoptosis at 18 h was evaluated by fluorescence microscopy and based on cell morphology. Apoptosis was significantly increased ($p<0.05$) by VT (250, 500 ng/ml) in SP cultures (Figure 4.1A). VT (500 ng/ml) also significantly increased TH and BM apoptotic morphology. Morphological changes were not noted in VT-treated PP cells. Concurrent with apoptosis induction, increased cytotoxicity was observed by MTT assay in SP and BM leukocytes exposed for 18 h to 250 ng/ml VT and all leukocytes exposed to 500 ng/ml (Figure 4.1B). The present study demonstrates that several primary murine leukocytes are sensitive to VT-induced cytotoxicity and apoptosis.

Sepsis (Oberholzer et al., 2001; Ayala et al., 1996) or administration of LPS to mice (Zhang et al., 1993; Zhang et al., 1994) results in apoptosis in lymphocytes of the BM, SP, and TH. In the present study, LPS concentrations up to 20 μg/ml did not alter apoptotic morphology in any of the primary leukocyte cultures (data not shown). However, all three LPS doses tested significantly increased MTT conversion, indicative of a proliferative response, in SP (Figure 4.2). Zhou et al. (2000) reported a synergistic increase in lymphocyte apoptosis in mice co-exposed to LPS and VT. As previously stated, LPS did not directly induce apoptosis in murine TH, SP, BM, or PP leukocyte cultures. However, VT inhibited the LPS-induced proliferative responses in SP leukocytes, but did not significantly alter apoptotic morphology in the co-treated cultures. The ability to inhibit protein synthesis by VT (Ueno, 1983) may have contributed to this reduced proliferative response. These results suggest the in vivo induction of apoptosis in immune tissues exposed to LPS alone or LPS and VT is not due to LPS directly, but may require a secondary mediator. Possible interactions between prostanoids, immunoglobulins (as antigen mimics), glucocorticoids, Fas, and TNF-α signaling components with VT were further investigated.

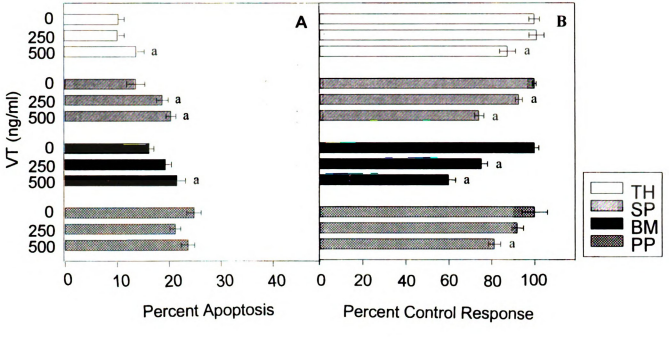

Figure 4.1. VT induced apoptosis (A) and cytotoxicity (B) in the primary murine leukocyte cultures. Primary murine leukocyte cultures were exposed to VT (0 - 500 ng/ml) for 18 h. Percent apoptosis was assessed by fluorescence microscopy. Cytotoxicity was measured by conversion of MTT during the final 4 h in culture. Data (n=4) represent the mean ± SEM. [a]A Student's t test was used to determine values significantly different from the respective tissue control value ($p < 0.05$). TH - thymocytes; SP - splenocytes; BM - bone marrow; PP - Peyer's patch.

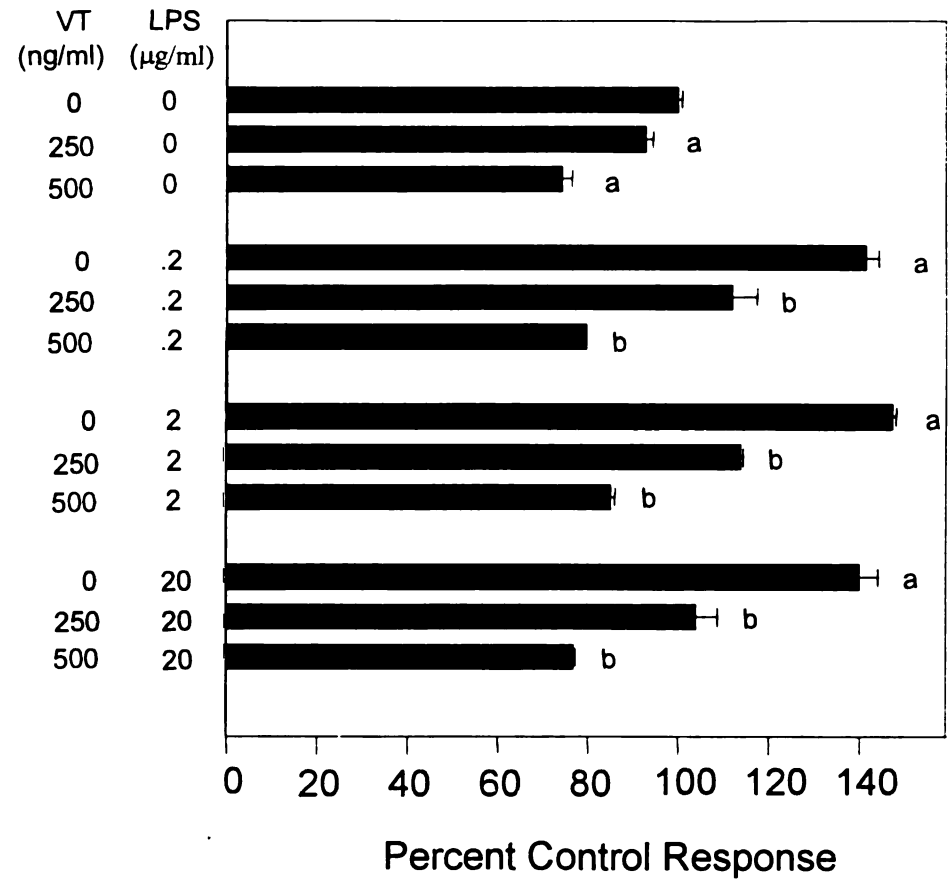

Figure 4.2. LPS-induced increases in splenocyte MTT conversion were inhibited by VT. Splenocytes were exposed to VT (0 - 500 ng/ml), LPS (0 - 20 μg/ml) or both for 18 h. Cytotoxicity was measured by conversion of MTT during the final 4 h in culture. Data (n=4) represent the mean percent control response ± SEM. [a]A Student's t test was used to determine values significantly different from the untreated control and [b]values significantly different from the respective LPS control ($p<0.05$).

Differential sensitivity of primary murine leukocytes to PGE_2 -induced apoptosis and cytotoxicity in the absence and presence of VT

Prostanoids, including PGE_2, increase in response to acute inflammation prior to leukocyte recruitment (Tilley et al., 2001). PGE_2 can activate or inhibit effector cell functions depending on stimuli and target cell. Receptors for prostanoids are expressed on TH, SP, BM, and macrophage cells. The ability of PGE_2 to induce apoptosis in immature B lymphocytes (Brown et al., 1992) and immature and mature T cells (Pica et al., 1996; Mastino et al., 1992) suggests prostanoids may be capable of interacting with chemical agents to alter immune cell responses by selectively affecting cell death. Sensitivity of unstimulated primary leukocyte cultures prepared from TH, SP, BM, and PP to PGE_2 was assessed. Microscopic analysis of PGE_2-induced apoptosis indicated a significant increase ($p<0.05$) in TH cultures exposed to 20 μM for 18 h (Figure 4.3A). Decreased MTT conversion (increased cytotoxicity) was observed in TH cultures exposed to 0.2 μM (75.7 ± 1.1%), 2 μM (60.0 ±3.3%), and 20 μM (57.2 ± 5.0%) PGE_2 (Figure 4.3B). No significant changes in apoptosis or cytotoxicity were observed in SP, BM, or PP leukocyte cultures. Apoptosis in TH exposed to a combination of VT at concentrations up to 500 ng/ml and PGE_2 was not statistically different than either TH single treatment (data not shown). The addition of VT to these cultures did not significantly alter TH apoptotic or cytotoxic responses. These results suggest VT and PGE_2 signaling pathways do not collaborate in primary leukocyte signaling.

Differential sensitivity of primary murine leukocytes to anti-IgM -induced apoptosis and cytotoxicity in the absence and presence of VT

Antigen receptor ligation has been used extensively as a model of clonal B cell

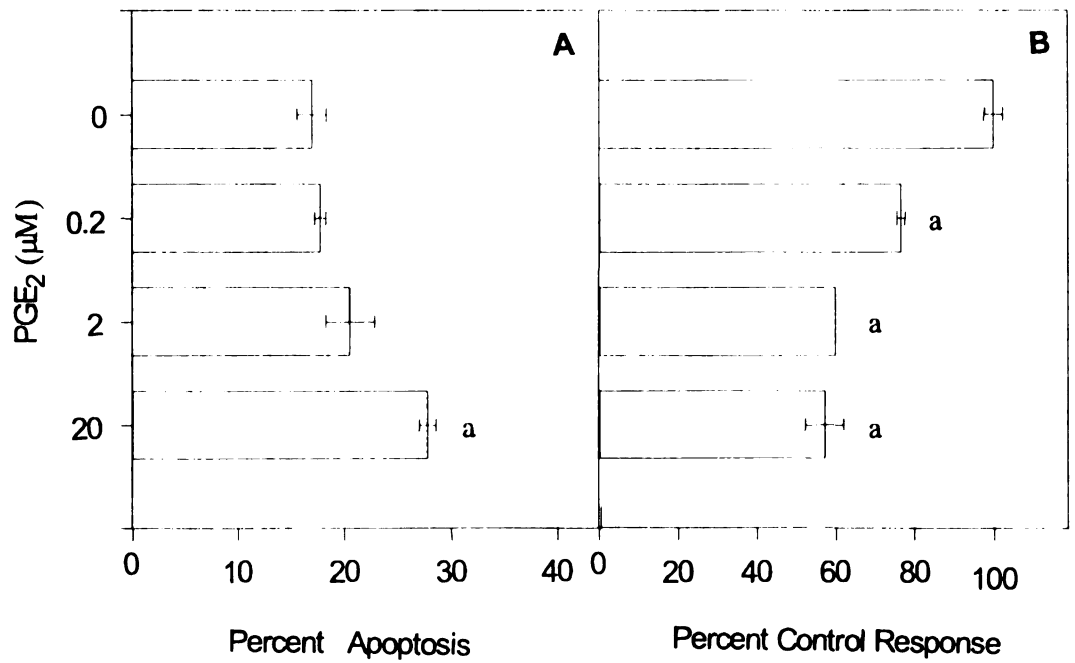

Figure 4.3. PGE_2 induced apoptosis (A) and cytotoxicity (B) in primary murine thymocyte cultures. Primary murine thymocyte cultures were exposed to PGE_2 (0 - 20 μM) for 18 h. Percent apoptosis was assessed by fluorescence microscopy. Cytotoxicity was measured by conversion of MTT during the final 4 h in culture. Data (n=4) represent the mean ± SEM. [a]A Student's t test was used to determine values significantly different from the respective tissue control value ($p < 0.05$).

deletion (Hasbold and Klaus, 1990; Joseph et al., 1995; Gottschalk and Quintans, 1995). Following anti-IgM crosslinking, B cells undergo cell cycle arrest and apoptosis. This process appears to be regulated by the B cell microenvironment (Modigliani et al., 1997) and a significant increase in ceramide levels is of critical importance (Gottschalk and Quintans, 1995). Sensitivity of unstimulated primary leukocyte cultures prepared from TH, SP, BM, and PP to anti-IgM (as an antigen mimic) was assessed. Anti-IgM (1 μg/ml) significantly increased SP leukocyte apoptosis (Figure 4.4A) and decreased MTT conversion (78.9 ± 5.3%, $p<0.05$; Figure 4.4B). Apoptotic morphology and cytotoxicity were not altered in TH, BM, or PP cultures. The combination of VT and anti-IgM was not significantly different than either SP single treatment (data not shown). These results suggest VT and antigen-dependent signaling pathways do not interact in primary leukocytes.

Differential sensitivity of primary murine leukocytes to DEX- induced apoptosis and cytotoxicity in the absence and presence of VT

Endogenous increases in glucocorticoids can result from both inflammatory conditions (Cabrera et al., 2000) and cell stress resulting from chemical exposure (Pruett et al., 1993). Glucocorticoids can both inhibit (Bailly-Maitre et al., 2001) and induce (Krishna et al., 1995; Andreau et al., 1998) apoptosis. The induction of lymphocyte apoptosis by glucocorticoids has been well characterized (Gruber et al, 1994; Krishna et al., 1995; Andreau et al, 1998) and provides a model in which two apoptotic inducers may interact.

Sensitivity of unstimulated primary leukocyte cultures prepared from TH, SP, BM, and PP to DEX was assessed. Apoptosis induction by DEX was observed for TH,

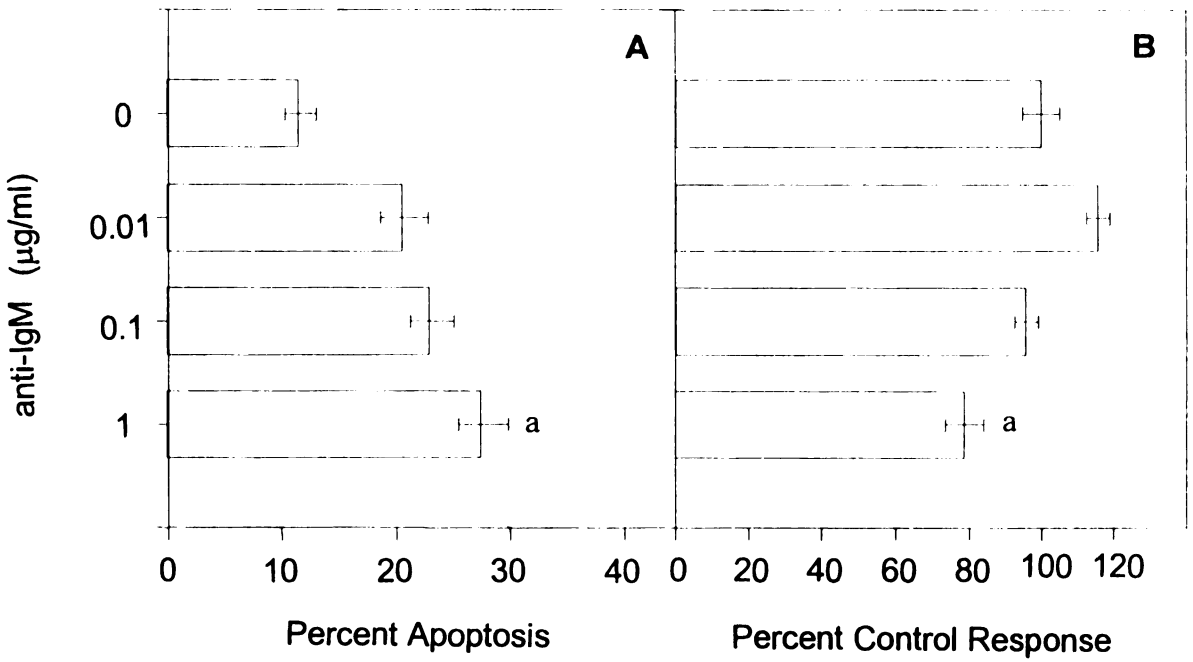

Figure 4.4. Anti-IgM induced apoptosis (A) and cytotoxicity (B) in primary murine splenocyte cultures. Primary murine splenocyte cultures were exposed to Anti-IgM (0.01 - 1 µg/ml) for 18 h. Percent apoptosis was assessed by fluorescence microscopy. Cytotoxicity was measured by conversion of MTT during the final 4 h in culture. Data (n=4) represent the mean ± SEM. [a]A Student's t test was used to determine values significantly different from the respective tissue control value ($p < 0.05$).

SP, and PP cultures (Figure 4.5). The effective doses resulting in 50% (ED_{50}) apoptosis for TH and SP were 23 and 2 nM, respectively. Maximum apoptosis observed in PP cultures was 43.77 ± 2.0%. BM apoptosis was not observed at concentrations of DEX up to 5 μM (data not shown). ED_{50} values for TH and SP cytotoxicity were 12 and 30 nM, respectively (data not shown). In a previous study, Pestka et. al (1994) demonstrated in vitro that DEX (100 nM)-induced SP apoptosis was significantly reduced by a high dose of VT (50,000 ng/ml). In the present study, induction of SP apoptosis by 10 nM DEX was significantly inhibited by 500 ng/ml VT (Figure 4.6). Interestingly, MTT-conversion results for VT plus DEX treated SP leukocytes was not significantly affected even though apoptosis was inhibited (data not shown). These data suggest metabolic activity (mitochondrial conversion of MTT) was arrested for at least a portion of the incubation period. It is not clear if the development of apoptosis was completely inhibited or just delayed in this model system.

The opposing effects on apoptosis by DEX and VT may involve NFκB. DEX-induced inactivation of NFκB has been described in both T cells (Ray and Prefontane, 1994; Scheinman et al., 1995) and B cells (Donjerkovic et al., 2000) while VT activates NFκB in T cells model (Ouyang et al., 1996). Wu et al. (1996) demonstrated the necessity of NFκB inhibition in the induction of B cell apoptosis. Here, apoptosis was induced in WEHI-231 B cells and normal murine splenic B cells by preventing the degradation of the inhibitor of NFκB, interfering with NFκB binding, and microinjecting IκB-α-GST protein. VT may be similarly upregulating NFκB and inhibiting or delaying DEX-induced SP apoptosis.

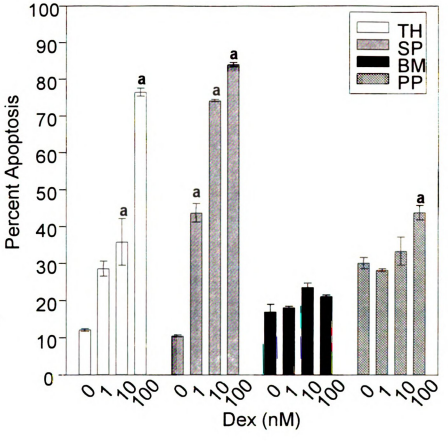

Figure 4.5. DEX induced apoptosis in primary murine thymocyte, splenocyte, and Peyer's patch cultures. Primary murine leukocyte cultures were exposed to DEX (0 - 100 nM) for 18 h. Percent apoptosis was assessed by fluorescence microscopy. Data (n=4) represent the mean ± SEM. [a]A Student's t test was used to determine values significantly different from the respective tissue control value ($p < 0.05$). TH - thymocytes; SP - splenocytes; BM - bone marrow; PP - Peyer's patch.

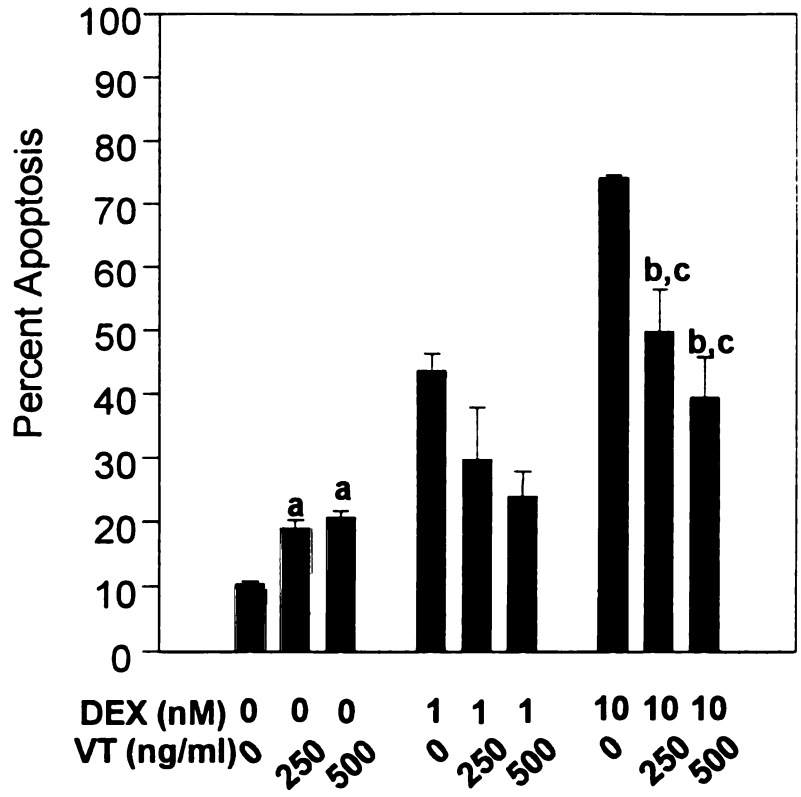

Figure 4.6. DEX-induced increases in splenocyte apoptosis were inhibited by VT. Splenocytes were exposed to VT (0 - 500 ng/ml), DEX (0 - 100 nM) or both for 18 h. Percent apoptosis was assessed by fluorescence microscopy. Data (n=4) represent the mean percent control response ± SEM . [a]A Student's t test was used to determine values significantly different from the untreated control, [b]values significantly different from the respective DEX control, and [c]values significantly different from the respective VT control ($p<0.05$).

Interestingly, the use of glucocorticoids in vivo has been investigated in the pharmacological treatment of trichothecene toxicity. Matsuoka and Kubota (1987) inhibited fusarenone-x induced gastro-intestinal permeability with hydrocortisone. In addition, DEX administration significantly increased the LD_{50} value of T-2 toxin in mice (Fricke and Jorge, 1991) and lethality in rats (Harvey et al., 1994). In the latter studies, the high dose required to reduce trichothecene toxicity suggests glucocorticoids were acting indirectly by reducing the inflammatory response rather than a direct receptor-mediated mechanism.

Differential sensitivity of primary murine leukocytes to anti-Fas-induced apoptosis and cytotoxicity in the presence and absence of VT

Fas ligand (FasL) and Fas receptor (FasR) are upregulated following sepsis (Ayala et al., 1998) and administration of LPS to mice (Kitamura et al., 2001). Binding of FasL to FasR results in the induction of apoptosis in thymocytes and B cells of BM, SP, and PP (Nilsson et al., 2000; Ayala et. al., 1998; Nishimura et al., 1997; Kakinuma et al., 1999). In the present study, sensitivity of unstimulated primary leukocyte cultures prepared from TH, SP, BM, and PP to anti-Fas was assessed. A significant increase in apoptotic morphology was noted in TH cell cultures exposed to anti-Fas (1 μg/ml) for 18 h. Whereas apoptosis in SP, BM, or PP were unaffected (Figure 4.7A). In addition, MTT conversion was significantly decreased in TH treated with 0.1 μg/ml (56.6 ± 4.8%) and 1 μg/ml anti-Fas (48.6 ± 2.4%; Figure 4.7B) A previous in vitro study required pre-treatment of primary SP cultures with LPS to sensitize the cells to Fas mediated apoptosis (Watanabe et al., 1995).

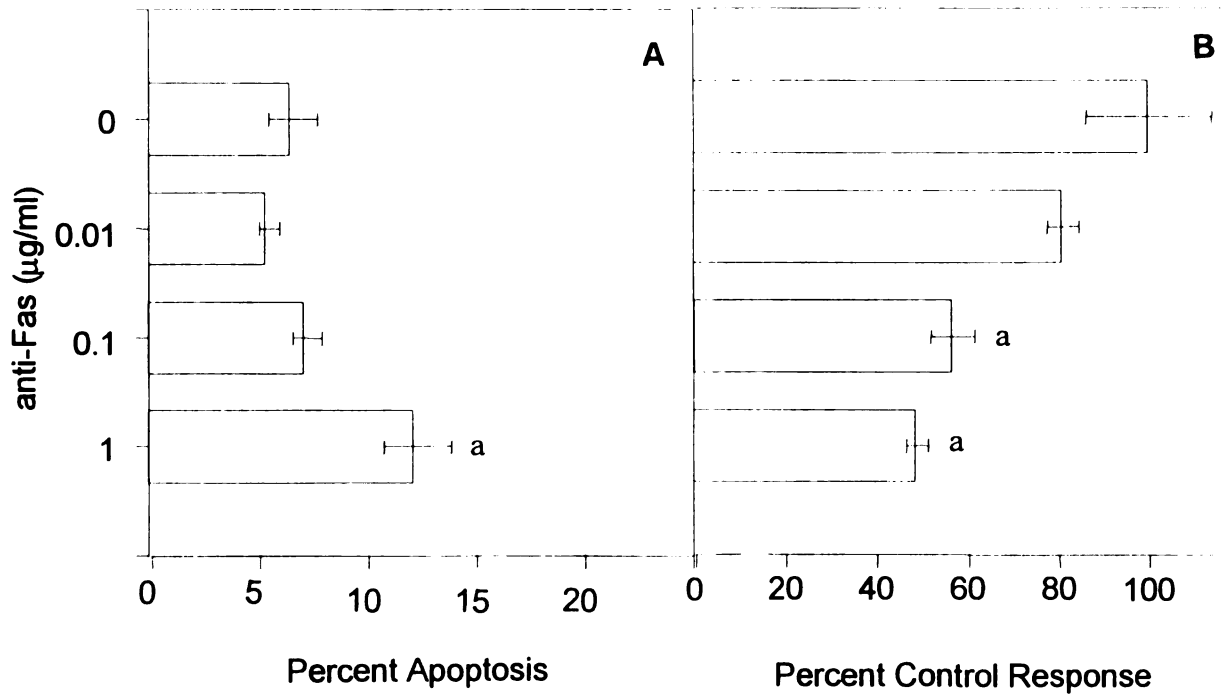

Figure 4.7. Anti-Fas induced apoptosis (A) and cytotoxicity (B) in primary murine thymocyte cultures. Primary murine thymocyte cultures were exposed to anti-Fas (0 - 1 µg/ml) for 18 h. Percent apoptosis was assessed by fluorescence microscopy Cytotoxicity was measured by conversion of MTT during the final 4 h in culture. Data (n=4) represent the mean ± SEM. [a]A Student's t test was used to determine values significantly different from the respective tissue control value ($p < 0.05$).

Apoptosis and cytotoxicity for VT (up to 500 ng/ml) and anti-Fas combined were not significantly different than the single-treatment TH cultures (data not shown). In contrast, the combination of VT (500 ng/ml) and anti-Fas (0.1 or 1 μg/ml) induced a level of apoptosis in BM leukocytes (Figure 4.8A) that was significantly greater than either single treatments alone ($p<0.05$). Percentages of apoptosis for the untreated control, anti-Fas (1 μg/ml), VT (500 ng/ml), and the combination were 17.6%, 15.1%, 23.7%, and 32.0% respectively. The expected mean additive increase over the untreated control after exposure to the combined toxins was 6.1%. Statistical analysis of the apoptosis data indicated that anti-Fas potentiated VT-induced BM apoptosis. This interaction was also observed for combinations of lower doses of VT (250 ng/ml) and anti-Fas (0.1 μg/ml). MTT conversion by BM cultures treated with VT (250 ng/ml) and anti-Fas (1 μg/ml) were significantly lower than each individual treatment ($p<0.05$). However, the combination treatments with 500 ng/ml VT were not statistically different from VT alone (Figure 4.8B). A similar potentiation of apoptosis was reported in murine granulosa cells co-treated with the translational inhibitor cycloheximide (CHX) and anti-Fas antibody (Quirk et al., 1998). Cells treated with anti-Fas alone did not undergo apoptosis. This potentiation of apoptosis may result from the upregulation of FasR by CHX, demonstrated both in vivo (Kimura and Yamamoto, 1997) and in a T cell model (Tang et al., 1999), which would sensitize the cells to Fas-mediated apoptosis. Similarly, VT may upregulate FasR and sensitize BM cells to Fas-mediated apoptosis.

Differential sensitivity of primary murine leukocytes to TNF-α-induced apoptosis and cytotoxicity in the presence and absence of VT

TNF-α is a potent proinflammatory cytokine produced by lymphocytes and other

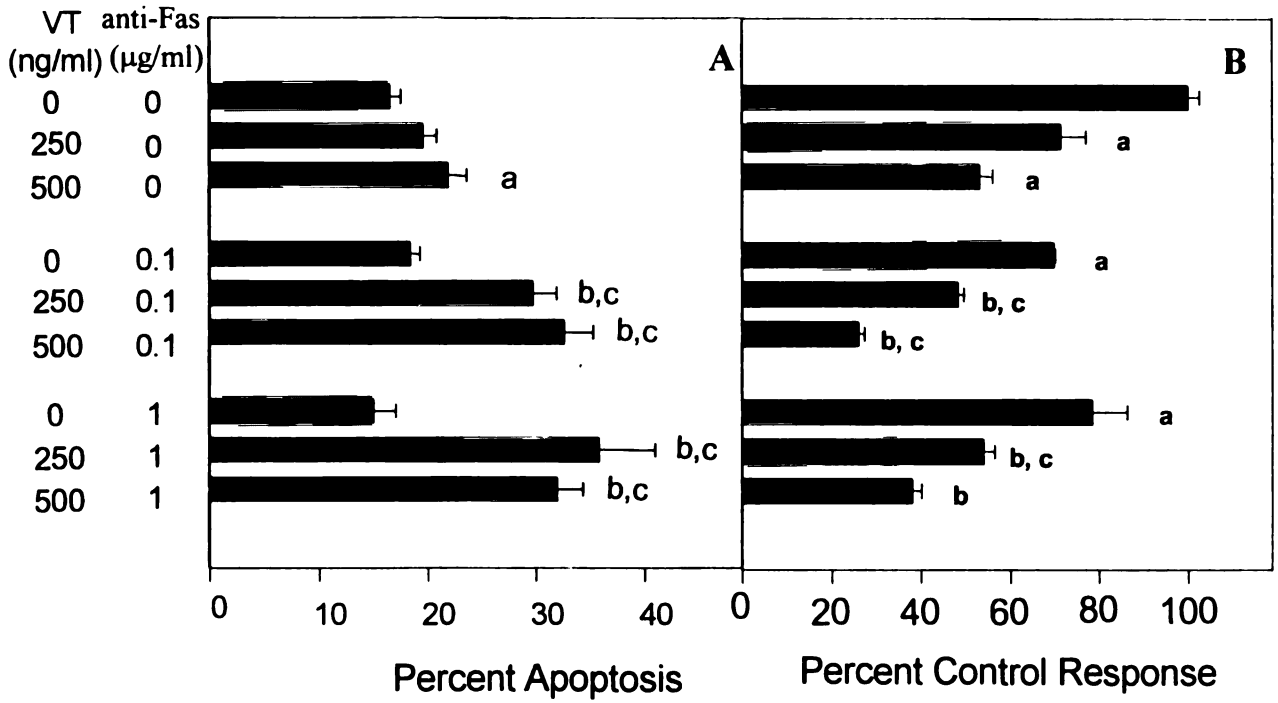

Figure 4.8. Anti-Fas potentiated VT-induced apoptosis (A) and cytotoxicity (B) in primary murine bone marrow cultures. Bone marrow leukocytes were exposed to VT (0-500 ng/ml), anti-Fas (0 - 1 μg/ml), or both for 18 h. Percent apoptosis was assessed by fluorescence microscopy. Cytotoxicity was measured by conversion of MTT during the final 4 h in culture. Data (n=4) represent the mean ± SEM. [a]A Student's t test was used to determine values significantly different from the untreated control, [b]values significantly different from the respective anti-Fas control, and [c]values significantly different from the respective VT control ($p<0.05$).

cells in response to inflammation or environmental stress (Baud and Karin, 2001). TNF-α induces a variety of cell responses including proliferation, differentiation, and apoptosis. The induction of apoptosis by TNF-α depends on recruitment of several signaling proteins to TNFR1 including TNFR1-associated death domain protein (TRADD), receptor-interacting protein 1 (RIP1), Fas-associated death domain protein (FADD), TNF-receptor associated factor 2 (TRAF2), and TNF-related apoptosis inducing ligand (TRAIL). Sensitivity of unstimulated primary leukocyte cultures prepared from TH, SP, BM, and PP to TNF-α-induced apoptosis was assessed in the present study. TNF-α (0.8 - 20 ng/ml) did not significantly increase apoptosis or cytotoxicity in any primary leukocyte cultures after 18 h (data not shown). However, the combination of VT (250 or 500 ng/ml) and TNF-α (4 or 20 ng/ml) significantly increased TH apoptosis (Figure 4.9A). The observed apoptosis was significantly higher than apoptosis induced by either mediator alone ($p<0.05$). Percentages of TH apoptosis for the untreated control, VT (500 ng/ml), TNF-α (20 ng/ml), and the combination were 8.8%, 13.8%, 10.1%, and 40.5% respectively. The expected mean additive increase over the untreated control after exposure to the combined toxins was 6.3%. Statistical analysis of the apoptosis data indicated TNF-α potentiated VT-induced TH apoptosis ($p<0.05$). This interaction was also observed for the combination of lower doses of VT (250 ng/ml) and TNF-α (4 ng/ml). MTT conversion by TH cultures treated with VT (250 or 500 ng/ml) and TNF-α (20 ng/ml) was significantly lower than each individual treatment (Figure 4.9B). Percent inhibition of MTT conversion for VT (500 ng/ml), TNF-α (20 ng/ml), and the combination was 7.7%, 3.6%, and 42.6% respectively. The expected mean additive inhibition over the untreated control after exposure to the combined toxins was 11.3%. Statistical analysis of MTT inhibition indicated TNF-α potentiated VT-induced

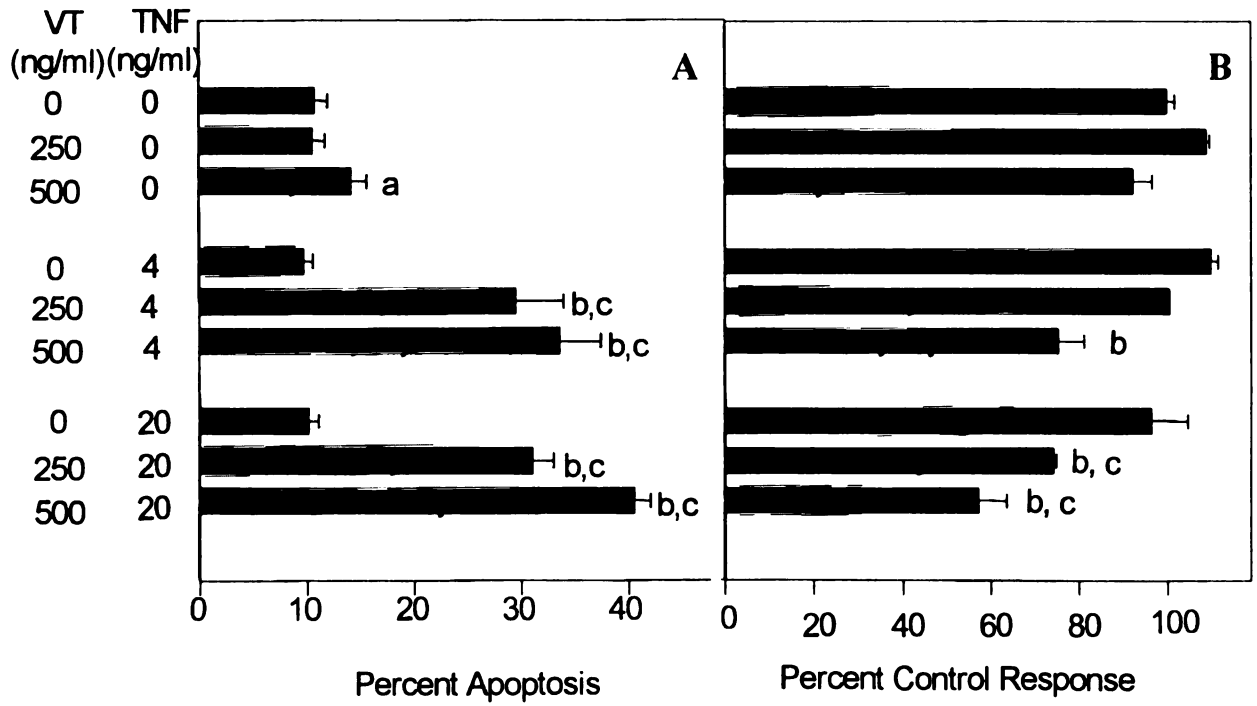

Figure 4.9. TNF-α potentiated VT-induced apoptosis (A)and cytotoxicity (B) in primary murine thymocyte cultures. Thymocyte cultures were exposed to VT (0-500 ng/ml), TNF-α (0 - 20 ng/ml), or both for 18 h. Percent apoptosis was assessed by fluorescence microscopy. Cytotoxicity was measured by conversion of MTT during the final 4 h in culture. Data (n=4) represent the mean ± SEM [a]A Student's t test was used to determine values significantly different from the untreated control, [b]values significantly different from the respective TNF-α control, and [c]values significantly different from the respective VT control ($p<0.05$).

cytotoxicity ($p<0.05$). The combination of VT and TNF-α had no significant effect on SP, BM, or PP apoptosis or cytotoxicity.

Apoptotic responses to TNF-α are thought to be dependent on the inhibition of genes involved in proliferation and activation responses by RNA or protein synthesis inhibitors (Baud and Karin, 2001). However, NFκB is required for activation-induced cell death of $CD4^+CD8^+$ thymocytes (Hettmann et al., 1999; Bessho et al., 1994), and the IkB kinase complex is essential for protection of T lymphocytes against anti-Fas and TNF-α-induced apoptosis (Senftleben et al., 2001). The upregulation of NFκB by VT (Ouyang et al., 1996) may be contributing to the increased apoptosis observed in TH leukocytes co-treated with TNF-α and VT. Recently, the upregulation of TRAIL by NFκB has been demonstrated in T cells (Siegmund et al., 2001; Baetu et al, 2001).

Cycloheximide induces T cell death in a FADD/caspase-8 dependent manner without Fas or TNF receptor I interaction (Tang et al., 1999). Similarly, VT-induced apoptosis may be FADD-dependent. FADD is a common component of both TNF-α and Fas death receptor pathways and may explain the potentiation of apoptosis in both TNF-α plus VT treated TH and anti-Fas plus VT treated BM leukocytes. In addition, LPS induces endothelial cell apoptosis in a FADD-dependent manner independent of TNF-α/Fas death receptor involvement (Choi et al., 1998). The induction of a FADD-dependent pathway may explain the in vivo induction of apoptosis by LPS plus VT (Zhou et al., 2000). While the receptor-proximal events of death receptor pathways are well defined, the role of other signal components, such as mitogen activated protein kinase (MAPK) activation are reportedly cell-type specific (Baud and Karin, 2001). We investigated signal events involved in the potentiation of VT induced apoptosis by TNF-α in TH leukocyte cultures using several pharmacological inhibitors.

Mechanism of TNF-α potentiation of VT-induced TH apoptosis involves reactive oxygen species, intracellular Ca^{2+}, mitogen activated protein kinases, and caspase-3

The potentiation of VT-induced apoptosis by TNF-α provides a model in which an inflammatory component significantly increases the immunotoxic response of a chemical. This model was further investigated to determine the upstream mechanisms involved in TH apoptosis. For these studies, cells were pretreated with each signaling inhibitor and the percent apoptosis was compared to the VT plus TNF-α treated control cultures and the untreated control.

N-acetyl-cysteine (NAC) replenishes intracellular glutathione, protecting the cell against the production of reactive oxygen species. NAC blocks apoptosis induced by TNF-α (Talley et al., 1995) and cycloheximide plus TNF-α co-treated cells (Cossarizza et al., 1995). A significant decrease in intracellular glutathione was reported in cycloheximide-treated Jurkat cells (Chiba et al., 1996). In the present study, VT plus TNF-α-induced TH apoptosis was significantly reduced by NAC (10.9 ± 0.5%; Figure 4.10). This value was not significantly different than the untreated control value (8.8 ± 0.3%). Previous studies indicate NAC blocks NFκB and JNK activation by TNF-α (Shrivastava and Aggrarwal, 1999) and NFκB resulting from Fas ligation (Giardina et al., 1999).

Ca^{2+} mobilization may influence apoptosis in a cell-type specific manner. For example, elevation of intracellular Ca^{2+} induces the appearance of phosphatidylserine on the membrane of apoptotic Jurkat cells (Hampton et al., 1996) but is not necessary for TNF-α-induced apoptosis in a rat/mouse T cell hybridoma (Denecker et al., 1997). In the present study, intracellular Ca^{2+} chelator BAPTA-AM significantly reduced VT plus TNF-α TH apoptosis (10.9 ± 0.9%; Figure 4.10). This value was not significantly

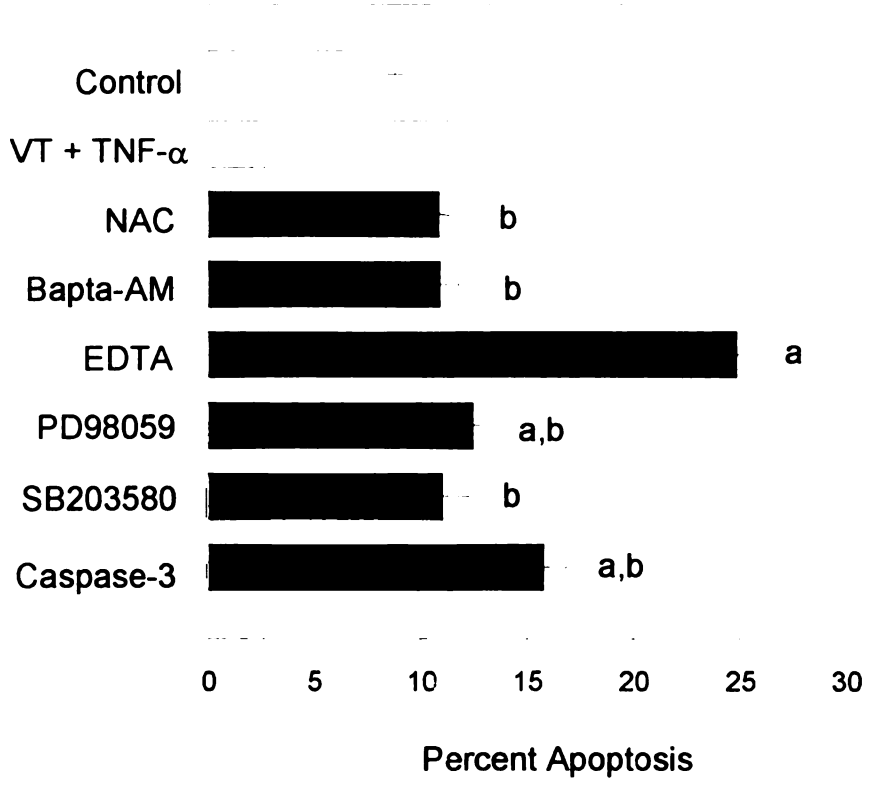

Figure 4.10. VT plus TNF-α induced apoptosis signal mechanisms involve reactive oxygen species, intracellular Ca^{2+}, mitogen activated protein kinases, and caspase-3. Thymocyte cultures were pre-treated 2 h with 1 μM of each inhibitor and exposed to VT (500 ng/ml), TNF-α (20 ng/ml), or both for 18 h. Percent apoptosis was assessed by fluorescence microscopy. Data (n=6) represent the mean ± SEM. [a]A student's t test was used to determine values significantly different from the untreated control or [b]VT plus TNF-α positive control ($p<0.05$).

different than the untreated control value (8.8 ± 0.3%). Extracellular Ca^{2+} chelator EDTA did not significantly alter TH apoptosis. In a previous study, FADD-DN T cells demonstrated an impaired release of intra-cellular, but not extra-cellular Ca^{2+} (Hueber et al., 2000). Interestingly, intracellular Ca^{2+} and ROS produced during TNF-α-induced apoptosis are interdependent (Ko et al., 2000). Production of ROS in BAPTA/AM treated fibroblasts was delayed while removal of ROS blocked the TNF-α mediated intracellular Ca^{2+} increases and apoptosis. Taken together, these results suggest that both ROS and intracellular Ca^{2+} may be necessary for VT plus TNF-α-induced apoptosis and these signals may be intertwined.

MAPKs are a group of serine/threonine specific protein kinases that connect cell surface signals through kinase cascades to transcription factors and ultimately modulate gene expression. c-Jun-N-terminal kinase (JNK), p38/SAPK, and ERK 1/2 are critical regulators of cell survival in Fas and TNF-α treated cells (Roulston et al., 1998; Tran et al., 2001). In the present study, PD98059, an inhibitor of MEK1 and subsequently ERK 1/2, inhibited VT plus TNF-α induced apoptosis (12.5 ± 0.5%), however, this value was significantly higher than control levels. Activation of ERK 1/2 by TNF-α is commonly associated with proliferation or activation of cells (McLeish et al., 1998). Recently, Bommhardt et al. (2000) demonstrated a role for ERK in thymocyte negative selection. In contrast, Tran, et al (2001) demonstrated that ERK activation could override apoptotic signals from death receptors. Interestingly, Davies et al. (2000) demonstrated that PD98059 (50 mM) can reduce both MEK1 and p38 activity to approximately 85% of the control value. In addition, Salh et al. (2000) described JNK inhibition by PD98059 in HT29 cells. Therefore, the role of ERK in VT plus TNF-α-induced apoptosis of TH is presently unclear.

The activation of p38 in response to TNF-α is biphasic, and both independent and dependent on caspase activation (Roulston et al., 1998; Herr et al., 1999). Apoptosis in the presence of SB203580, a highly selective inhibitor of p38, was significantly decreased to control levels (11.1 ± 1.2%) in VT plus TNF-α co-treated thymocytes. Caspase activation is critical in the induction of apoptosis by TNF-α (Belka et al., 2001; Aggarwal et al., 2000; MacFarlane et al., 2000). Caspase-3 inhibitor I, a specific but reversible inhibitor, reduced apoptosis to 15.8 ± 1.1%, which was significantly higher than control values. These results suggest p38 and Caspase-3 may play critical roles in VT plus TNF-α-induced TH apoptosis.

CONCLUSION

Apoptosis is a mechanism of cell death which contributes to homeostasis in the immune system by removing self-reactive lymphocytes (Cohen et al., 1992). Negative selection of lymphocytes has been well characterized in the thymus (T cells) and germinal centers of the SP and PP (B cells). Immune cell apoptosis may also result from chemical insult. Signaling components of both cellular stress and inflammation may interact with a chemical agent to alter immune cell responses. This study demonstrates that VT, a potent protein synthesis inhibitor, could inhibit or enhance immune cell apoptosis and cytotoxicity as exemplified by (1) VT inhibition of LPS-induced proliferation and DEX-induced apoptosis in SP leukocytes and (2) Potentiation of VT-induced apoptosis in BM leukocytes by anti-Fas and TH leukocytes by TNF-α. The potentiation of VT-induced apoptosis by TNF-α was further characterized and pharmacological inhibition studies suggest critical roles for ROS, intracellular Ca^{2+},

p38/SAPK, and caspase activation. Future studies will begin to decipher the role of these mediators in the potentiation of VT-induced apoptosis by TNF-α.

CHAPTER 5

Mechanisms of Trichothecene-Induced Jurkat T Cell Apoptosis: Dose Response and Potentiation by TNF-α

INTRODUCTION

Fusarium, *Stachybotrys*, and *Myrothecium* produce biologically active fungal metabolites called trichothecenes (Bondy and Pestka, 2000). Human and animal exposure to trichothecenes may occur through consumption of contaminated grains or inhalation of mold spores. The most common trichothecene contaminant of grain crops in the United States and Canada is vomitoxin (VT, deoxynivalenol) (Rotter et al., 1996). VT is resistant to milling, processing, and baking and may readily enter cereal-based food products intended for human consumption (Abouzied et al., 1991).

Leukocytes of the immune system are particularly sensitive to VT and the trichothecenes. Trichothecenes are immunosuppressive at high doses resulting from both inhibition of protein synthesis and induction of leukocyte death by apoptosis in the bone marrow, lymph nodes, spleen, and thymus. (Bondy and Pestka, 2000). Apoptosis is a critical regulatory pathway of the immune system that restricts excessive inflammation and prevents autoimmunity through activation of death receptors (Dong, et al., 2002). In addition, apoptosis may result from cellular stress (i.e. UV light, viral infection, cytokines, and heat shock) or chemical insult (Saini and Walker, 1998). Recently, apoptosis induction by ribotoxic stress resulting from ribosomal cleavage (Iordanov et

al., 1997) or ribosomal binding (Shifrin and Anderson, 1999) by translational inhibitors has been described.

Despite the high potential for human exposure, little information exists on the role of apoptosis in VT-induced immunosuppression and the mechanisms involved in apoptosis induction. Induction of apoptosis is characterized by exposure to extracellular stimuli, such as VT, and the initiation of a signaling pathway. The pathway triggered is largely dependent on the specific stimulus and the type of target cell (Saini and Walker, 1998).

Mitogen activated protein kinases (MAPKs) are centrally important in determining cellular responses to extracellular stimuli. MAPKs are divided into three distinct, but partially overlapping signaling pathways that include ERK1/2 (p44/p42), JNK1/2 (p54/p46), and p38. Phosphorylation and subsequent activation of transcription factors by MAPKs leads to expression of genes critical for apoptosis induction including signaling components of death receptor pathways (Hsu et al., 1999; Faris et al., 1998). Activation of MAPKs has been previously reported and linked to apoptosis induction by trichothecenes (Yang et al., 2000; Shifrin and Anderson, 1999).

As previously reported in Chapter 4, anti-Fas antibody in murine bone marrow cells and TNF-α in murine thymocytes potentiated VT-induced apoptosis. Previous in vivo studies in our lab demonstrated increased trichothecene-induced apoptosis and mortality in the presence of lipopolysaccharide (LPS), the biologically active component of gram negative bacteria (Zhou et al., 2000; Zhou et al., 1999). The mechanisms involved in this synergistic toxicity have not been elucidated. The potentiation of VT-induced apoptosis by TNF-α was significantly reduced by pharmacological inhibitors of MAPKs. These results suggest death receptor pathways may converge or cooperate

with VT-induced cell signal mechanisms in some cell types and this process may involve MAPKs.

The objective of this study was to characterize VT-induced apoptosis in a human T cell model focusing on both dose-reponse effects and potentiation by the proinflammatory cytokine TNF-α. In addition, the relationship between these effectors and activation of second messengers (i.e. intracellular calcium and reactive oxygen species), upregulation of three MAPK family members, Bcl-2 expression, and caspase substrate cleavage was investigated.

MATERIALS AND METHODS

Chemicals and Reagents

Chemicals and reagents were purchased from Sigma Chemical Company (St. Louis, MO) unless otherwise noted. VT, anisomycin (AN), and monensin were dissolved in 100% ethanol and diluted in supplemented RPMI-1640 medium. Final ethanol concentration in the culture media was less than 0.01% (v/v) which did not induce apoptosis or cytotoxicity. TNF-α (R & D Systems, Minneapolis, MN) was dissolved in 0.01 M phosphate buffered saline (PBS, pH 7.2) and diluted in supplemented RPMI-1640 medium for a final concentration in culture of 1000 U/ml or 20 ng/ml. Diphenylene-iodonium chloride (DPI), BAPTA-AM, PD98059, SB203580, and Caspase 3 Inhibitor I were purchased from Calbiochem (San Diego, CA) and dissolved in cell culture grade dimethylsulfoxide (DMSO). Final DMSO concentrations in cell culture media was less than 0.1% (v/v) which did not induce apoptosis or cytotoxicity.

Cell Culture

Jurkat T lymphocytes (American Type Cell Culture, Manassas, VA) were grown in RPMI-1640 medium supplemented with 100 U/ml penicillin, 100 μg/ml streptomycin, 50 μM 2-mercaptoethanol, 2 mM glutamine, 10 mM HEPES (Sigma Chemical Company), 1 mM sodium pyruvate, 1 mM non-essential amino acids, and 10% (v/v) fetal bovine serum (FBS, Gibco Life Technologies, Rockville, MD). Cell number and viability was assessed by trypan blue dye exclusion using a hemocytometer (Stiles, 1986).

Apoptosis Assay

Jurkat cells (5 x 10^5/ml) were cultured in 96 well plates (300 μl/well) as described. Apoptotic cells were quantitated by fluorescence microscopy as described by Duke and Cohen (1995). Microtiter plates were centrifuged at 450 x g for 10 min and 250 μl of supernatant was removed. Five μl of DNA staining reagent (acridine orange (100 μg/ml) and ethidium bromide (100 μg/ml) in 0.01 M PBS) was added to each well. Cells were classified as apoptotic or normal based on chromatin organization. A normal nucleus appeared small and highly condensed or fragmented. Percent apoptosis was calculated as follows: number of cells with apoptotic nuclei/total cell number x 100.

MTT conversion assay for cytotoxicity

Following treatment, 20 μl of a 5 mg/ml solution of 3- (4,5 dimethylthiazol-2-ul)-2,5-diphenyl tetrazolium bromide (MTT) in 0.01 M PBS was added to each well for the final 4 h of the 18 h incubation period (Marin, et al., 1996). Microtiter plates were centrifuged at 450 x g for 20 min and media was aspirated to minimize formazan crystal

loss. The resultant crystals were dissolved in 150 µl DMSO for 15 min. Optical density was measured using a Vmax Microplate Reader (Molecular Devices, Menlo Park, CA) at dual wavelengths, 570 nm and 690 nm. Percent control response was calculated as follows: ((1-absorbance of treatment/absorbance of control) x 100).

Spectrofluorometric detection of intracellular Ca^{2+}

Intracellular Ca^{2+} was measured as described by McCormack and Cobbold (1991). Cells (1 x 10^7) were resuspended in 0.75 ml of incubation media (120 mM NaCl, 20 mM HEPES, 4.7 mM KCl, 1.2 mM KH^2PO_4, 1.2 mM $MgSO_4$, 1.25 mM $CaCl_2$, 10 mM glucose, pH 7.4 containing 2% (w/v) bovine serum albumin (BSA)) and combined with 0.25 ml of loading solution (containing a final concentration of 0.025% pluronic F127 and 20 µM Fluo-3-AM in incubation buffer) for 30 min at 35°C water bath. Cells were then washed three times at 450 x g in incubation media without BSA and diluted to a concentration of 2 x 10^6/ml. Cells (150 µl/well) were aliquoted into Fluoronunc 96 well plates (Fisher Scientific, Pittsburgh, PA). Background fluorescence was recorded (485 nm excitation, 534 nm emission) using a CytoFluor II microwell fluorescence reader and the CytofluorII software Version 2.0 (Biosearch Incorporated, Bedford, MA). When baseline fluorescence stabilized, ionomycin (positive control), VT, TNF-α, or combination treatments were added and fluorescence intensity was recorded at several time points.

Spectrofluorometric detection of reactive oxygen species (ROS)

Intracellular levels of reactive oxygen species (ROS) were monitored spectrofluorometrically (Kim et al., 1996) as described above for intracellular Ca^{2+}

detection. Briefly, cells were resuspended in 0.75 ml of incubation media and combined with 0.25 ml of loading solution (containing dichlorofluorescin diacetate (DCFDA) in incubation buffer) for 15 min at 35°C water bath. Cells were then washed three times as described, diluted to a concentration of 2 x 10^6/ml, and aliquoted into fluoronunc 96 well plates. When baseline fluorescence stabilized, H_2O_2 (positive control), VT, TNF-α, or combination treatments were added and fluorescence intensity was recorded at several time points.

Western blot analysis for mitogen activated protein kinase (MAPK) and Bcl_2 expression

Phosphorylation of MAPKs or alterations in Bcl_2 were assessed by Western blotting using phospho-p44/p42 ERK, phospho-p38 MAPK, phospho-JNK specific rabbit IgG antibody (Cell Signaling, Beverly, MA) or Bcl_2 (Santa Cruz Biotech, Santa Cruz, CA) as previously described (Yang et al., 2000). Briefly, cells were suspended in lysis buffer (10 mM Tris pH 7.4, 1 mM sodium orthovanadate, 1% (w/v) SDS) on ice for 30 min and sonicated. Lysates were centrifuged at 4000 x g for 5 min at 4°C and protein concentration in the supernatant was determined using a Bio-Rad Protein Assay kit (Bio-Rad Laboratories, Melville, NY). Total cell lysates (10 μg) were resolved using 10% (w/v) SDS-PAGE. Gels were electrophorhetically transferred to polyvinylidene difluoride membrane (PVDF). Membranes were probed with the primary antibodies (1:1000 dilution) described above and stripped per manufacturer's protocol and probed with p44/p42 MAPK specific antibody (Santa Cruz Biotech), p38 MAPK specific antibody (Cell Signaling) and JNK specific antibody (Santa Cruz Biotech) diluted 1:1000 and recognizing both phosphorylated and unphosphorylated forms of each MAPK to verify total MAPK protein levels. To verify loading for Bcl_2, membranes were stripped

as described and probed with actin specific antibodies diluted 1:2000 (Cell Signaling). After incubation with horseradish peroxidase-conjugated anti-rabbit IgG antibodies diluted 1:2000 (Cell Signaling), the membrane was developed with a chemiluminescence detection kit (Amersham, Arlington Heights, IL).

Fluorescence assay for caspase-3 activity

DEVD-specific caspase activity was measured as previously described (Shifrin and Anderson, 1999). Cells (5 x 10^5/ml) were resuspended in 0.1 ml of lysis buffer (20 mM HEPES, pH 7.1, 1% (v/v) Triton X 100, 10 mM KCl, 1.5 mM $MgCl_2$, 1 mM EDTA, 1 mM EGTA, 1 mM dithiothreitol, 0.1 mM phenylmethylsulfonyl fluoride, 5 μg/ml pepstatin, 10 μg/ml leupeptin, 2 μg/ml aprotinin, 25 ug/ml N-acetyl-leu-leu-norleucinal (Calbiochem)), incubated on ice for 10 min, vortexed for 5 s and lysates were clarified for 10 min at 4000 x g at 4°C. DEVD-specific activity was determined by mixing 50 μg of protein with 0.2 ml of reaction buffer (100 mM HEPES, pH 7.1, 10% sucrose, 0.1% CHAPS, 10 mM dithiothreitol, 0.1 mg/ml bovine serum albumin and 2 μM DEVD-AMC) and incubating at 30°C for 20 min. Caspase activity was calculated by measuring fluorescence of released AMC with excitation at 360 nm and emission at 460 nm.

Statistical analysis

The data were analyzed using Systat version 5.0 (Evanston, IL). A Student's t test was used to compare two groups while multiple groups were compared using a one way analysis of variance (ANOVA) and a Tukey test for mean separation. A p value < 0.05 was considered statically significant. Samples receiving two treatments were analyzed

for synergy/potentiation by randomly combining single treatment replicates to calculate an expected mean additive response with variance. This calculated value was compared to actual co-treated samples using a Mann Whitney Rank Sum test. A p value < 0.05 was considered statistically significant.

RESULTS

Time course of VT-induced apoptosis

VT induces apoptosis in both murine and human leukocytes in vitro (Yang et al., 2000; Shifrin and Anderson, 1999) and in vivo (Zhou et al., 2000). The dose dependent induction of apoptosis in Jurkat cells over a 24 h period was characterized. Apoptotic cell morphology, assessed by fluorescence microscopy, was significantly increased over the untreated controls by 6 h of exposure to VT (500 - 1000 ng/ml, Figure 5.1 A). This elevation in apoptosis was observed throughout the remaining 24 h sample period. VT (100 ng/ml) did not significantly alter Jurkat cell morphology up to 24 h of exposure.

Similarly, a significant increase in apoptosis was observed in cells exposed to VT plus TNF-α between 6 - 24 h of exposure (Figure 5.1 B). The observed apoptosis was significantly higher than apoptosis induced by either mediator alone between 15 to 24 h. VT (250 ng/ml) alone significantly increased apoptosis between 15 - 24 h, while TNF-α had no effect. Percentages of Jurkat apoptosis at 18 h for the untreated control, VT (250 ng/ml), TNF-α (20 ng/ml), and the combination were 2.1%, 18.2%, 0.8%, and 40.2% respectively. The expected mean additive increase over the untreated control after exposure to the combined toxins was 16.9%. Statistical analysis of the apoptosis data indicated TNF-α potentiated VT-induced Jurkat apoptosis ($p<0.05$). The signal

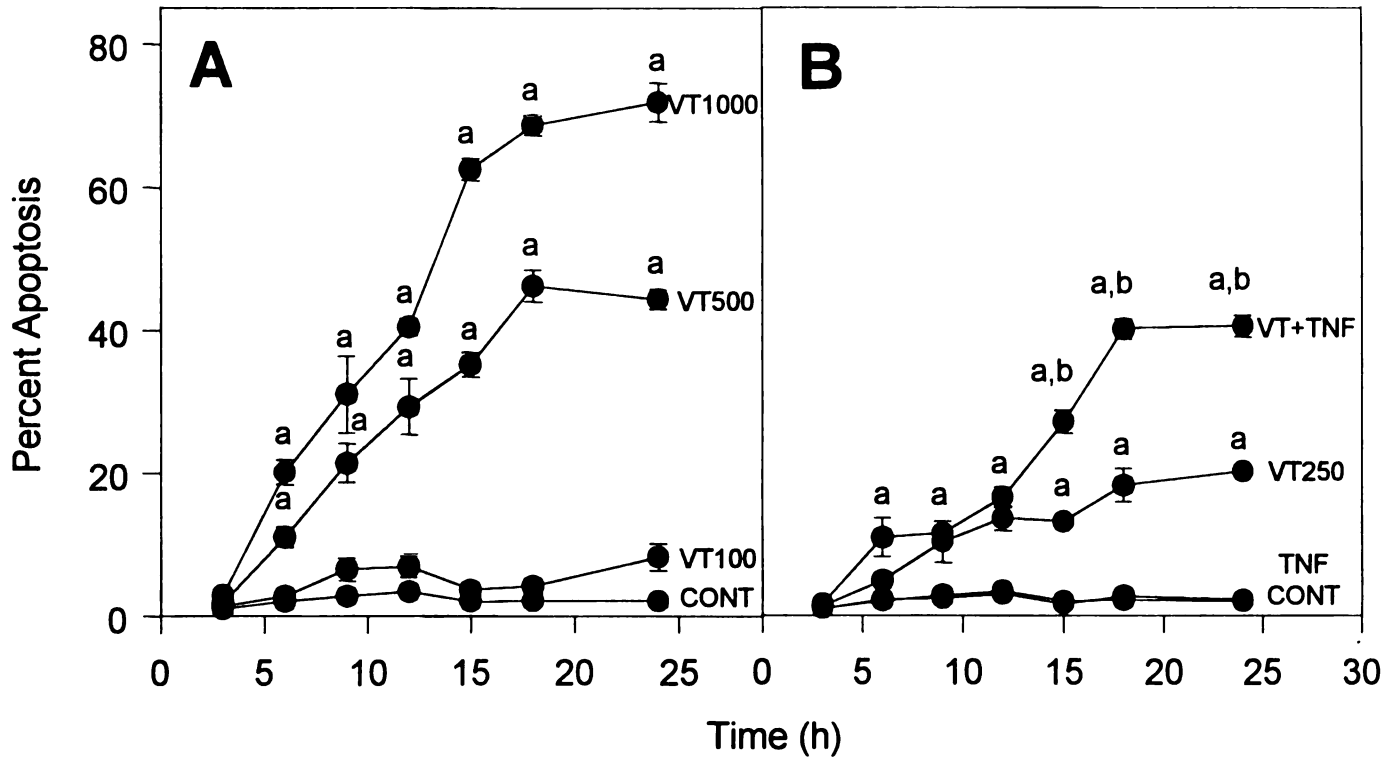

Figure 5.1. Time course of VT-induced apoptosis in Jurkat T cells: dose dependence (A) and potentiation by TNF-α (B). Jurkat cells were exposed to VT (0-1000 ng/ml), TNF-α (20 ng/ml) or VT (250 ng/ml) plus TNF-α (20 ng/ml) for 24 h. Percent apoptosis was assessed by fluorescence microscopy at various time intervals (3-24 h). Data (n=6) represent the mean ± SEM. [a]A Student's t test was used to determine values significantly different from the untreated control. [b]ANOVA was used to compare VT (250 ng/ml), TNF-α (20 ng/ml), and VT plus TNF-α treatments.

transduction mechanisms involved in the induction of apoptosis by VT alone and in the presence of TNF-α were further investigated.

Intracellular calcium modulation by VT

Disruption of calcium homeostasis is frequently associated with cell injury and apoptosis in a variety of tissues (Penninger and Kroemer, 1998). A rapid, transient increase of intracellular Ca^{2+} was reported following exposure to the trichothecene T-2 toxin in HL-60 cells prior to the induction of apoptosis (Yoshino et al., 1996).

Apoptosis induction was further characterized using pharmacological inhibitors. Jurkat cells were treated with each inhibitor for 1 h prior to the addition of VT (500 ng/ml) or co-incubated for 18 h. The intracellular calcium chelator, BAPTA-AM (10 – 25 M) did not significantly influence VT (500 ng/ml)-induced apoptosis or cytotoxicity (Figure 5.2 A). In contrast, the potentiation of VT (250 ng/ml)-induced apoptosis by TNF-α could be significantly reduced following a 1 h pretreatment with BAPTA-AM (10 – 25 mM; Figure 5.2 B). In addition, BAPTA-AM (25 mM) significantly decreased VT plus TNF-α-induced cytotoxicity (Table 5.1).

The role of Ca^{2+} in VT and VT plus TNF-α-induced apoptosis was further assessed. Jurkat cells were loaded with FLUO-3-AM, a fluorogenic calcium probe. Following loading, cells were treated with VT, TNF-α, VT plus TNF-α, or ionomycin as a positive control. VT, TNF-α, or VT plus TNF-α did not significantly alter fluorescence intensity following 10 min of exposure (data not shown, Figure 5.3). Ionomycin induced a rapid increase in fluorescence intensity that peaked at 7 min of exposure and was maintained through 10 min. The results suggest intracellular calcium increases did not

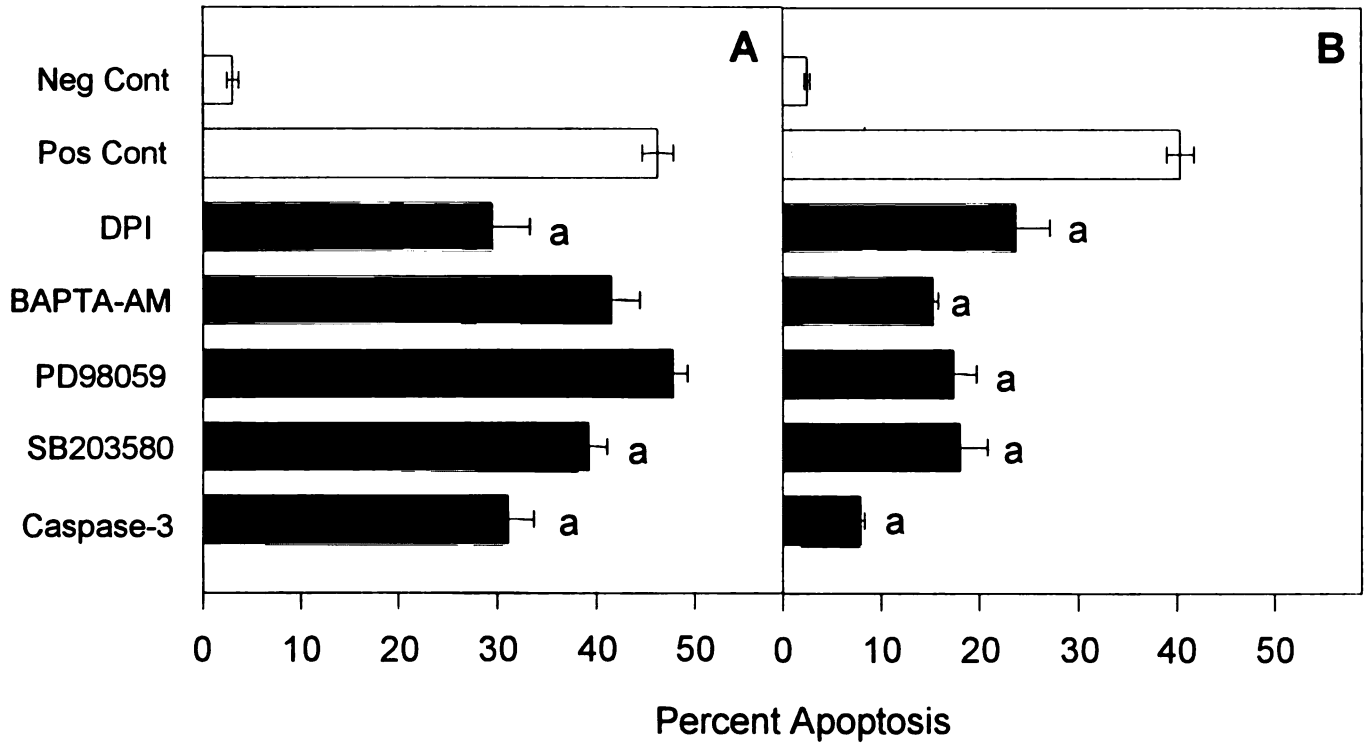

Figure 5.2. Inhibition of VT-induced apoptosis by pharmacological agents. Jurkat cells were pretreated 1 h with each pharmacological agent and exposed to media (negative control), VT (500 ng/ml, positive control, A), or VT (250 ng/ml) plus TNF-α (20 ng/ml, positive control B) for 18 h. Percent apoptosis was assessed by fluorescence microscopy. Data (n=6) represent the mean ± SEM. [a]A Student's t test was used to determine values significantly different from the respective positive control.

Table 5.1. Dose response relationships of pharmacological inhibitors (1 h pre-incubation) on VT-induced cytotoxicity measured by MTT conversion assay.

Treatment	VT (500 ng/ml) Percent Control Response	VT (250 ng/ml) + TNF-α (20 ng/ml) Percent Control Response
DPI 0 μM	23.8 ± 2.4	35.5 ± 1.7
DPI 10 μM	25.2 ± 0.3	45.2 ± 0.7[a]
DPI 25 μM	24.6 ± 1.8	41.0 ± 2.4
DPI 50 μM	12.5 ± 0.4	49.2 ± 3.0[a]
BAPTA-AM 0 μM	23.2 ± 0.9	35.3 ± 1.6
BAPTA-AM 10 μM	21.9 ± 0.9	39.1 ± 2.0
BAPTA-AM 25 μM	24.8 ± 0.7	46.9 ± 0.8[a]
BAPTA-AM 50 μM	25.6 ± 2.2	31.1 ± 0.8
PD98059 0 μM	29.9 ± 4.5	52.7 ± 2.8
PD98059 10 μM	38.1 ± 3.7	58.7 ± 1.2
PD98059 25 μM	37.0 ± 3.4	57.4 ± 2.8
PD98059 50 μM	32.1 ± 1.2	54.1 ± 4.3
SB203580 0 μM	32.9 ± 0.7	50.4 ± 2.8
SB203580 10 μM	51.0 ± 5.7[a]	65.7 ± 4.8[a]
SB203580 25 μM	58.4 ± 4.0[a]	86.1 ± 7.2[a]
SB203580 50 μM	48.9 ± 4.4[a]	84.5 ± 1.7[a]
Monensin 0 μM	25.5 ± 0.8	40.1 ± 3.2
Monensin 10 μM	25.4 ± 1.0	35.6 ± 1.6
Monensin 25 μM	22.5 ± 1	45.0 ± 0.8
Monension 50 μM	21.1 ± 0.2	29.6 ± 0.9

Data (n=3) represent mean percent control response ± SEM. [a]A Student's t test was used to determine values significantly different from the respective untreated control.

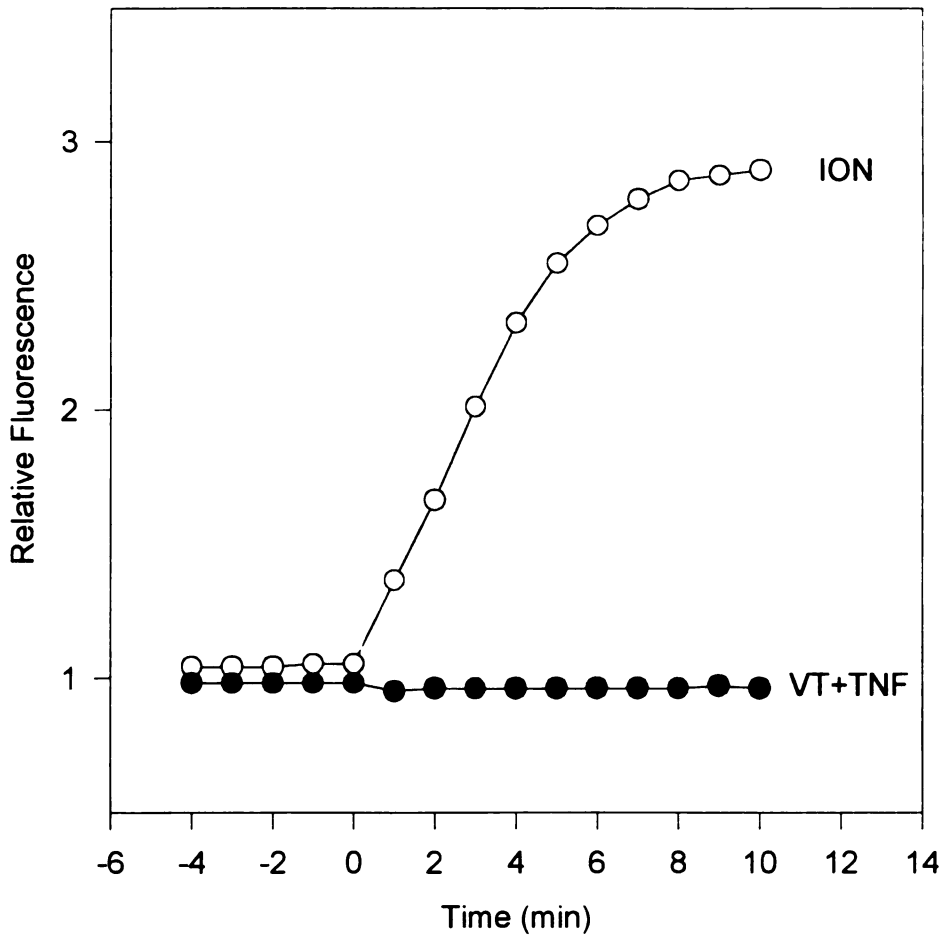

Fig 5.3. Intracellular calcium modulation by VT. Jurkat cells were loaded with FLUO-3-AM as described in Materials and Methods. When background fluorescence was stable, ionomycin (1 μM, positive control), VT (250 ng/ml), TNF-α (20 ng/ml), or VT (250 ng/ml) plus TNF-α (20 ng/ml) was added. Fluorescence intensity was monitored using a Cytofluor II microwell plate reader. Data (n=3) represents mean ± SEM.

occur as an early signal in VT (250 ng/ml)-, TNF-α-, or VT plus TNF-α-induced apoptosis.

Alterations in reactive oxygen species (ROS) by VT

Reactive oxygen species (ROS) are generated during mitochondrial respiration and have been implicated in cellular signaling including the induction of apoptosis (Davis et al., 2001). Suneja et al. (1989) reported free radical generation following oral exposure to trichothecenes in a rat model. In the present study, apoptosis induction by VT (500 ng/ml) was significantly reduced by pretreatment with DPI (10 μM), an irreversible inhibitor of NADPH oxidoreductase (Figure 5.2 A). However, cytotoxicity was significantly increased when cells were co-incubated with DPI (50 μM) and VT (500 ng/ml) (Table 5.1). The potentiation of VT (250 ng/ml)-induced apoptosis by TNF-α could be significantly reduced following a 1 h pretreatment with DPI (10 μM; Figure 5.2 B). In addition, DPI (10, 50 μM) significantly decreased VT plus TNF-α-induced cytotoxicity (Table 5.1).

To further assess the role of ROS, Jurkat cells were loaded with DCFDA, a fluorogenic oxygen radical probe. Following loading, cells were treated with VT (0 - 1000 ng/ml), TNF-α, VT (250 ng/ml) plus TNF-α, or H_2O_2 as a positive control. VT, TNF-α, or VT plus TNF-α did not significantly alter fluorescence intensity following 5 min of exposure (data not shown, Figure 5.4). H_2O_2 induced a rapid increase in fluorescence intensity. The results suggest generation of ROS did not occur as an early signal in VT- or VT plus TNF-α-induced apoptosis.

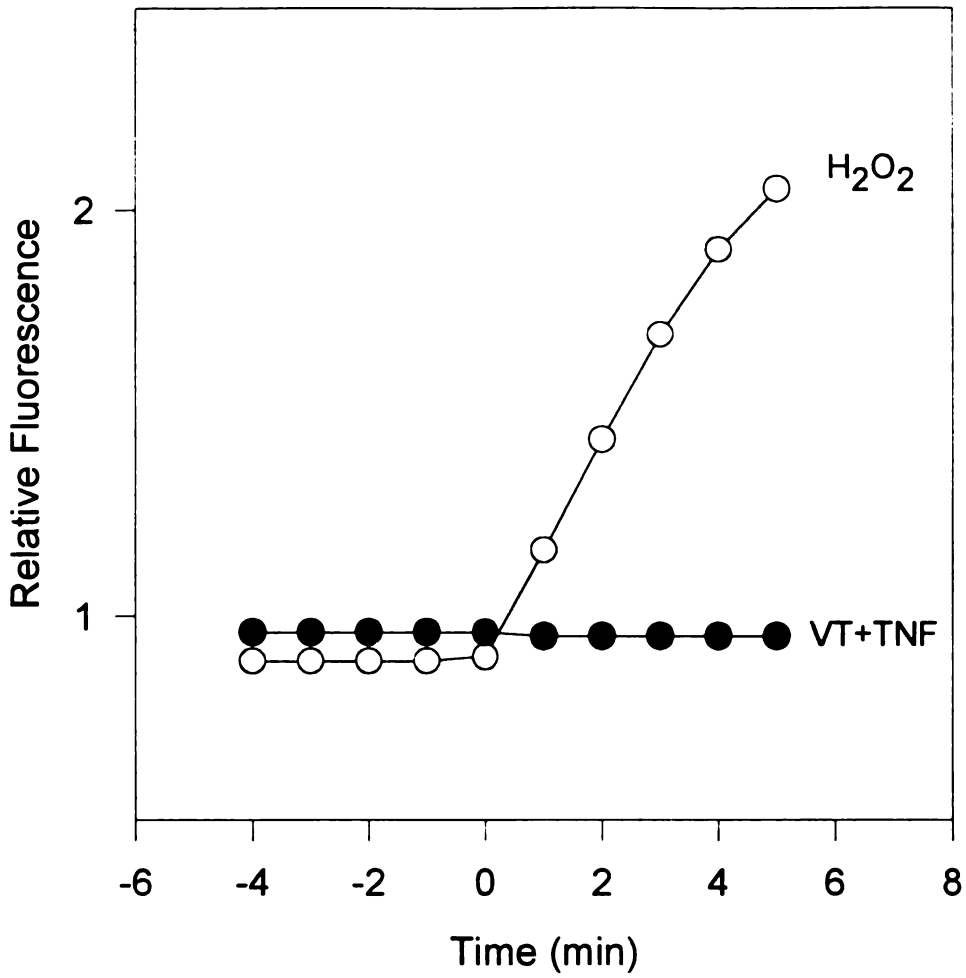

Figure 5.4. Elevation of reactive oxygen species (ROS) by VT. Jurkat cells were loaded with DCFDA as described in Materials and Methods. When background fluorescence was stable, H_2O_2 (1 μM, positive control), VT (0 - 10 μg/ml), TNF-α (20 ng/ml), or VT (250 ng/ml) plus TNF-α (20 ng/ml) was added. Fluorescence intensity was monitored using a Cytofluor II microwell plate reader. Data (n=3) represents mean ± SEM.

VT-induced activation of ERK 1/2

The MAPKs, ERK1/2, have been linked to the induction of negative selection in thymocytes (Bommhardt et al., 2000), apoptosis induced by loss of anchorage (Zugasti et al., 2001), and activation-induced cell death in Jurkat cells (van den Brink, et. al, 1999). Several trichothecenes induce ERK1/2 (Yang et al., 2000). In the present study MEK1 inhibitor PD98059 (10 μM) did not significantly influence VT-induced apoptosis when cells were pre-treated for 1 h. Similarly, pre-incubation with PD98059 (10 – 50 μM) did not alter VT-induced cytotoxicity. However, co-incubation with 0.1 μM PD98059 protected Jurkat cells from VT-induced cytotoxic effects (Table 5.2).

Western blot analysis of VT treated cells demonstrated ERK 2 phosphorylation between 0.25 - 4 h in cells treated with VT 250 and 500 ng/ml (Figure 5.5 A). ERK 2 was up-regulated between 0.25 - 1 h in cells treated with VT (1000 ng/ml). VT (100 ng/ml), a dose that does not alter apoptotic cell morphology, did not significantly change ERK1/2 phosphorylation up to 4 h after treatment. Comparison of the treatments at 0.25, 1, and 2 h did not demonstrate dose-dependent phophorylation of ERK 2 (data not shown, Figure 5.5 B) possibly due to maximal activation by 0.25 h.

The potentiation of VT (250 ng/ml)-induced apoptosis by TNF-α could be significantly reduced following a 1 h pretreatment with PD98059 (10 μM; Figure 5.2 B). Pre-incubation with PD98059 did not significantly alter VT plus TNF-α-induced cytotoxicity. However, 18 h co-incubation with PD98059 (0.1 μM) resulted in a significant decrease in MTT-based cytotoxicity for VT plus TNF-α treated cells (Table 5.2). Western blot analysis of VT plus TNF-α treated cells demonstrated ERK 2 phosphorylation was up-regulated between 0.25 - 1 h (Figure 5.5 A). TNF-α (20 ng/ml) did not activate ERK1/2 at any time point tested (0 - 4 h, data not shown). Total ERK1/2

Table 5.2. Dose response relationships of several pharmacological inhibitors (18 h co-incubation) on VT-induced cytotoxicity measured by MTT conversion assay.

Treatment	VT (500 ng/ml) Percent Control Response	VT (250 ng/ml) + TNF-α (20 ng/ml) Percent Control Response
No Treatment	64.35 ± 2.50	74.93 ± 4.39
DPI 1 μM	64.92 ± 6.01	57.41 ± 8.97
DPI 0.1 μM	61.65 ± 8.71	83.48 ± 12.15
PD98059 1 μM	51.55 ± 2.85	58.52 ± 5.13
PD98059 0.1 μM	80.94 ± 3.85[a]	104.41 ± 5.36[a]
SB203580 1 μM	53.99 ± 6.71	58.06 ± 3.44
SB203580 0.1 μM	68.82 ± 10.99	79.38 ± 7.21
Monensin 1 μM	37.37 ± 0.46	67.97 ± 5.29
Monensin 0.1 μM	74.04 ± 5.05	78.00 ± 6.06

Data (n=3) represent mean percent control response ± SEM. [a]A Student's t test was used to determine values significantly different from the respective untreated control.

Figure 5.5. VT-induced phosphorylation of ERK1/2 . Lysates (10 μg) from Jurkat cells were incubated in the absence and presence of VT (100 - 1000 ng/ml), TNF-α (20 ng/ml), or VT (250 ng/ml) plus TNF-α (20 ng/ml) for 0 - 4 h (A). Dose dependent increases in p-ERK after 15 min of exposure (B) were investigated by Western blot analysis using phospho-specific ERK1/2 antibodies as described. Anisomycin (AN) was used as a positive control. The blots were stripped and total ERK levels were confirmed using p44/p42 specific antibodies recognizing both phosphorylated and unphosphorylated forms (B, second panel). Two bands were detected corresponding to ERK1/2. Results are representative of two experiments.

A

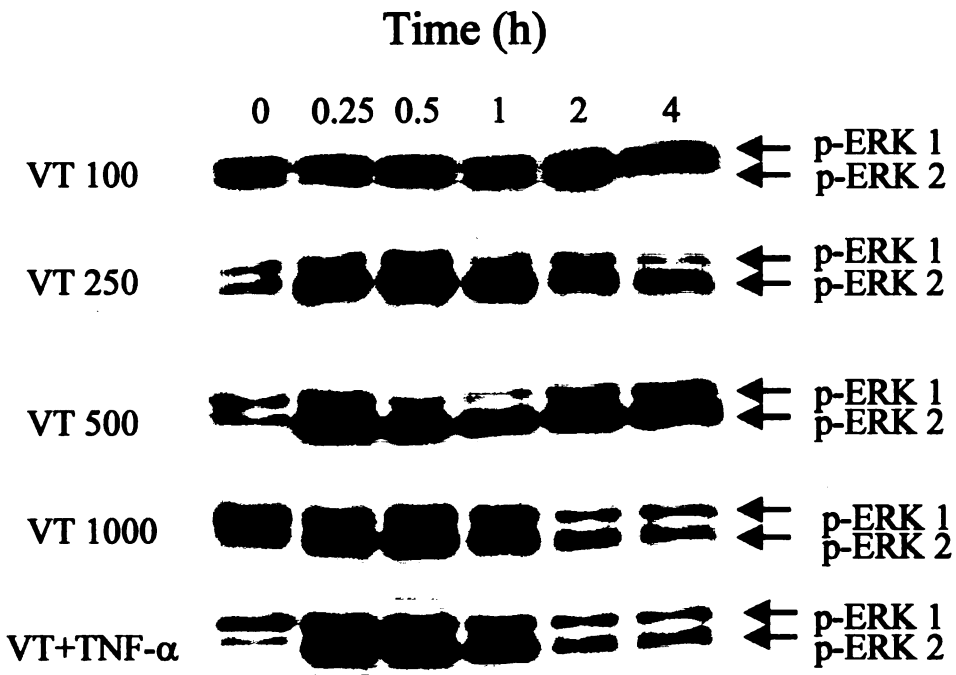
Time (h)
0
0.25
0.5
1
2
4
VT 100
VT 250
VT 500
VT 1000
VT+TNF-α
p-ERK 1
p-ERK 2

B

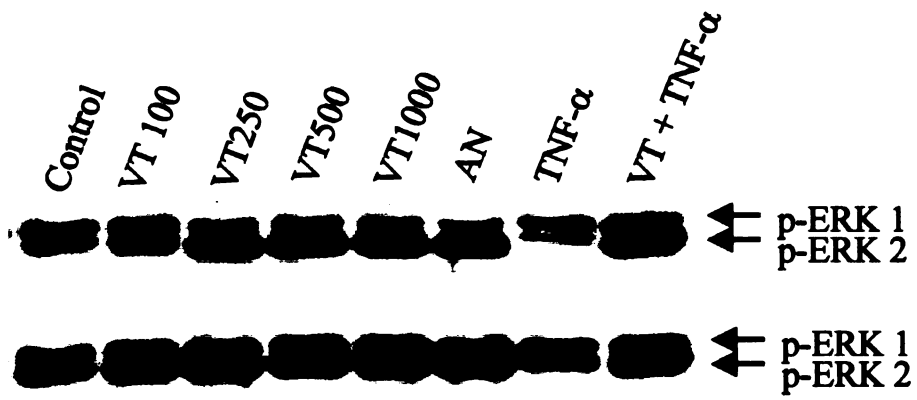
Control
VT 100
VT250
VT500
VT1000
AN
TNF-α
VT + TNF-α
p-ERK 1
p-ERK 2
p-ERK 1
p-ERK 2

(phosphorylated and unphosphorylated) was confirmed to be unchanged by the various treatments in Figure 5.5 B (second panel). These results suggest a role for ERK 2 in VT and VT plus TNF-α-induced apoptosis.

VT-induced activation of p38 and JNK 1/2

Activation of p38 and JNK MAPK is associated with stress stimuli such as UV radiation, heat shock, cytokines, and osmotic shock (Kortenjann and Shaw, 1995). Trichothecenes induce a ribotoxic stress response that activates both p38 and JNK (Shifrin and Anderson, 1999; Yang et al., 2000). Shifrin and Anderson (1999) demonstrated phosphorylation of p38 and JNK substrate c-Jun after 2 h of exposure to 3 μg/ml VT. Yang, et al (2000) could not detect p38 or JNK phosphorylation at a low VT (10 ng/ml) dose, but inhibited apoptosis induced by a high dose of VT (2.5 - 5 μg/ml) with SB203580.

In the present study, SB203580 (10 - 50 μM), a selective inhibitor of p38 MAPK kinase, significantly reduced VT-induced apoptosis and cytotoxicity when pre-incubated with cells 1 h prior to the addition of toxin. Western blot analysis of p38 indicated a prolonged phosphorylation of p38 between (0 - 4 h) in cells treated with 250 - 1000 ng/ml VT (Figure 5.6 A). VT (100 ng/ml) transiently increased p-p38 with maximal phosphorylation at 1 h. A dose dependent increase in p-p38 was observed after 2 h exposure (Figure 5.6 B). Total p38 (phosphorylated and unphosphorylated) was confirmed to be unchanged in Figure 5.6 B (second panel).

The potentiation of VT (250 ng/ml)-induced apoptosis by TNF-α could be significantly reduced following a 1 h pretreatment with SB203580 (10 μM, Figure 5.2 B). SB203580 (10 - 50 μM) significantly decreased VT plus TNF-α-induced

Figure 5.6. VT-induced phosphorylation of p38 MAPK. Lysates (10 μg) from Jurkat cells were incubated in the absence and presence of VT (100 - 1000 ng/ml), TNF-α (20 ng/ml), or VT (250 ng/ml) plus TNF-α (20 ng/ml) for 0 - 4 h (A). Dose dependent increases in p-p38 after 2 h of exposure (B) were investigated by Western blot analysis using phospho-specific p38 MAPK antibodies as described. Anisomycin (AN) was used as a positive control. The blots were stripped and total p38 levels were confirmed using p38 specific antibodies recognizing both phosphorylated and unphosphorylated forms (B, second panel). One band was detected corresponding to p38. Results are representative of two experiments.

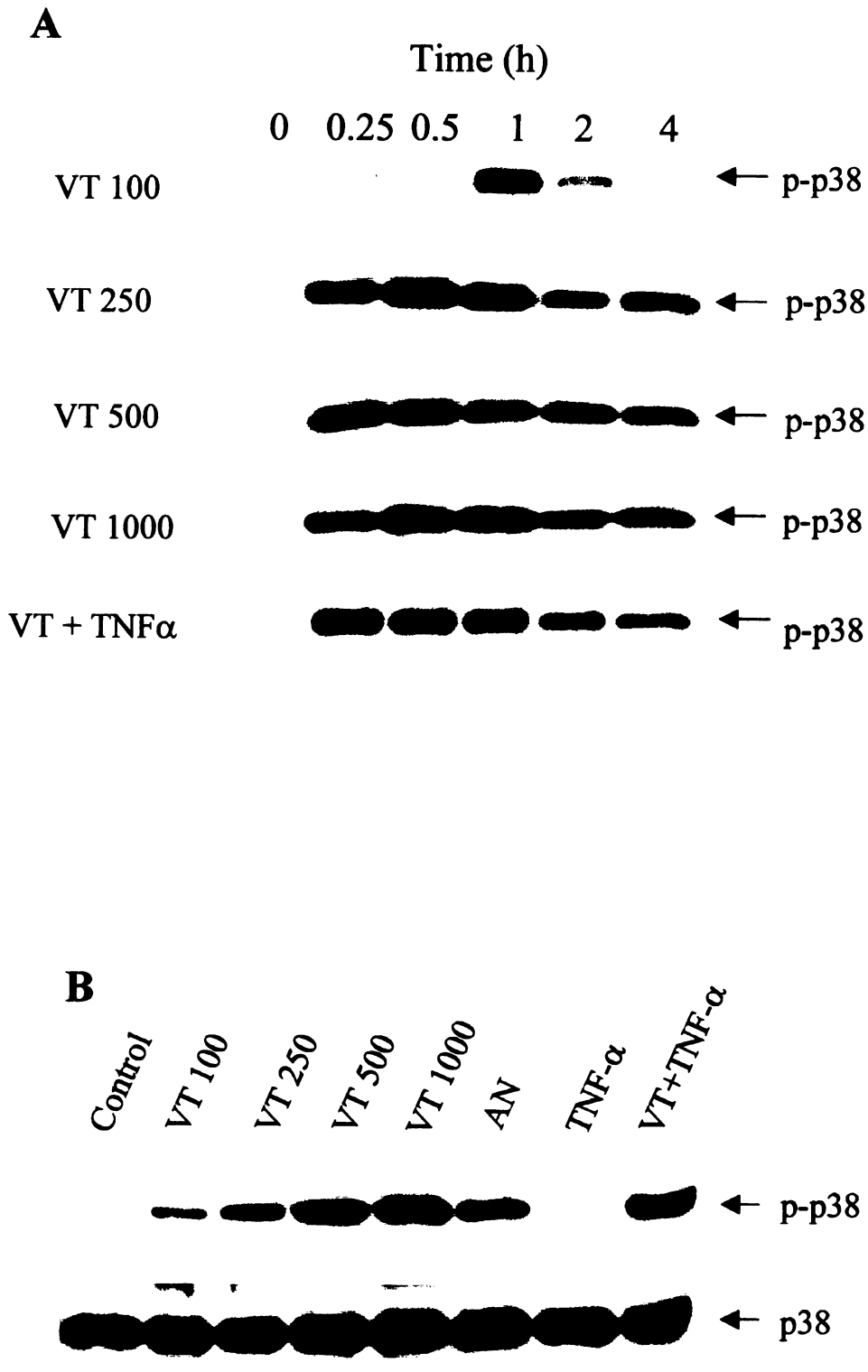
A
Time (h)
0 0.25 0.5 1 2 4
VT 100
VT 250
VT 500
VT 1000
VT + TNFα
p-p38
B
Control
VT 100
VT 250
VT 500
VT 1000
AN
TNF-α
VT+TNF-α
p-p38
p38

cytotoxicity (Table 5.1). A prolonged activation of p38 between (0 - 4 h) was observed in cells treated with VT plus TNF-α (Figure 5.6 A). In addition, the combination of VT plus TNF-α increased p-p38 expression greater than either individual treatment alone (Figure 5.6 B).

Phosphorylation of JNK1/2 was observed between 0.25 - 2 h following VT (500 - 1000 ng/ml) exposure. VT (250 ng/ml) transiently increased p-JNK (0.25 - 1 h) while VT (100 ng/ml) induced activation at 1 h (Figure 5.7 A). A dose dependent activation of JNK was demonstrated following 2 h VT exposure (Figure 5.7 B). Total JNK (phosphorylated and unphosphorylated) was confirmed to be unchanged in Figure 5.7 B (second panel).

VT plus TNF-α transiently increased p-JNK (0.25 - 1 h). Induction of JNK at 2 h by VT plus TNF-α resembled the individual VT (250 ng/ml) treatment. TNF-α did not induce significant phosphorylation of JNK at any time point tested (0 – 4 h). These results support a role for stress-activated p38 and JNK in VT and VT plus TNF-α-induced T cell apoptosis.

Modulation of Bcl_2 expression by VT

Bcl_2 family of proteins encompasses both anti-apoptotic and pro-apoptotic members that control the involvement of the mitochondria in the apoptotic process by controlling the formation of pores in the membrane (Tsujimoto and Shimizu, 2000). Bcl_2 expression in VT-treated Jurkat cells was further assessed. Bcl_2 expression was not significantly altered in cells exposed to VT (500 ng/ml) or VT plus TNF-α (data not shown) Bcl_2 levels in cells treated with 1000 ng/ml VT were unchanged between 0 - 15 h (Figure 5.8). Levels dropped significantly at 18 h which corresponded to approximately

Figure 5.7. VT-induced phosphorylation of JNK1/2. Lysates (10 μg) from Jurkat cells were incubated in the absence and presence of VT (100 - 1000 ng/ml), TNF-α (20 ng/ml), or VT (250 ng/ml) plus TNF-α (20 ng/ml) for 0 - 4 h (A). Dose dependent increases in p-JNK after 2 h of exposure (B) were investigated by Western blot analysis using phospho-specific JNK antibodies as described. Anisomycin (AN) was used as a positive control. The blots were stripped and total JNK levels were confirmed using JNK1/2 specific antibodies recognizing both phosphorylated and unphosphorylated forms (B, second panel). Two bands were detected corresponding to JNK 1/2. Results are representative of two experiments.

A

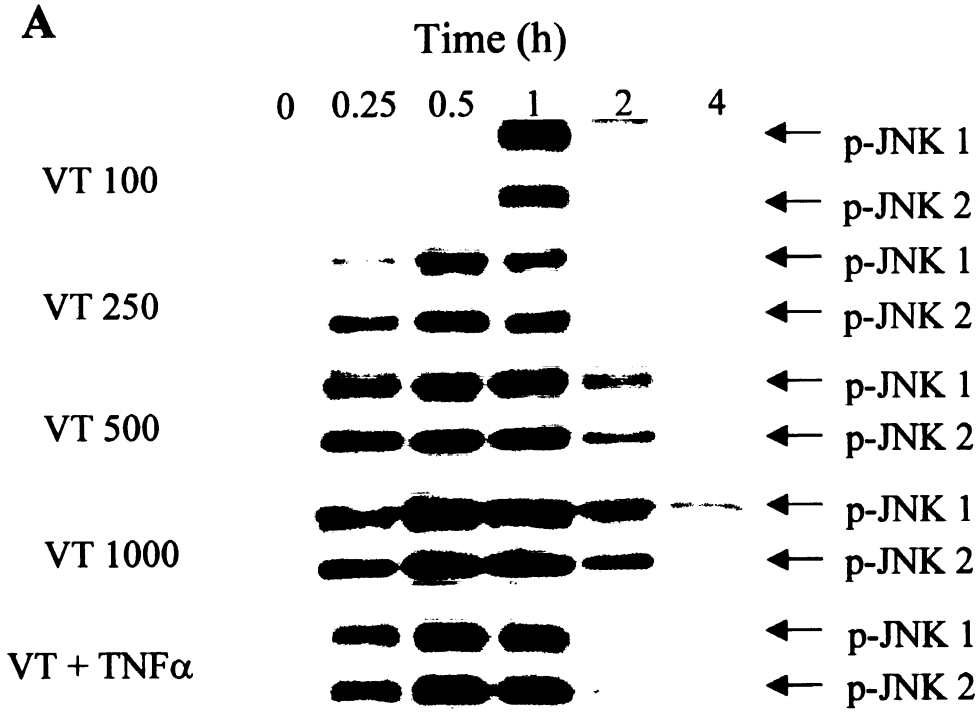
Time (h)
0
0.25
0.5
1
2
4
VT 100
VT 250
VT 500
VT 1000
VT + TNFα
p-JNK 1
p-JNK 2
p-JNK 1
p-JNK 2
p-JNK 1
p-JNK 2
p-JNK 1
p-JNK 2
p-JNK 1
p-JNK 2

B

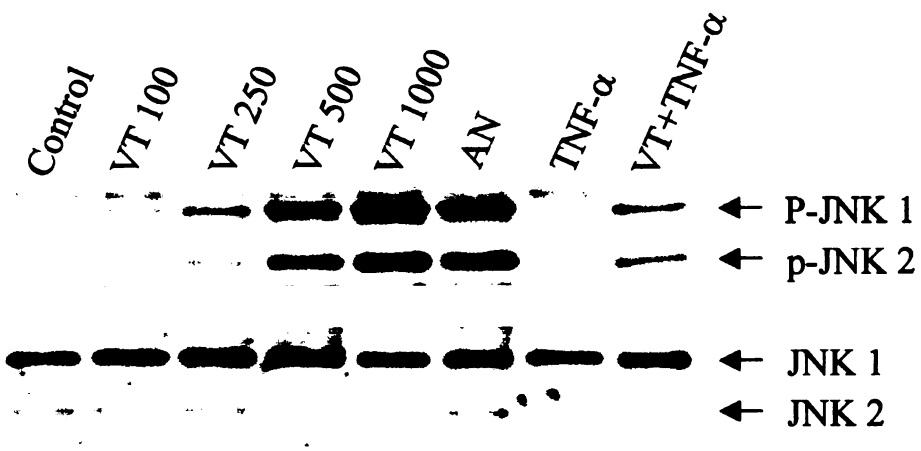
Control
VT 100
VT 250
VT 500
VT 1000
AN
TNF-α
VT+TNF-α
P-JNK 1
p-JNK 2
JNK 1
JNK 2

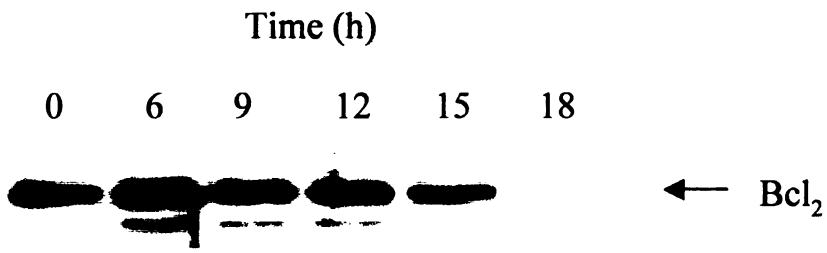

Figure 5.8. Modulation of Bcl_2 expression by VT. Lysates (10 μg) from Jurkat cells were incubated in the absence or presence of VT (1000 ng/ml) up to 18 h. Alterations in Bcl_2 expression were analyzed by Western blot analysis. One band was detected corresponding to Bcl_2. Results are representative of two experiments.

70% apoptotic morphology in the cell population. The results suggest Bcl_2 did not play a role in VT-induced or VT plus TNF-α-induced apoptosis and support a previous study (Okumura et al., 2000) in which Bcl_2 levels were not altered in T-2 toxin induced apoptosis.

VT-induced activation of caspase-3

Activation of caspases during apoptosis results in the cleavage of cellular substrates critical for the development of an apoptotic morphology (Cohen, 1997). Several trichothecene mycotoxins activate caspases (Shifrin and Anderson, 1999). In the present study, Caspase-3 Inhibitor I (10 μM), a reversible Caspase-3 inhibitor, effectively reduced VT-induced apoptosis and VT plus TNF-α induced apoptosis (Figure 5.2). Caspase activation was not elevated following 1 h exposure to VT (data not shown). However, significant increases in caspase activation were noted at 3 and 5 h exposure to VT (500 - 1000 ng/ml; Figure 5.9 A) and VT plus TNF-α (Figure 5.9 B). Caspase activation by VT plus TNF-α was significantly greater than either individual treatment alone. Caspase substrate cleavage remained elevated at 7 h post-exposure (data not shown). VT (100 ng/ml) and TNF-α alone did not induce measurable caspase substrate cleavage.

The ability of pharmacological inhibitors to block caspase activation was evaluated. Monensin, DPI, and BAPTA-AM did not significantly alter caspase substrate cleavage at 3 h (Table 5.3). MAPK inhibitors SB203580 and PD98059 did not reduce VT (500 ng/ml) caspase activation (Table 5.4). However, VT plus TNF-α-induced caspase fluorescence was significantly reduced by SB203580. These results support previous studies indicating a role for caspase activation in trichothecene-induced

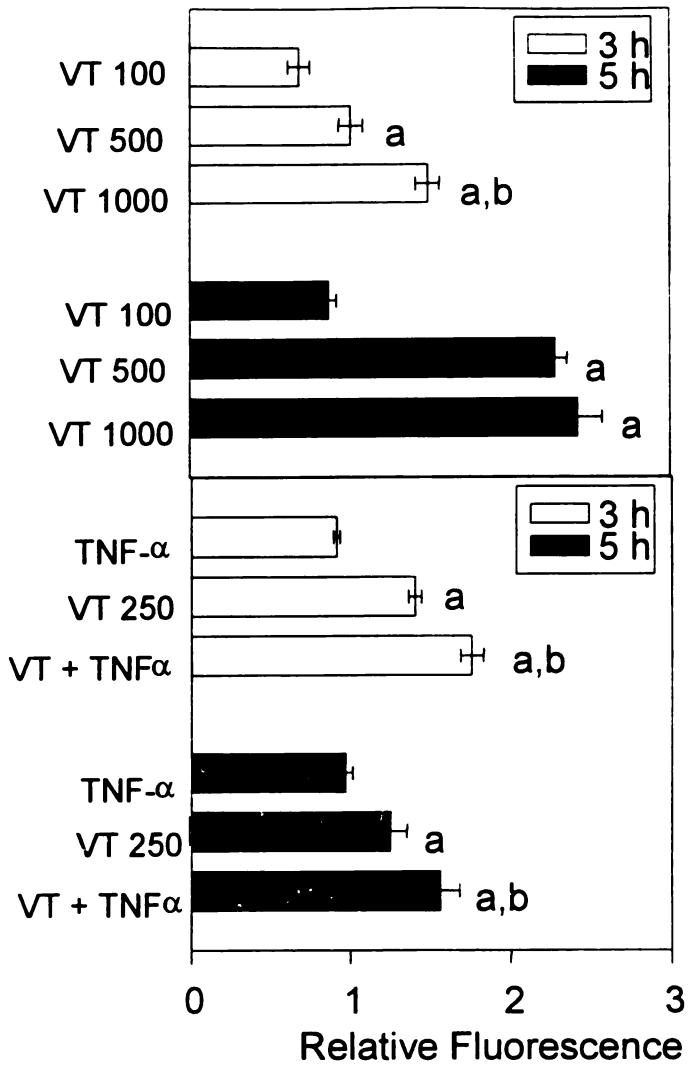

Figure 5.9. VT-induced activation of Caspase-3. Jurkat cells were treated with VT (0 - 1000 ng/ml), TNF-α (20 ng/ml), or VT (250 ng/ml) + TNF-α (20 ng/ml) for 3 or 5 h. Cell lysates (50 μg) were incubated with fluorogenic caspase substrate DEVD-AMC (2 μM) as described. Fluorescence intensity was measured using a Cytofluor II microwell plate reader. Data (n=6) represents mean fluorescence intensity ± SEM. [a] A Student's t test was used to determine values significantly different from the untreated control. [b]ANOVA was used to compare VT (250 ng/ml), TNF-α (20 ng/ml), and VT plus TNF-α treatments.

Table 5.3. Effect of pharmacological inhibitors on VT-induced caspase-3 activity.

Treatment	VT (500 ng/ml) Relative Fluorescence	VT (250 ng/ml) + TNF-α (20 ng/ml) Relative Fluorescence
No Treatment	1.6 ± 0.09	1.7 ± 0.09
Monensin 10 μM	1.77 ± 0.02	1.67 ± 0.01
DPI 40 μM	1.63 ± 0.04	1.58 ± 0.09
BAPTA-AM 5 μM	1.85 ± 0.04	1.8 ± 0.03

Table 5.4. Effect of MAPK inhibitors on VT-induced caspase-3 activity.

Treatment	VT (500 ng/ml) Relative Fluorescence	VT (250 ng/ml) + TNF-α (20 ng/ml) Relative Fluorescence
No Treatment	1.46 ± 0.04	1.3 ± 0.04
SB230580 10 μM	1.3 ± 0.02	0.95 ± 0.01
PD98059 10 μM	1.56 ± 0.01	1.61 ± 0.04

apoptosis (Nagase et al., 2001; Shifrin and Anderson, 1999) that is partially mediated by p38 MAPK.

DISCUSSION

Vomitoxin (VT) is the most frequently encountered food-borne trichothecene worldwide (Rotter et al., 1996). Trichothecenes can impair immune function and exposure may increase an individual's susceptibility to *Candida*, *Salmonella*, and *Listeria* (Bondy and Pestka, 2000). TNF-α, a cytokine released under conditions of inflammation or environmental stress, may play a role in pathogen susceptibility following VT exposure. The potentiation of VT-induced apoptosis by TNF-α, suggests the possibility for ribotoxic stress response and cytokine signaling pathways to converge and contribute to immunosuppression. In addition, this interaction provides a model in which toxic effects of a chemical may be amplified by an immune or inflammatory response at the cellular level. This study addressed the kinetics of the second messengers intracellular $Ca^{2+}$and ROS, MAPK activation, Bcl_2 expression, and caspase enzymatic activity in the development of VT-induced T cell apoptosis to gain insight into mechanisms by which VT alters immune function and contributes to the manifestation of immune suppression.

Induction of intracellular $Ca^{2+}$and ROS has been implicated as both an early signal to activate MAPKs (Seo et al., 2001; Yu et al., 2000) or a late signal as a result of mitochondrial permeability (Castedo et al., 1996)) in the induction of apoptosis. Neither intracellular Ca^{2+} nor ROS increased during early exposure to VT. However, pre-incubation with BAPTA-AM significantly reduced VT plus TNF-α-induced apoptosis and cytotoxicity. Pre-incubation with DPI significantly reduced both VT (500

ng/ml) and VT plus TNF-α induced apoptosis. It is most likely that calcium and ROS may be increasing at a later time point during the apoptotic process. Our results differ from a previous report that the trichothecene T-2 toxin transiently increased intracellular calcium between 3 - 5 min of exposure in HL-60 cells (Yoshino et al., 1996). The reason for this difference may be stimulus dependent, cell-type specific effect, or due to assay sensitivity.

Intracellular $Ca^{2+}$and ROS are frequently associated with the development of irreversible damage to the mitochondria. Initially, increases in oxidant production by the mitochondria can no longer be inactivated by endogenous antioxidants (Chakraborti, et al, 1999). This stimulates a cascade of events involving calcium release from the mitochondria that stimulates calcium dependent proteases, nucleases, and phospholipases critical in the development of an apoptotic morphology. Pore formation in the mitochondrial membrane is mediated by the Bcl_2 protein family. In the present study, Bcl_2 levels were not altered by VT treatment suggesting another member of the Bcl_2 family may be important in trichothecene-induced apoptosis. In support of these findings, Okumura et al. (2000) could not demonstrate a role for Bcl_2 in T-2 toxin induced apoptosis.

Pore formation is followed by the release in cytochrome c and activation of the caspase family. Fluorogenic caspase substrate cleavage was significantly increased by VT following 3 h of toxin exposure and throughout the 7 h sample period. Caspase activation by 3 h is in agreement with previous studies in which caspase activation was increased by several trichothecenes by 3 h (Nagase et al., 2001; Shifrin and Anderson, 1999). Caspase activation induced by VT plus TNF-α at 3 and 5 h was significantly

increased over either individual treatment alone suggesting caspase activation may be a signaling step where ribotoxic stressors and cytokine signaling pathways converge.

MAPK phosphorylation appears to be an early, critical signal for the development of VT-induced apoptosis. Phosphorylation of several transcription factors by the MAPKs may be critical to cellular responses to stress or apoptosis (Widmann et al., 1999). For example, ERK1/2 activates Elk-1 and nur 77(Pavlovic et al., 2000; Widmann et al., 1999), p38 activates ATF-2 (Cho et al., 2001) and JNK activates c-Jun (Faris et al., 1998; Behrens et al., 2001). Induction of human T cell apoptosis by VT or VT plus TNF-α was associated with the up-regulation of ERK1/2, p38, and JNK1/2 MAPKs. Levels of VT (100 ng/ml) that did not increase apoptosis did not increase ERK1/2 phosphorylation and caused only a transient increase in p38 and JNK 1 h after exposure. These data suggest prolonged activation of MAPKs and the resultant transcriptional activation may be critical to apoptosis induction.

A protective effect of ERK1/2 in a mouse macrophage model of VT-induced apoptosis was previously described (Yang et al., 2000). In that study, when MEK1 and subsequently ERK1/2, was blocked by pretreatment with 40 μM PD98059, VT (2.5 and 5 mg/ml)-induced apoptosis was drastically increased. In the present study, VT (250 ng/ml) plus TNF-α induced apoptosis was significantly reduced by pretreatment with 10 μM PD98059. However, cytotoxicity measured by MTT conversion assay was not recovered in cells pretreated with 10 – 50 μM. This suggests development of apoptotic morphology may have been delayed, but not reversed. Co-incubation with PD98059 (0.1 μM) resulted in a significant reversal of cytotoxicity in both VT (500 ng/ml) and VT plus TNF-α treated cells. Data presented here suggests ERK 2 may contribute to the induction of apoptosis under conditions of low toxin concentrations. Exposure to 2.5 – 5

μg/ml VT (2.5 – 5 times greater than the highest concentration used in this study) may have caused rapid, severe damage that triggered ERK activation as a cell survival mechanism (Yang et al., 2000). Up-regulation of ERK 2 has been commonly associated with T cell antigen receptor ligation and activation-induced T cell death (Izquierdo et al., 1994; Izquierdo et al., 1993). However, previous reports of the inhibition of p38 (Davies, et al., 2000) and JNK (Salh, et al., 2000) by PD98059 require further confirmation of the role of ERK in this apoptotic model.

Prolonged phosphorylation of p38 and JNK are more commonly associated with stress stimuli and apoptosis (Chen et al., 1996). Shifrin and Anderson (1999) demonstrated up-regulation of p38 and JNK for several trichothecenes. Yang et al. (2000) reported a correlation between stress-activated protein kinases (i.e. p38 and JNK) and apoptosis induced by trichothecenes. Similarly, we observed prolonged activation of p38 and JNK for levels of VT that induced apoptosis and this activation was dose dependent at 2 h. In addition, p38 phosphorylation was significantly increased in VT plus TNF-α over either individual treatment at 2 h, suggesting p38 may represent a point where ribotoxic stressors and cytokine signaling pathways converge. Low levels of VT that did not induce apoptosis triggered only a transient increase in p38 and JNK detectable at 1 h. Also in agreement with Yang et al. (2000), SB203580 could partially block VT-induced apoptosis suggesting p38 could contribute to trichothecene-induced apoptosis. The role of JNK in VT-induced T cell apoptosis has not been deciphered, but will require use of a dominant negative mutant JNK kinase 1 (SEK1) or the recently available pharmacological inhibitor of JNK.

While the role of ERK 2, p38, and JNK1/2 in T cell apoptosis is not completely understood, all three phosphorylate Elk-1 (Zinck et al., 1995; Shao et al., 1998) and

NFκB (Lee, et al., 1997; Schwenger, et al., 1998; Zhao and Lee, 1999), common transcription factors associated with apoptosis. Elk-1 regulates c-fos transcription and prolonged activation by protein synthesis inhibitors anisomycin and cycloheximide is mediated by ERK, p38, and JNK (Zinck, et al., 1995). NFκB is induced by VT (Ouyang et al., 1996) and TNF-α (Kasof et al., 2001). The up-regulation of death receptor 6 (DR6) by TNF-α was recently demonstrated to occur via NFκB activation (Kasof et al., 2001). The ability of all three MAPKs to activate Elk-1 and NFκB suggests a point of signaling convergence in which inhibition by pharmacological agents may be overcome by the remaining active MAPKs. This may explain the partial inhibition observed when cells were pre-incubated with PD98059 or SB203580.

MacFarlane et al. (2000) presented a kinetic model of receptor (TRAIL and Fas) and chemical (lactacystin)-induced apoptosis in Jurkat T celis. In this model, receptor-induced apoptosis resulted in a rapid onset of apoptotic morphology. TRAIL induced 70% apoptosis by 2 h while Fas induced 70% apoptosis by 8 h. Chemical-induced apoptosis reached 70% by 18 h following lactacystin exposure. Caspase-3 activation in TRAIL- and Fas-mediated apoptosis was maximal by 1 and 2 h, respectively. Chemical-induced caspase activity significantly increased by 12 h post-exposure. MacFarlane et al. (2000) reported maximal p38 and JNK phosphorylation 1 h after caspase induction by TRAIL and 2 h after caspase induction by Fas. In the chemical model of apoptosis, p38 and JNK phosphorylation peaked at 8 h, prior to caspase activation. Neither model of apoptosis could be inhibited by SB203580 leading the authors to conclude p38 does not play a critical role in the induction of apoptosis in Jurkat T cells. Similar to chemical-induced apoptosis, VT apoptotoic morphology peaked at 18 h, and phosphorylation of MAPKs was demonstrated prior to caspase

enzyme activity. In contrast to the chemical-induced apoptotsis, caspase-3 activity increased much earlier (3 h) and SB203580 significantly inhibited the development of apoptotic morphology. Taken together, these data suggest ribotoxic stressors may present a third kinetic model of apoptotic development in Jurkat T cells and this pathway may involve components of both death receptor and chemical induced pathways presented by MacFarlane et al. (2000).

CHAPTER 6

Summary

Toxins encountered in food and the environment pose a health risk to humans and animals. The unscheduled induction of apoptosis by these compounds may contribute to immune suppression by decreasing the number of leukocytes in the immune system and decreasing host-resistance to pathogens. Comparisons made here among naturally occurring translational inhibitors suggest trichothecene mycotoxins are among the most potent inducers of apoptosis and cytotoxicity in lymphocytes.

The worldwide occurrence of the trichothecenes and the potential for their use as biological warfare agents requires an improved understanding of the mechanism of action of this group of toxins. The studies presented here identified several structural characteristics of the trichothecenes critical for biological activity. These factors influence both cellular transport and binding of these compounds to the site of action and may facilitate risk assessment studies to predict the toxicity of the untested compounds in this group of mycotoxins.

Deoxynivalenol (DON, vomitoxin, VT) is the most common food-borne trichothecene (Rotter et al., 1996). Despite the high potential for human exposure, little information exists on the role of apoptosis and cytotoxicity in DON-induced immune suppression. Recent studies demonstrated increased DON toxicity in the presence of bacterial lipopolysaccharide (LPS; Zhou et al., 2000; Zhou et al., 1999). The mechanisms involved in the potentiation of DON toxicity by LPS have not been elucidated, but suggest trichothecene toxicity may be augmented by signal components involved in cell stress and inflammatory responses. The studies presented here

demonstrated a potentiation of DON induced apoptosis and cytotoxicity by TNF-α and Fas ligand. The present studies suggest cell signaling by translational inhibitors such as DON may cooperate with death receptor or cytokine signal pathway components to increase lymphocyte cell death.

Mitogen activated protein kinases (MAPKs) are serine/threonine specific protein kinases that connect cell surface signals through kinase cascades to transcription factors. These studies suggest that prolonged activation of MAPKs is crucial for the induction of apoptosis by DON and the potentiation of DON-induced apoptosis by TNF-α. The phosphorylation of transcription factors by MAPKs drives gene expression. The identification of transcription factors activated by DON through MAPK cascades should be the focus of future studies. Taken together, these studies have contributed to our mechanistic understanding of trichothecene toxicity and may facilitate risk assessment studies for this group of natural toxins.

LITERATURE CITED

Abouzied, M. M., J. I. Azcona, W. E. Braselton, and J. J. Pestka. 1991. Immunochemical assessment of mycotoxins in 1989 grain foods: evidence for deoxynivalenol (vomitoxin) contamination. Appl. Environ. Microbiol. 57:672-677.

Aggarwal, S., S. Gollapudi, L. Yel, A. S. Gupta, and S. Gupta. 2000. TNF-alpha-induced apoptosis in neonatal lymphocytes: TNFRp55 expression and downstream pathways of apoptosis. Genes Immun. 1:271-279.

Albers, R., P. A. van der, M. Bol, W. Seinen, and R. Pieters. 1996. Stress proteins (HSP) and chemical-induced autoimmunity. Toxicol. Appl. Pharmacol. 140:70-76.

Anderson, D. W., R. M. Black, C. G. Lee, C. Pottage, R. L. Rickard, M. S. Sandford, T. D. Webber, and N. E. Williams. 1989. Structure-activity studies of trichothecenes: cytotoxicity of analogues and reaction products derived from T-2 toxin and neosolaniol. J. Med. Chem. 32:555-562.

Andreau, K., C. Lemaire, V. Souvannavong, and A. Adam. 1998. Induction of apoptosis by dexamethasone in the B cell lineage. Immunopharmacology 40:67-76.

Ayala, A., C. D. Herdon, D. L. Lehman, C. A. Ayala, and I. H. Chaudry. 1996. Differential induction of apoptosis in lymphoid tissues during sepsis: variation in onset, frequency, and the nature of the mediators. Blood 87:4261-4275.

Ayala, A., X. Y. Xin, C. A. Ayala, D. E. Sonefeld, S. M. Karr, T. A. Evans, and I. H. Chaudry. 1998. Increased mucosal B-lymphocyte apoptosis during polymicrobial sepsis is a Fas ligand but not an endotoxin-mediated process. Blood 91:1362-1372.

Baetu, T. M., H. Kwon, S. Sharma, N. Grandvaux, and J. Hiscott. 2001. Disruption of NF-kappaB signaling reveals a novel role for NF-kappaB in the regulation of TNF-related apoptosis-inducing ligand expression. J. Immunol. 167:3164-3173.

Bailly-Maitre, B., G. de Sousa, K. Boulukos, J. Gugenheim, and R. Rahmani. 2001. Dexamethasone inhibits spontaneous apoptosis in primary cultures of human and rat hepatocytes via Bcl-2 and Bcl-xL induction. Cell Death. Differ. 8:279-288.

Bamburg, J. R. 1972. The biological activities and detection of naturally occurring 12,13-epoxy-delta9-trichothecenes. Clin. Toxicol. 5:495-515.

Bamburg, J. R., N. V. Riggs, and F. M. Strong. 1968. The structures of toxins from two strains of Fusarium tricinctum. Tetrahedron 24:3329-3336.

Barratt, M. D. 1995a. Quantitative structure activity relationships for skin corrosivity of organic acids, bases and phenols. Toxicol. Lett. 75:169-176.

Barratt, M. D. 1998b. Integrating computer prediction systems with in vitro methods towards a better understanding of toxicology. Toxicol. Lett. 102-103:617-621.

Barratt, M. D. 1998. Integration of QSAR and in vitro toxicology. Environ. Health Perspect. 106 Suppl 2:459-465.

Baud, V. and M. Karin. 2001. Signal transduction by tumor necrosis factor and its relatives. Trends Cell Biol. 11:372-377.

Behrens, A., K. Sabapathy, I. Graef, M. Cleary, G. R. Crabtree, and E. F. Wagner. 2001. Jun N-terminal kinase 2 modulates thymocyte apoptosis and T cell activation through c-Jun and nuclear factor of activated T cell (NF-AT). Proc. Natl. Acad. Sci. U. S. A 98:1769-1774.

Belka, C., B. Schmid, P. Marini, E. Durand, J. Rudner, H. Faltin, M. Bamberg, K. Schulze-Osthoff, and W. Budach. 2001. Sensitization of resistant lymphoma cells to irradiation-induced apoptosis by the death ligand TRAIL. Oncogene 20:2190-2196.

Benigni, R. and C. Andreoli. 1993. Rodent carcinogenicity and toxicity, in vitro mutagenicity, and their physical chemical determinants. Mutat. Res. 297:281-292.

Bessho, R., K. Matsubara, M. Kubota, K. Kuwakado, H. Hirota, Y. Wakazono, Y. W. Lin, A. Okuda, M. Kawai, R. Nishikomori, and . 1994. Pyrrolidine dithiocarbamate, a potent inhibitor of nuclear factor kappa B (NF-kappa B) activation, prevents apoptosis in human promyelocytic leukemia HL-60 cells and thymocytes. Biochem. Pharmacol. 48:1883-1889.

Bommhardt, U., Y. Scheuring, C. Bickel, R. Zamoyska, and T. Hunig. 2000. MEK activity regulates negative selection of immature CD4+CD8+ thymocytes. J. Immunol. 164:2326-2337.

Bondy, G. S. and J. J. Pestka. 2000. Immunomodulation by fungal toxins. J. Toxicol. Environ. Health B Crit Rev. 3:109-143.

Brown, D. M. and R. P. Phipps. 1995. Characterization and regulation of prostaglandin E2 receptors on normal and malignant murine B lymphocytes. Cell Immunol. 161:79-87.

Brown, D. M., G. L. Warner, J. E. Ales-Martinez, D. W. Scott, and R. P. Phipps. 1992. Prostaglandin E2 induces apoptosis in immature normal and malignant B lymphocytes. Clin. Immunol. Immunopathol. 63:221-229.

Cabrera, R., S. M. Korte, E. G. Lentjes, F. Romijn, E. Schonbaum, A. De Nicola, and E. R. De Kloet. 2000. The amount of free corticosterone is increased during lipopolysaccharide-induced fever. Life Sci. 66:553-562.

Carsetti, R., G. Kohler, and M. C. Lamers. 1995. Transitional B cells are the target of negative selection in the B cell compartment. J. Exp. Med. 181:2129-2140.

Casarett, L.J., Amdur, M.O., Klaassen, C.D. 1996. Casarett and Doull's toxicology: the basic science of poisons. McGraw-Hill, Health Professions Division, New York.

Castedo, M., T. Hirsch, S. A. Susin, N. Zamzami, P. Marchetti, A. Macho, and G. Kroemer. 1996. Sequential acquisition of mitochondrial and plasma membrane alterations during early lymphocyte apoptosis. J. Immunol. 157:512-521.

Chakraborti, T., S. Das, M. Mondal, S. Roychoudhury, and S. Chakraborti. 1999. Oxidant, mitochondria and calcium: an overview. Cell Signal. 11:77-85.

Chen, X. Q., W. D. Zhang, Y. G. Song, and D. Y. Zhou. 1998. Induction of apoptosis of lymphocytes in rat mucosal immune system. World J. Gastroenterol. 4:19-23.

Chen, Y. and M. Z. Lai. 2001. c-Jun NH2-terminal kinase activation leads to a FADD-dependent but Fas ligand-independent cell death in Jurkat T cells. J. Biol. Chem. 276:8350-8357.

Chen, Y. R., X. Wang, D. Templeton, R. J. Davis, and T. H. Tan. 1996. The role of c-Jun N-terminal kinase (JNK) in apoptosis induced by ultraviolet C and gamma radiation. Duration of JNK activation may determine cell death and proliferation. J. Biol. Chem. 271:31929-31936.

Chiba, T., S. Takahashi, N. Sato, S. Ishii, and K. Kikuchi. 1996. Fas-mediated apoptosis is modulated by intracellular glutathione in human T cells. Eur. J. Immunol. 26:1164-1169.

Cho, S. G., A. Bhoumik, L. Broday, V. Ivanov, B. Rosenstein, and Z. Ronai. 2001. TIP49b, a regulator of activating transcription factor 2 response to stress and DNA damage. Mol. Cell Biol. 21:8398-8413.

Choi, K. B., F. Wong, J. M. Harlan, P. M. Chaudhary, L. Hood, and A. Karsan. 1998. Lipopolysaccharide mediates endothelial apoptosis by a FADD-dependent pathway. J. Biol. Chem. 273:20185-20188.

Cohen, A., V. Madrid-Marina, Z. Estrov, M. H. Freedman, C. A. Lingwood, and H. M. Dosch. 1990. Expression of glycolipid receptors to Shiga-like toxin on human B lymphocytes: a mechanism for the failure of long-lived antibody response to dysenteric disease. Int. Immunol. 2:1-8.

Cohen, G. M. 1997. Caspases: the executioners of apoptosis. Biochem. J. 326:1-16.

Cohen, J. J., R. C. Duke, V. A. Fadok, and K. S. Sellins. 1992. Apoptosis and programmed cell death in immunity. Annu. Rev. Immunol. 10:267-293.

Cossarizza, A., C. Franceschi, D. Monti, S. Salvioli, E. Bellesia, R. Rivabene, L. Biondo, G. Rainaldi, A. Tinari, and W. Malorni. 1995. Protective effect of N-acetylcysteine in tumor necrosis factor-alpha- induced apoptosis in U937 cells: the role of mitochondria. Exp. Cell Res. 220:232-240.

Davies, S. P., H. Reddy, M. Caivano, and P. Cohen. 2000. Specificity and mechanism of action of some commonly used protein kinase inhibitors. Biochem. J. 351:95-105.

Davis, W., Jr., Z. Ronai, and K. D. Tew. 2001. Cellular thiols and reactive oxygen species in drug-induced apoptosis. J. Pharmacol. Exp. Ther. 296:1-6.

Dearborn, D. G., I. Yike, W. G. Sorenson, M. J. Miller, and R. A. Etzel. 1999. Overview of investigations into pulmonary hemorrhage among infants in Cleveland, Ohio. Environ. Health Perspect. 107:495-499.

Denecker, G., P. Vandenabeele, J. Grooten, L. C. Penning, W. Declercq, R. Beyaert, W. A. Buurman, and W. Fiers. 1997. Differential role of calcium in tumour necrosis factor-mediated apoptosis and secretion of granulocyte-macrophage colony-stimulating factor in a T cell hybridoma. Cytokine 9:631-638.

Dong, C., R. J. Davis, and R. A. Flavell. 2002. Map kinases in the immune response. Annu. Rev. Immunol. 20:55-72.

Donjerkovic, D., C. M. Mueller, and D. W. Scott. 2000. Steroid- and retinoid-mediated growth arrest and apoptosis in WEHI-231 cells: role of NF-kappaB, c-Myc and CKI p27(Kip1). Eur. J. Immunol. 30:1154-1161.

Duke, R. C. and J. J. Cohen. 1995. Morphological, biochemical, and flow cytometric assays of apoptosis. Current Protocols in Immunology3.17.1-3.17.33.

Ehrlich, K. C. and K. W. Daigle. 1987. Protein synthesis inhibition by 8-oxo-12,13-epoxytrichothecenes. Biochim. Biophys. Acta 923:206-213.

El Mauhoub, M., M. M. Khalifa, O. B. Jaswal, and M. S. Garrah. 1983. "Ricin syndrome". A possible new teratogenic syndrome associated with ingestion of castor oil seed in early pregnancy: a case report. Ann. Trop. Paediatr. 3:57-61.

Elidemir, O., G. N. Colasurdo, S. N. Rossmann, and L. L. Fan. 1999. Isolation of Stachybotrys from the lung of a child with pulmonary hemosiderosis. Pediatrics 104:964-966.

Emmendoerffer, A., M. Hecht, T. Boeker, M. Mueller, and U. Heinrich. 2000. Role of inflammation in chemical-induced lung cancer. Toxicol. Lett. 112-113:185-191.

FAO/WHO. 2002. Evaluation of certain mycotoxins in food. Fifty-sixth report of the Joint FAO/WHO Expert Committee on Food Additives. World Health Organ Tech. Rep. Ser. 906:1-62.

Faris, M., N. Kokot, K. Latinis, S. Kasibhatla, D. R. Green, G. A. Koretzky, and A. Nel. 1998. The c-Jun N-terminal kinase cascade plays a role in stress-induced apoptosis in Jurkat cells by up-regulating Fas ligand expression. J. Immunol. 160:134-144.

Forsell, J. H., J. R. Kateley, T. Yoshizawa, and J. J. Pestka. 1985. Inhibition of mitogen-induced blastogenesis in human lymphocytes by T-2 toxin and its metabolites. Appl. Environ. Microbiol. 49:1523-1526.

Fricke, R. F. and J. Jorge. 1991. Beneficial effect of dexamethasone in decreasing the lethality of acute T-2 toxicosis. Gen. Pharmacol. 22:1087-1091.

Garvy, B. A., L. E. King, W. G. Telford, L. A. Morford, and P. J. Fraker. 1993. Chronic elevation of plasma corticosterone causes reductions in the number of cycling cells of the B lineage in murine bone marrow and induces apoptosis. Immunology 80:587-592.

Geier, A., I. Bar-Shalom, R. Beery, M. Haimsohn, R. Hemi, Z. Malik, B. Lunenfeld, and A. Karasik. 1996. Induction of apoptosis in MDA-231 cells by protein synthesis inhibitors is suppressed by multiple agents. Cancer Invest 14:435-444.

Geier, A., R. Beery, M. Haimshon, R. Hemi, and B. Lunenfeld. 1992. Serum and insulin inhibit cell death induced by cycloheximide in the human breast cancer cell line MCF-7. In Vitro Cell Dev. Biol. 28A:415-418.

Giardina, C., H. Boulares, and M. S. Inan. 1999. NSAIDs and butyrate sensitize a human colorectal cancer cell line to TNF-alpha and Fas ligation: the role of reactive oxygen species. Biochim. Biophys. Acta 1448:425-438.

Gittens, R. 1985. Canonical analysis: a review with applications in ecology. Springer Verlag, Berlin.

Gottschalk, A. R. and J. Quintans. 1995. Apoptosis in B lymphocytes: the WEHI-231 perspective. Immunol. Cell Biol. 73:8-16.

Griffiths, G. D., M. D. Leek, and D. J. Gee. 1987. The toxic plant proteins ricin and abrin induce apoptotic changes in mammalian lymphoid tissues and intestine. J. Pathol. 151:221-229.

Grove J.F. 1993. Macrocyclic Trichothecenes. Nat. Prod. 10:429-448.

Grove, J. F. 1996. Non-macrocyclic trichothecenes. Prog.Chem.Org.Nat.Prod. 69: 1-70.

Grove, J. F. and P. H. Mortimer. 1969. The cytotoxicity of some transformation products of diacetoxyscirpenol. Biochem. Pharmacol. 18:1473-1478.

Gruber, J., R. Sgonc, Y. H. Hu, H. Beug, and G. Wick. 1994. Thymocyte apoptosis induced by elevated endogenous corticosterone levels. Eur. J Immunol. 24:1115-1121.

Hampton, M. B., D. M. Vanags, M. I. Porn-Ares, and S. Orrenius. 1996. Involvement of extracellular calcium in phosphatidylserine exposure during apoptosis. FEBS Lett. 399:277-282.

Hanelt, M., M. Gareis, and B. Kollarczik. 1994. Cytotoxicity of mycotoxins evaluated by the MTT-cell culture assay. Mycopathologia 128:167-174.

Harvey, P. W., G. Healing, S. J. Rees, D. J. Everett, and A. Cockburn. 1994. Glucocorticosteroid interactions with natural toxins: a mini review. Nat. Toxins. 2:341-346.

Hasbold, J. and G. G. Klaus. 1990. Anti-immunoglobulin antibodies induce apoptosis in immature B cell lymphomas. Eur. J. Immunol. 20:1685-1690.

Herr, I., D. Wilhelm, E. Meyer, I. Jeremias, P. Angel, and K. M. Debatin. 1999. JNK/SAPK activity contributes to TRAIL-induced apoptosis. Cell Death. Differ. 6:130-135.

Hettmann, T., J. DiDonato, M. Karin, and J. M. Leiden. 1999. An essential role for nuclear factor kappaB in promoting double positive thymocyte apoptosis. J. Exp. Med. 189:145-158.

Heyndrickx, A., N. Sookvanichsilp, and H. M. Van-den. 1984. Detection of trichothecene mycotoxins (yellow rain) in blood, urine and faeces of Iranian soldiers treated as victims of a gas attack. Arch. Belg. Suppl:143-146.

Hsu, S. C., M. A. Gavrilin, M. H. Tsai, J. Han, and M. Z. Lai. 1999. p38 mitogen-activated protein kinase is involved in Fas ligand expression. J. Biol. Chem. 274:25769-25776.

Hueber, A. O., M. Zornig, A. M. Bernard, M. Chautan, and G. Evan. 2000. A dominant negative Fas-associated death domain protein mutant inhibits proliferation and leads to impaired calcium mobilization in both T- cells and fibroblasts. J. Biol. Chem. 275:10453-10462.

Iordanov, M. S., D. Pribnow, J. L. Magun, T. H. Dinh, J. A. Pearson, S. L. Chen, and B. E. Magun. 1997. Ribotoxic stress response: activation of the stress-activated protein kinase JNK1 by inhibitors of the peptidyl transferase reaction and by sequence-specific RNA damage to the alpha-sarcin/ricin loop in the 28S rRNA. Mol. Cell Biol. 17:3373-3381.

Ishii, H. H., M. R. Etheridge, and G. C. Gobe. 1995. Cycloheximide-induced apoptosis in Burkitt lymphoma (BJA-B) cells with and without Epstein-Barr virus infection. Immunol. Cell Biol. 73:463-468.

Islam, Z., M. Nagase, T. Yoshizawa, K. Yamauchi, and N. Sakato. 1998. T-2 toxin induces thymic apoptosis in vivo in mice. Toxicol. Appl. Pharmacol. 148:205-214.

Izquierdo, M., S. Bowden, and D. Cantrell. 1994. The role of Raf-1 in the regulation of extracellular signal-regulated kinase 2 by the T cell antigen receptor. J. Exp. Med. 180:401-406.

Izquierdo, M., S. J. Leevers, C. J. Marshall, and D. Cantrell. 1993. p21ras couples the T cell antigen receptor to extracellular signal- regulated kinase 2 in T lymphocytes. J. Exp. Med. 178 :1199-1208.

Johanning, E., R. Biagini, D. Hull, P. Morey, B. Jarvis, and P. Landsbergis. 1996. Health and immunology study following exposure to toxigenic fungi (Stachybotrys chartarum) in a water-damaged office environment. Int. Arch. Occup. Environ. Health 68:207-218.

Joseph, L. F., S. Ezhevsky, and D. W. Scott. 1995. Lymphoma models for B-cell activation and tolerance: anti- immunoglobulin M treatment induces growth arrest by preventing the formation of an active kinase complex which phosphorylates retinoblastoma gene product in G1. Cell Growth Differ. 6:51-57.

Kakinuma, C., K. Takagaki, T. Yatomi, N. Nakamura, S. Nagata, A. Uemura, and Y. Shibutani. 1999. Acute toxicity of an anti-Fas antibody in mice. Toxicol. Pathol. 27:412-420.

Kasof, G. M., J. J. Lu, D. Liu, B. Speer, K. N. Mongan, B. C. Gomes, and M. V. Lorenzi. 2001. Tumor necrosis factor-alpha induces the expression of DR6, a member of the TNF receptor family, through activation of NF-kappaB. Oncogene 20:7965-7975.

Kim, Y.-M., T. R. Billiar, and J. R. Lancaster. 1996. Reactive Oxygen and Nitrogen Metabolites and Related Enzymes, p. 171.1-171.10. *In* L. A. Herzenberg, D. M. Weir, and C. Blackwell, Weir's Handbook of Experimental Immunology. Blackwell Science, Cambridge, MASS.

Kimura, K. and M. Yamamoto. 1997. Rapid induction of Fas antigen mRNA expression in vivo by cycloheximide. Cell Biochem. Funct. 15:81-86.

Kitamura, Y., S. Hashimoto, N. Mizuta, A. Kobayashi, K. Kooguchi, I. Fujiwara, and H. Nakajima. 2001. Fas/FasL-dependent apoptosis of alveolar cells after lipopolysaccharide-induced lung injury in mice. Am. J. Respir. Crit Care Med. 163:762-769.

Kiyokawa, N., T. Mori, T. Taguchi, M. Saito, K. Mimori, T. Suzuki, T. Sekino, N. Sato, H. Nakajima, Y. U. Katagiri, T. Takeda, and J. Fujimoto. 2001. Activation of the caspase cascade during Stx1-induced apoptosis in Burkitt's lymphoma cells. J. Cell Biochem. 81:128-142.

Ko, S., T. T. Kwok, K. P. Fung, Y. M. Choy, C. Y. Lee, and S. K. Kong. 2000. Slow rise of Ca2+ and slow release of reactive oxygen species are two cross-talked events important in tumour necrosis factor-alpha-mediated apoptosis. Free Radic. Res. 33:295-304.

Kodama, T., K. Nagayama, K. Yamada, Y. Ohba, Y. Akeda, and T. Honda. 1999. Induction of apoptosis in human renal proximal tubular epithelial cells by Escherichia coli verocytotoxin 1 in vitro. Med. Microbiol. Immunol. (Berl) 188:73-78.

Kollarczik, B., M. Gareis, and M. Hanelt. 1994. In vitro transformation of the Fusarium mycotoxins deoxynivalenol and zearalenone by the normal gut microflora of pigs. Nat. Toxins. 2:105-110.

Kortenjann, M. and P. E. Shaw. 1995. The growing family of MAP kinases: regulation and specificity. Crit Rev. Oncog. 6:99-115.

Koury, M. J. 1992. Programmed cell death (apoptosis) in hematopoiesis. Exp. Hematol. 20:391-394.

Krishna, G., G. Urda, W. Tefera, N. D. Lalwani, and J. Theiss. 1995. Simultaneous evaluation of dexamethasone-induced apoptosis and micronuclei in rat primary spleen cell cultures. Mutat. Res. 332:1-8.

Kulkarni, A., Y. Han, and A. J. Hopfinger. 2002. Predicting Caco-2 cell permeation coefficients of organic molecules using membrane-interaction QSAR analysis. J. Chem. Inf. Comput. Sci. 42:331-342.

Lee, F. S., J. Hagler, Z. J. Chen, and T. Maniatis. 1997. Activation of the IkappaB alpha kinase complex by MEKK1, a kinase of the JNK pathway. Cell 88:213-222.

Li, F. Q., X. Y. Luo, and T. Yoshizawa. 1999. Mycotoxins (trichothecenes, zearalenone and fumonisins) in cereals associated with human red-mold intoxications stored since 1989 and 1991 in China. Nat. Toxins. 7:93-97.

Li, J., R. Zheng, J. Li, and Z. Wang. 2001. Mechanisms of the induction of apoptosis in human hepatoma cells by tumour necrosis factor-alpha. Cell Biol. Int. 25:1213-1219.

Liao, J. H., B. H. Zhou, M. Q. Chai, and J. G. Song. 2001. Cycloheximide blocks TGF-|A(1)-induced apoptosis in murine hepatocytes. Acta Pharmacol. Sin. 22:176-182.

Lingwood, C. A. 1996. Role of verotoxin receptors in pathogenesis. Trends Microbiol. 4:147-153.

Lopez de Compadre, R. L., A. K. Debnath, A. J. Shusterman, and C. Hansch. 1990. LUMO energies and hydrophobicity as determinants of mutagenicity by nitroaromatic compounds in Salmonella typhimurium. Environ. Mol. Mutagen. 15:44-55.

Luster, M. I., P. P. Simeonova, R. M. Gallucci, A. Bruccoleri, M. E. Blazka, B. Yucesoy, and J. M. Matheson. 2000. The role of tumor necrosis factor alpha in chemical-induced hepatotoxicity. Ann. N. Y. Acad. Sci. 919:214-220.

MacFarlane, M., G. M. Cohen, and M. Dickens. 2000. JNK (c-Jun N-terminal kinase) and p38 activation in receptor-mediated and chemically-induced apoptosis of T-cells: differential requirements for caspase activation. Biochem. J. 348 Pt 1:93-101.

Mahmoudi, M. and M. E. Gershwin. 2000. Sick building syndrome. III. Stachybotrys chartarum. J. Asthma 37:191-198.

Marin, M. L., J. Murtha, W. Dong, and J. J. Pestka. 1996. Effects of mycotoxins on cytokine production and proliferation in EL-4 thymoma cells. J. Toxicol. Environ. Health 48:379-396.

Mastino, A., M. Piacentini, S. Grelli, C. Favalli, F. Autuori, L. Tentori, S. Oliverio, and E. Garaci. 1992. Induction of apoptosis in thymocytes by prostaglandin E2 in vivo. Dev. Immunol. 2 :263-271.

Matsuoka, Y. and K. Kubota. 1987. Characteristics of inflammation induced by fusarenon-X, a trichothecene mycotoxin from Fusarium species. Toxicol. Appl. Pharmacol. 91:333-340.

McCormack, J.G., Cobbold, P.H. 1991. Cellular calcium: a practical approach. Oxford University Press, New York.

McGovern, T. W., G. W. Christopher, and E. M. Eitzen. 1999. Cutaneous manifestations of biological warfare and related threat agents. Arch. Dermatol. 135:311-322.

McLeish, K. R., C. Knall, R. A. Ward, P. Gerwins, P. Y. Coxon, J. B. Klein, and G. L. Johnson. 1998. Activation of mitogen-activated protein kinase cascades during priming of human neutrophils by TNF-alpha and GM-CSF. J. Leukoc. Biol. 64:537-545.

Mekenyan, O. G. and G. D. Veith. 1993. Relationships between descriptors for hydrophobicity and soft electrophilicity in predicting toxicity. SAR QSAR. Environ. Res. 1:335-344.

Minervini, F., W. Dong, and J. Pestka. 1993. In vitro vomitoxin exposure alters IgA and IgM secretion by CH12LX B cells. Relationship to proliferation and macromolecular synthesis. Mycopathologia 121:33-40.

Modigliani, Y., J. Demengeot, R. Vasconcellos, J. Andersson, A. Coutinho, and A. Grandien. 1997. Differential sensitivity of B lymphocyte populations to IgM receptor ligation is determined by local factors. Int. Immunol. 9:755-762.

Mori, T., N. Kiyokawa, Y. U. Katagiri, T. Taguchi, T. Suzuki, T. Sekino, N. Sato, K. Ohmi, H. Nakajima, T. Takeda, and J. Fujimoto. 2000. Globotriaosyl ceramide (CD77/Gb3) in the glycolipid-enriched membrane domain participates in B-cell receptor-mediated apoptosis by regulating lyn kinase activity in human B cells. Exp. Hematol. 28:1260-1268.

Nagase, M., M. M. Alam, A. Tsushima, T. Yoshizawa, and N. Sakato. 2001. Apoptosis induction by T-2 toxin: activation of caspase-9, caspase-3, and DFF-40/CAD through cytosolic release of cytochrome c in HL-60 cells. Biosci. Biotechnol. Biochem. 65:1741-1747.

Nakao, H. and T. Takeda. 2000. Escherichia coli Shiga toxin. J Nat. Toxins. 9:299-313.

Nava, V. E., O. Cuvillier, L. C. Edsall, K. Kimura, S. Milstien, E. P. Gelmann, and S. Spiegel. 2000. Sphingosine enhances apoptosis of radiation-resistant prostate cancer cells. Cancer Res. 60:4468-4474.

Nikulin, M., K. Reijula, B. B. Jarvis, and E. L. Hintikka. 1996. Experimental lung mycotoxicosis in mice induced by Stachybotrys atra. Int. J. Exp. Pathol. 77:213-218.

Nikulin, M., K. Reijula, B. B. Jarvis, P. Veijalainen, and E. L. Hintikka. 1997. Effects of intranasal exposure to spores of Stachybotrys atra in mice. Fundam. Appl. Toxicol. 35:182-188.

Nilsson, N., S. Ingvarsson, and C. A. Borrebaeck. 2000. Immature B cells in bone marrow express Fas/FasL. Scand. J. Immunol. 51:279-284.

Nishimura, Y., Y. Hirabayashi, Y. Matsuzaki, P. Musette, A. Ishii, H. Nakauchi, T. Inoue, and S. Yonehara. 1997. In vivo analysis of Fas antigen-mediated apoptosis: effects of agonistic anti-mouse Fas mAb on thymus, spleen and liver. Int. Immunol. 9:307-316.

Oberholzer, C., A. Oberholzer, M. Clare-Salzler, and L. L. Moldawer. 2001. Apoptosis in sepsis: a new target for therapeutic exploration. FASEB J. 15:879-892.

Okumura, H., N. Yoshino, T. Ihara, M. Sugamata, and Y. Ueno. 2000. Induction of apoptotic cell death by trichothecenes. Mycotoxins 50:41-44.

Onel, K. B., C. L. Tucek-Szabo, D. Ashany, E. Lacy, J. Nikolic-Zugic, and K. B. Elkon. 1995. Expression and function of the murine CD95/FasR/APO-1 receptor in relation to B cell ontogeny. Eur. J. Immunol. 25:2940-2947.

Ouyang, Y. L., S. Li, and J. J. Pestka. 1996. Effects of vomitoxin (deoxynivalenol) on transcription factor NF-kappa B/Rel binding activity in murine EL-4 thymoma and primary CD4+ T cells. Toxicol. Appl. Pharmacol. 140:328-336.

Palatnick, W. and M. Tenenbein. 2000. Hepatotoxicity from castor bean ingestion in a child. J. Toxicol. Clin. Toxicol. 38:67-69.

Pavlovic, D., N. A. Andersen, T. Mandrup-Poulsen, and D. L. Eizirik. 2000. Activation of extracellular signal-regulated kinase (ERK)1/2 contributes to cytokine-induced apoptosis in purified rat pancreatic beta-cells. Eur. Cytokine Netw. 11:267-274.

Penninger, J. M. and G. Kroemer. 1998. Molecular and cellular mechanisms of T lymphocyte apoptosis. Adv. Immunol. 68:51-144.:51-144.

Peraica, M., B. Radic, A. Lucic, and M. Pavlovic. 1999. Toxic effects of mycotoxins in humans. Bull. World Health Organ 77:754-766.

Pestka, J. J., D. Yan, and L. E. King. 1994. Flow cytometric analysis of the effects of in vitro exposure to vomitoxin (deoxynivalenol) on apoptosis in murine T, B and IgA+ cells. Food Chem. Toxicol. 32:1125-1136.

Pica, F., O. Franzese, C. D'Onofrio, E. Bonmassar, C. Favalli, and E. Garaci. 1996. Prostaglandin E2 induces apoptosis in resting immature and mature human lymphocytes:

a c-Myc-dependent and Bcl-2-independent associated pathway. J. Pharmacol. Exp. Ther. 277:1793-1800.

Pijpers, A. H., P. A. van Setten, L. P. van den Heuvel, K. J. Assmann, H. B. Dijkman, A. H. Pennings, L. A. Monnens, and V. W. van Hinsbergh. 2001. Verocytotoxin-induced apoptosis of human microvascular endothelial cells. J. Am. Soc. Nephrol. 12:767-778.

Pruett, S. B., D. K. Ensley, and P. L. Crittenden. 1993. The role of chemical-induced stress responses in immunosuppression: a review of quantitative associations and cause-effect relationships between chemical-induced stress responses and immunosuppression. J. Toxicol. Environ. Health 39:163-192.

Purdy, R. 1996. A Mechanism-mediated Model for Carcinogenicity: Model Content and Prediction of the Outcome of Rodent Carcinogenicity Bioassays Currently Being Conducted on 25 Organic Chemicals. Environ. Health Perspect. 104S:1085-1094.

Quirk, S. M., D. A. Porter, S. C. Huber, and R. G. Cowan . 1998. Potentiation of Fas-mediated apoptosis of murine granulosa cells by interferon-gamma, tumor necrosis factor-alpha, and cycloheximide.

Ramu, A., B. Yagen, and N. Ramu. 1989. The cytotoxicity of T-2 toxin and related 12,13-epoxytrichothecenes to Adriamycin-sensitive and -resistant P388 leukemia cells. Cancer Chemother. Pharmacol. 24:264-267.

Ray, A. and K. E. Prefontaine. 1994. Physical association and functional antagonism between the p65 subunit of transcription factor NF-kappa B and the glucocorticoid receptor. Proc. Natl. Acad. Sci. U. S. A 91:752-756.

Roth, R. A., J. R. Harkema, J. P. Pestka, and P. E. Ganey. 1997. Is exposure to bacterial endotoxin a determinant of susceptibility to intoxication from xenobiotic agents? Toxicol. Appl. Pharmacol. 147:300-311.

Rotter, B. A., D. B. Prelusky, and J. J. Pestka. 1996. Toxicology of deoxynivalenol (vomitoxin). J. Toxicol. Environ. Health 48:1-34.

Roulston, A., C. Reinhard, P. Amiri, and L. T. Williams. 1998. Early activation of c-Jun N-terminal kinase and p38 kinase regulate cell survival in response to tumor necrosis factor alpha. J. Biol. Chem. 273:10232-10239.

Saini, K. S. and N. I. Walker. 1998. Biochemical and molecular mechanisms regulating apoptosis. Mol. Cell Biochem. 178:9-25.

Salh, B. S., J. Martens, R. S. Hundal, N. Yoganathan, D. Charest, A. Mui, and A. Gomez-Munoz. 2000. PD98059 attenuates hydrogen peroxide-induced cell death through inhibition of Jun N-Terminal Kinase in HT29 cells. Mol. Cell Biol. Res. Commun. 4:158-165.

Sandvig, K. and B. van Deurs. 2000. Entry of ricin and Shiga toxin into cells: molecular mechanisms and medical perspectives. EMBO J. 19:5943-5950.

Scheinman, R. I., P. C. Cogswell, A. K. Lofquist, and A. S. Baldwin, Jr. 1995. Role of transcriptional activation of I kappa B alpha in mediation of immunosuppression by glucocorticoids. Science 270:283-286.

Schwenger, P., D. Alpert, E. Y. Skolnik, and J. Vilcek. 1998. Activation of p38 mitogen-activated protein kinase by sodium salicylate leads to inhibition of tumor necrosis factor-induced IkappaB alpha phosphorylation and degradation. Mol. Cell Biol. 18:78-84.

Scott, P. M. 1997. Multi-year monitoring of Canadian grains and grain-based foods for trichothecenes and zearalenone. Food Addit Contam 14:333-339.

Senftleben, U., Z. W. Li, V. Baud, and M. Karin. 2001. IKKbeta is essential for protecting T cells from TNFalpha-induced apoptosis. Immunity. 14:217-230.

Seo, S. R., S. A. Chong, S. I. Lee, J. Y. Sung, Y. S. Ahn, K. C. Chung, and J. T. Seo. 2001. Zn2+-induced ERK activation mediated by reactive oxygen species causes cell death in differentiated PC12 cells. J. Neurochem. 78:600-610.

Shao, N., Y. Chai, J. Q. Cui, N. Wang, K. Aysola, E. S. Reddy, and V. N. Rao. 1998. Induction of apoptosis by Elk-1 and deltaElk-1 proteins. Oncogene 17:527-532.

Shifrin, V. I. and P. Anderson. 1999. Trichothecene mycotoxins trigger a ribotoxic stress response that activates c-Jun N-terminal kinase and p38 mitogen-activated protein kinase and induces apoptosis. J. Biol. Chem. 274:13985-13992.

Shinozuka, J., L. Guanmin, K. Uetsuka, H. Nakayama, and K. Doi. 1997. Process of the development of T-2 toxin-induced apoptosis in the lymphoid organs of mice. Exp. Anim 46:117-126.

Shinozuka, J., G. Li, W. Kiatipattanasakul, K. Uetsuka, H. Nakayama, and K. Doi. 1997. T-2 toxin-induced apoptosis in lymphoid organs of mice. Exp. Toxicol. Pathol. 49:387-392.

Shrivastava, A. and B. B. Aggarwal. 1999. Antioxidants differentially regulate activation of nuclear factor-kappa B, activator protein-1, c-jun amino-terminal kinases, and apoptosis induced by tumor necrosis factor: evidence that JNK and NF-kappa B activation are not linked to apoptosis. Antioxid. Redox. Signal. 1:181-191.

Siegmund, D., A. Hausser, N. Peters, P. Scheurich, and H. Wajant. 2001. Tumor necrosis factor (TNF) and phorbol ester induce TNF-related apoptosis-inducing ligand (TRAIL) under critical involvement of NF- kappa B essential modulator (NEMO)/IKKgamma. J. Biol. Chem. 276:43708-43712.

Smoragiewicz, W., B. Cossette, A. Boutard, and K. Krzystyniak. 1993. Trichothecene mycotoxins in the dust of ventilation systems in office buildings. Int. Arch. Occup. Environ. Health 65:113-117.

Snyder, P. 1986. Qualitative, Quantitative and Technological Aspects of the Trichothecene Mycotoxins. J. Food Prot. 49:544-569.

Stiles, G. L. 1986. Photoaffinity cross-linked A1 adenosine receptor-binding subunits. Homologous glycoprotein expression by different tissues. J. Biol. Chem. 261:10839-10843.

Suneja, S. K., D. S. Wagle, and G. C. Ram. 1989. Effect of oral administration of T-2 toxin on glutathione shuttle enzymes, microsomal reductases and lipid peroxidation in rat liver. Toxicon 27:995-1001.

Tai, J. H. and J. J. Pestka. 1988. Synergistic interaction between the trichothecene T-2 toxin and Salmonella typhimurium lipopolysaccharide in C3H/HeN and C3H/HeJ mice. Toxicol. Lett. 44:191-200.

Takahashi, K., O. Inanami, M. Hayashi, and M. Kuwabara. 2002. Protein synthesis-dependent apoptotic signalling pathway in X- irradiated MOLT-4 human leukaemia cell line. Int. J. Radiat. Biol. 78:115-124.

Talley, A. K., S. Dewhurst, S. W. Perry, S. C. Dollard, S. Gummuluru, S. M. Fine, D. New, L. G. Epstein, H. E. Gendelman, and H. A. Gelbard. 1995. Tumor necrosis factor alpha-induced apoptosis in human neuronal cells: protection by the antioxidant N-acetylcysteine and the genes bcl-2 and crmA. Mol. Cell Biol. 15:2359-2366.

Tang, D., J. M. Lahti, J. Grenet, and V. J. Kidd. 1999. Cycloheximide-induced T-cell death is mediated by a Fas-associated death domain-dependent mechanism. J. Biol. Chem. 274:7245-7252.

Thompson, W. L. and R. W. Wannemacher, Jr. 1986. Structure-function relationships of 12,13-epoxytrichothecene mycotoxins in cell culture: comparison to whole animal lethality. Toxicon 24:985-994.

Tilley, S. L., T. M. Coffman, and B. H. Koller. 2001. Mixed messages: modulation of inflammation and immune responses by prostaglandins and thromboxanes. J. Clin. Invest 108:15-23.

Tong, W., R. Perkins, R. Strelitz, E. R. Collantes, S. Keenan, W. J. Welsh, W. S. Branham, and D. M. Sheehan. 1997. Quantitative structure-activity relationships (QSARs) for estrogen binding to the estrogen receptor: predictions across species. Environ. Health Perspect. 105:1116-1124.

Tran, S. E., T. H. Holmstrom, M. Ahonen, V. M. Kahari, and J. E. Eriksson. 2001. MAPK/ERK overrides the apoptotic signaling from Fas, TNF, and TRAIL receptors. J. Biol. Chem. 276:16484-16490.

Tsujimoto, Y. and S. Shimizu. 2000. Bcl-2 family: life-or-death switch. FEBS Lett. 466:6-10.

Tuomi, T., L. Saarinen, and K. Reijula. 1998. Detection of polar and macrocyclic trichothecene mycotoxins from indoor environments. Analyst 123:1835-1841.

Tuppurainen, K. 1999. Frontier orbital energies, hydrophobicity and steric factors as physical QSAR descriptors of molecular mutagenicity. A review with a case study: MX compounds. Chemosphere 38:3015-3030.

Ueno, Y. 1983. General toxicology., p. 135-146. *In* Y. Ueno (ed.), Trichothecenes: Chemical, Biological, and Toxicological Aspects. Elsevier, New York.

van den Brink, M. R., R. Kapeller, J. C. Pratt, J. H. Chang, and S. J. Burakoff. 1999. The extracellular signal-regulated kinase pathway is required for activation-induced cell death of T cells. J. Biol. Chem. 274:11178-11185.

Wang, J., D. W. Fitzpatrick, and J. R. Wilson. 1993. Effect of dietary T-2 toxin on biogenic monoamines in discrete areas of the rat brain. Food Chem. Toxicol. 31:191-197.

Wang, Z. G., J. N. Feng, and Z. Tong. 1993a. Human toxicosis caused by moldy rice contaminated with fusarium and T-2 toxin. Biomed. Environ. Sci. 6:65-70.

Warner, G. L., J. W. Ludlow, D. A. Nelson, A. Gaur, and D. W. Scott. 1992. Anti-immunoglobulin treatment of murine B-cell lymphomas induces active transforming growth factor beta but pRB hypophosphorylation is transforming growth factor beta independent. Cell Growth Differ. 3:175-181.

Watanabe, D., T. Suda, and S. Nagata. 1995. Expression of Fas in B cells of the mouse germinal center and Fas- dependent killing of activated B cells. Int. Immunol. 7:1949-1956.

Wei, C. M. and C. S. McLaughlin. 1974. Structure-function relationship in the 12,13-epoxytrichothecenes. Novel inhibitors of protein synthesis. Biochem. Biophys. Res. Commun. 57:838-844.

WHO. 1990. Trichothecenes in Selected mycotoxins: ochratoxins, thichothecenes, ergot, p. 71-164. *In* WHO Task Force, WHO, Geneva.

Wickman, M., S. Gravesen, S. L. Nordvall, G. Pershagen, and J. Sundell. 1992. Indoor viable dust-bound microfungi in relation to residential characteristics, living habits, and symptoms in atopic and control children. J. Allergy Clin. Immunol. 89:752-759.

Widmann, C., S. Gibson, M. B. Jarpe, and G. L. Johnson. 1999. Mitogen-activated protein kinase: conservation of a three-kinase module from yeast to human. Physiol Rev. 79:143-180.

Widmann, C., S. Gibson, and G. L. Johnson. 1998. Caspase-dependent cleavage of signaling proteins during apoptosis. A turn-off mechanism for anti-apoptotic signals. J. Biol. Chem. 273:7141-7147.

Witt, M. F. and J. J. Pestka. 1990. Uptake of the naturally occurring 3-alpha-hydroxy isomer of T-2 toxin by a murine B cell hybridoma. Food Chem. Toxicol. 28:21-28.

Wolf-Hall, C. E., M. A. Hanna, and L. B. Bullerman. 1999. Stability of deoxynivalenol in heat-treated foods. J. Food Prot. 62:962-964.

Wu, M., H. Lee, R. E. Bellas, S. L. Schauer, M. Arsura, D. Katz, M. J. FitzGerald, T. L. Rothstein, D. H. Sherr, and G. E. Sonenshein. 1996. Inhibition of NF-kappaB/Rel induces apoptosis of murine B cells. EMBO J. 15:4682-4690.

Yang, G. H., B. B. Jarvis, Y. J. Chung, and J. J. Pestka . 2000. Apoptosis induction by the satratoxins and other trichothecene mycotoxins: relationship to ERK, p38 MAPK, and SAPK/JNK activation. Toxicol. Appl. Pharmacol. 164:149-160.

Yike, I., T. Allan, W. G. Sorenson, and D. G. Dearborn. 1999. Highly sensitive protein translation assay for trichothecene toxicity in airborne particulates: comparison with cytotoxicity assays. Appl. Environ. Microbiol. 65:88-94.

Yoshino, N., M. Takizawa, H. Akiba, H. Okumura, F. Tashiro, M. Honda, and Y. Ueno. 1996. Transient elevation of intracellular calcium ion levels as an early event in T-2 toxin-induced apoptosis in human promyelotic cell line HL-60. Nat. Toxins. 4:234-241.

Yoshino, N., M. Takizawa, F. Tashiro, M. Honda, and Y. Ueno. 1997. T-2 toxin induced apoptosis in human peripheral blood lymphocytes in vitro. Research Communications in Biochemistry and Cell & Molecular Biology 1:218-228.

Yoshizawa, T., T. Sakamoto, Y. Anayno, and C. J. Mirocha . 1981. 3' Hydroxy T-2 and 3' hydroxy HT-2 toxins: new metabolites of T-2 toxin, a trichothecene mycotoxin in animals. Agriultural and Biological Chemistry 46:2613-2615.

Yoshizawa, T., T. Sakamoto, and K. Okamoto. 1984. In vitro formation of 3'-hydroxy T-2 and 3'-hydroxy HT-2 toxins from T- 2 toxin by liver homogenates from mice and monkeys. Appl. Environ. Microbiol. 47:130-134.

Yu, Z. P., M. Matsuoka, B. Wispriyono, Y. Iryo, and H. Igisu. 2000. Activation of mitogen-activated protein kinases by tributyltin in CCRF- CEM cells: role of intracellular Ca(2+). Toxicol. Appl. Pharmacol. 168:200-207.

Zhang, X. M., A. Morikawa, K. Takahashi, G. Z. Jiang, Y. Kato, T. Sugiyama, M. Kawai, M. Fukada, and T. Yokochi. 1994. Localization of apoptosis (programmed cell death) in mice by administration of lipopolysaccharide. Microbiol. Immunol. 38:669-671.

Zhang, Y. H., K. Takahashi, G. Z. Jiang, M. Kawai, M. Fukada, and T. Yokochi. 1993. In vivo induction of apoptosis (programmed cell death) in mouse thymus by administration of lipopolysaccharide. Infect. Immun. 61:5044-5048.

Zhao, Q. and F. S. Lee. 1999. Mitogen-activated protein kinase/ERK kinase kinases 2 and 3 activate nuclear factor-kappaB through IkappaB kinase-alpha and IkappaB kinase-beta. J. Biol. Chem. 274:8355-8358.

Zhou, H. R., J. R. Harkema, J. A. Hotchkiss, D. Yan, R. A. Roth, and J. J. Pestka. 2000. Lipopolysaccharide and the trichothecene vomitoxin (deoxynivalenol) synergistically induce apoptosis in murine lymphoid organs. Toxicol. Sci. 53:253-263.

Zhou, H. R., J. R. Harkema, D. Yan, and J. J. Pestka. 1999. Amplified proinflammatory cytokine expression and toxicity in mice coexposed to lipopolysaccharide and the trichothecene vomitoxin (deoxynivalenol). J. Toxicol. Environ. Health 57:115-136.

Zilinskas, R. A. 1997. Iraq's biological weapons. The past as future? JAMA 278:418-424.

Zinck, R., M. A. Cahill, M. Kracht, C. Sachsenmaier, R. A. Hipskind, and A. Nordheim. 1995. Protein synthesis inhibitors reveal differential regulation of mitogen- activated protein kinase and stress-activated protein kinase pathways that converge on Elk-1. Mol. Cell Biol. 15:4930-4938.

Zugasti, O., W. Rul, P. Roux, C. Peyssonnaux, A. Eychene, T. F. Franke, P. Fort, and U. Hibner. 2001. Raf-MEK-Erk cascade in anoikis is controlled by Rac1 and Cdc42 via Akt. Mol. Cell Biol. 21:6706-6717.